Supporting Information for:

Ligand Redox Non-Innocence in [Co^{III}(TAML)]$^{0/-}$ Complexes Affects Nitrene Formation

Nicolaas P. van Leest,[†] Martijn A. Tepaske,[†] Jean-Pierre H. Oudsen,[§] Bas Venderbosch,[§] Niels R. Rietdijk,[†] Maxime A. Siegler,[‡] Moniek Tromp,[§] Jarl Ivar van der Vlugt[†] and Bas de Bruin[†,*]

[†]*Homogeneous, Supramolecular and Bio-Inspired Catalysis Group and* [§]*Sustainable Materials Characterization Group. Van 't Hoff Institute for Molecular Sciences (HIMS), University of Amsterdam, Science Park 904, 1098 XH Amsterdam, The Netherlands.* [*] *b.debruin@uva.nl*
[‡]*Department of Chemistry, Johns Hopkins University, Baltimore, Maryland 21218, United States*

Table of contents

General Considerations S2
Synthesis and characterization of complexes, reagents and substrates S6
Synthesis and characterization of nitrene-complexes S15
(Spectro)electrochemistry S21
UV-Vis studies S23
Catalytic aziridination S25
Density Functional Theory Calculations S26
Complete Active Space Self Consistent Field Calculations S34
List of xyz coordinates for all DFT calculated structures S48
References in the Supporting Information S57

General Considerations

Chemicals and solvents

All reagents were of commercial grade and used without further purification, unless noted otherwise. All reactions and measurements (except NMR studies) were performed under an inert atmosphere in a N_2 filled glovebox or by using standard Schlenk techniques (under Ar), unless noted otherwise. CH_2Cl_2 was distilled from CaH_2, toluene was distilled from sodium, THF and benzene were distilled from sodium benzophenone ketyl and CH_3CN was dried over molecular sieves prior to use. All solvents were deaerated by three freeze-pump-thaw cycles and backfilled with argon or sparged with argon prior to use. Styrene was filtered over basic alumina prior to use.

NMR spectroscopy

^{1}H, ^{13}C and ^{31}P NMR spectra were recorded on a Bruker DRX 500, Bruker AMX 400, Bruker DRX 300 or Varian Mercury 300 spectrometer at r.t. and the reported ppm values are relative to $SiMe_4$ for ^{1}H and ^{13}C by referencing the residual solvent peak to $SiMe_4$.[1] ^{31}P was referenced to H_3PO_4.

Magnetic moment measurements using Evans' method

Magnetic moments were determined according to reported procedures by solvation of a known amount of the analyte in a known amount of deuterated solvent with an internal standard in an NMR tube.[2] A capillary containing the deuterated solvent and internal standard was inserted in the NMR tube and a ^{1}H NMR spectrum was recorded. The mass susceptibility (χ in cm^3g^{-1}) of the analyte was calculated with equation (1), wherein ν_0 is the operating frequency of the NMR spectrometer (Hz), c is the concentration of the analyte in the solution (g L^{-1}) and M is the molar mass of the analyte. The molar susceptibility (χ_M in cm^3mol^{-1}) can be calculated by equation (2). χ_M^P is the pure paramagnetic molar susceptibility and can be calculated by equation (3) in which χ_M^{Dia} (the diamagnetic molar susceptibility) is a correction on χ_M to account for the diamagnetic contributions within the analyte. The diamagnetic molar susceptibility (χ_M^{Dia}) can be calculated by using Pascal's constants, which are tabulated in literature for different atoms and bond-types.[3] With equation (4), χ_M^P can be used to calculate the effective magnetic moment (μ_{eff}) of the analyte, in which k is the Boltzmann constant, T is the temperature in Kelvin, N_A is the Avogadro constant and μ_B is the Bohr magneton. The electron spin quantum number (S) can now be calculated with equation (5) from the effective magnetic moment by solving for S. Here, g is obtained from an EPR measurement or taken as the g_e-value for the free electron (2.0023).

$$(1)\quad \chi = \frac{3000\times\Delta\nu}{4\pi\times\nu_0\times c\times M}$$

$$(2)\quad \chi_M = \chi \times \mathrm{M}$$

$$(3)\quad \chi_M^P = \chi_M - \chi_M^{Dia}$$

$$(4)\quad \mu_{eff} = \sqrt{\frac{3\times k\times T\times \chi_M^P}{N_A\times \mu_B^2}} \approx 2.82787\sqrt{T\times\chi_M}$$

$$(5)\quad \mu_{eff} = g\sqrt{S(S+1)}$$

Electrochemical measurements

Cyclic voltammograms were recorded using a 663 VA stand with a PGSTAT302N potentiostat (Metrohm/Autolab) in a single-cell three electrode system with a glassy carbon working electrode, Pt auxiliary electrode and leak-free Ag/AgCl (3.5 M KCl) reference electrode. Potentials are reported versus $Fc^{+/0}$ by addition of Fc during the last scan and referencing to this redox couple.

Spectroelectrochemistry

Spectroelectrochemical measurements were conducted by using a standard OTTLE cell[4] with a Pt grid working electrode, Pt auxiliary electrode and a Ag wire reference electrode, coupled to an Autolab PGSTAT302N potentiostat and double beam Shimadzu UV-2600 spectrometer.

UV-Vis spectroscopy

UV-Vis spectra were recorded on a Hewlett Packard 8453 or a double beam Shimadzu UV-2600 spectrometer in a 1.0 cm Teflon screw-cap quartz cuvette under Argon using the solvent as a background.

EPR spectroscopy

EPR spectra were recorded on a Bruker EMX X-band spectrometer equipped with a He cryostat. The spectra were analyzed and simulated using the W95EPR program of Prof. F. Neese (MPI Muelheim).

Mass spectrometry

CSI and ESI mass spectra were collected on an AccuTOF LC, JMS-T100LP Mass spectrometer (JEOL, Japan). The CSI apparatus features a liquid nitrogen cooling device to maintain the temperature of the capillary and spray itself between 0 °C and –50 °C. Typical measurement conditions are as follows: Positive-ion mode; Needle voltage 2000V, Orifice 1 voltage 90V, Orifice 2 voltage 9V, Ring Lens voltage 22V. Orifice 300C, Desolvating Chamber 30 0C, spray temperature –40 0C. For ESI, typical measurement conditions are as follows: Positive-ion mode; Needle voltage 2500V, Orifice 1 voltage 120V, Orifice 2 voltage 9V, Ring Lens voltage 22V. Orifice 1 80 °C, desolvating Chamber 250 °C. Flow injection with a flow rate of 0.01 ml/min. All mass spectra were recorded with an average duration of 0.5 min.

FD Mass spectra were collected on an AccuTOF GC v 4g, JMS-T100GCV Mass spectrometer (JEOL, Japan). FD/FI probe (FD/FI) equipped with FD Emitter, Carbotec or Linden (Germany), FD 13 µm. Current rate 51.2 mA/min over 1.2 min. FI Emitter, Carbotec or Linden (Germany), FI 10 µm. Flashing current 40 mA on every spectra of 30 ms. Typical measurement conditions are: Counter electrode –10kV, Ion source 37V. LiFDi probe (FD/FI) equipped with FD Emitter, Linden CMS GmbH (Germany), FD 13 µm. Current rate 51.2 mA/min over 1.2 min. Typical measurement conditions are: Counter electrode –10kV, Ion source 37V.

X-Ray crystallography

X-ray intensities were measured on a Bruker D8 Quest Eco diffractometer equipped with a Triumph monochromator (λ = 0.71073 Å) and a CMOS Photon 100 detector at a temperature of 150(2) K. Intensity data were integrated with the Bruker APEX2 software.[5] Absorption correction and scaling was performed with SADABS.[6] The structures were solved using intrinsic phasing with the program SHELXT.[7] Least-squares refinement was performed with SHELXL-2013[8] against F^2 of all reflections. Non-hydrogen atoms were refined with anisotropic displacement parameters. The H atoms were placed at calculated positions using the instructions AFIX 13, AFIX 43 or AFIX 137 with isotropic displacement parameters having values 1.2 or 1.5 times U_{eq} of the attached C atoms.

Co K-edge XAS measurements

Co K-edge XAS experiments were performed at Diamond Light Source on beamline B18 in Didcott, UK (proposal number SP22432). All measurements were done in fluorescence mode in toluene solutions. Solutions containing the complexes were kept frozen using a Cryojet set to a temperature of 100K.[9] Measurements were performed with a Si(111) double monochromator in combination with a 36 element Ge detector. A typical measurement required 4 minutes. Around 25 scans were required to obtain good signal-to-noise ratio in the data. All acquired spectra were calibrated to a Co foil. Normalization of the Co K-edge XANES data was done using the Matlab software package. This was achieved by fitting a second-order polynomial function to the pre-edge and fitting a third-order polynomial function to the post-edge. All sample preparations were performed in a glovebox containing an Ar atmosphere with less than 1 ppm of O_2 and H_2O. The analyte solutions were filtered prior to use over a syringe filter (PTFE 0.45 µm) and transferred to a Kapton® tube and taken out of the glovebox, rapidly frozen into liquid nitrogen and transferred to the beamline for measurement.

DFT calculations

DFT geometry optimizations were performed on full atomic models (no simplifications) using TURBOMOLE 7.3[10] coupled to the PQS Baker optimizer[11] via the BOpt package.[12] The calculations were performed at the BP86[13]/def2-TZVP[14] level of theory (unless noted otherwise) with strict convergence criteria (scfconv = 9) on an m4 grid, using Grimme's version 3 (disp3, "zero damping") dispersion corrections.[15] All minima (no imaginary frequencies) were characterized by numerically calculating the Hessian matrix. Energy output was reported in Hartree and was converted to kcal mol^{-1} by multiplication with 627.503.

When applicable, corrected broken symmetry energies ε_{BS} of the open-shell singlets (S = 0) were estimated from the energy (ε_S) of the optimized single-determinant broken symmetry solution and the energy (ε_{S+1}) from a separate unrestricted triplet single-point calculation at the same level, using the approximate correction formula (6).[12]

$$(6)\quad \varepsilon \approx \frac{S_{S+1}^2 \times \varepsilon_S - S_S^2 \times \varepsilon_{S+1}}{S_{S+1}^2 - S_S^2}$$

EPR parameters were calculated with the ORCA 4.1[16] software package at the B3LYP[17]/TZ2P[14] level, using the coordinates from the structures optimized in TURBOMOLE as the input.

Graphical representations of structures and visualization of orbitals were generated using IboView.[18] Spin densities were generated using IQMol (http://iqmol.org/).

NEVPT2-CASSCF calculations

NEVPT2 corrected CASSCF calculations were performed with the ORCA 4.1[16] software package on geometries optimized in TURBOMOLE at the doublet (neutral complexes) or triplet (anionic complexes) spin surface, as these were in-line with experimentally found spin states. The def2-TZVP[14] basis set was used together with the RIJCOSX[19] approximation in conjunction with the def2-TZVP/C fitting basis set to reduce computational cost. In all cases, the single root spin states (doublet, quartet *or* singlet, triplet, quintet for neutral or anionic complexes, respectively) were calculated. For refined energy values NEVPT2[20] calculations using the RI approximation were carried out on converged CASSCF wavefunctions. Canonical orbitals were generated for visualization using IboView.[18] Energy output was reported in Hartree and was converted to kcal mol^{-1} by multiplication with 627.503.

A general flow-scheme for these calculations is described below, including the input for the calculations in brackets:

1. The molecule was aligned properly along the x, y and z axis and QRO-type orbitals were generated in a single-point calculation by usage of the UNO keyword.
   [!BP86 def2-TZVP def2-TZVP/C RIJCOSX UNO Normalprint KeepDens]
2. The QRO orbitals were used for a restricted open-shell Kohn-Sham (ROKS) calculation.
   [! ROKS BP86 def2-TZVP def2-TZVP/C RIJCOSX Normalprint noiter MOREAD
   %moinp "orbitals.qro"]
3. Löwdin population analysis and visualization using IboView were used to identify the orbitals of interest (all metal d orbitals, relevant ligand π orbitals and relevant metal-ligand bonding and antibonding orbitals) and rotate these into the active space.
   [! ROKS BP86 def2-TZVP def2-TZVP/C RIJCOSX Normalprint noiter MOREAD
   %moinp "orbitals.gbw"]
   %scf rotate {orbital number, active space location} end end]
4. The single root CASSCF calculation was performed.
   [! def2-TZVP def2-TZVP/C RIJCOSX Normalprint MOREAD
   %moinp "orbitals.gbw"

```
%casscf
trafostep ri
nel (number of active electrons)
norb (number of active orbitals)
mult (multiplicity)
end]
```

5. The converged CASSCF calculation was analyzed for convergence and preservation of the active space, and if necessary orbitals were rotated back into the active space (step 3) and the calculation was repeated (step 4). The NEVPT2 correction was then applied and the orbitals were transformed to canonical orbitals for final visualization and (total) energy evaluation.

   ```
   [! def2-TZVP def2-TZVP/C RIJCOSX Normalprint MOREAD SOMF(1X) RI-NEVPT2
   %moinp "orbitals.gbw"
   %casscf
   trafostep ri
   nel (number of active electrons)
   norb (number of active orbitals)
   mult (multiplicity)
   actorbs canonorbs
   intorbs canonorbs
   extorbs canonorbs
   end]
   ```

6. The converged NEVPT2 corrected CASSCF calculation can be used to calculate absorption energies and associated orbitals by inclusion of a number of roots (nroots).

   ```
   [! def2-TZVP def2-TZVP/C RIJCOSX Normalprint MOREAD SOMF(1X) RI-NEVPT2
   %moinp "orbitals.gbw"
   %casscf
   trafostep ri
   nel (number of active electrons)
   norb (number of active orbitals)
   mult (multiplicity)
   nroots (number of roots)
   actorbs canonorbs
   intorbs canonorbs
   extorbs canonorbs
   end]
   ```

Synthesis and characterization of complexes, reagents and substrates

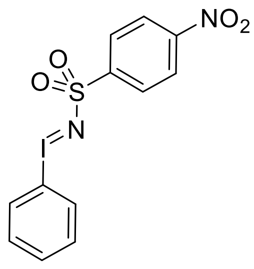

PhINNs

PhINNs was prepared according to a literature procedure and the spectroscopic data of the product matched those previously reported.[21] $PhI(OAc)_2$ (3.00 g; 9.3 mmol; 1.2 eq) was added portionwise to a stirred solution of KOH (1.09 g; 19.38 mmol; 2.5 eq) and $NsNH_2$ (1.57 g; 7.75 mmol; 1.0 eq) in MeOH (35 mL) at 0 °C under an N_2 atmosphere. The yellow suspension was stirred for 30 min at 0 °C and for 3 h at r.t., after which stirring was stopped and the reaction mixture was left to stand overnight in absence of light. The yellow precipitate was collected by filtration was washed with ice-cold MeOH (3×15 mL) and dried *in vacuo* at 60 °C. The product was obtained as a yellow solid in 2.84 g; 7.03 mmol; 90.6% isolated yield.

^{1}H NMR (300 MHz, DMSO-*d*$_6$) δ 8.03 (d, *J* = 8.8 Hz, 2H), 7.85 – 7.63 (m, 4H), 7.40 (t, *J* = 7.4 Hz, 1H), 7.25 (t, *J* = 7.7 Hz, 2H).

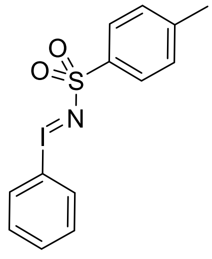

PhINTs

PhINTs was prepared according to a literature procedure and the spectroscopic data of the product matched those previously reported.[22] $PhI(OAc)_2$ (3.22 g; 10.0 mmol; 1.0 eq) was added to a stirred solution of KOH (1.40 g; 25.0 mmol; 2.5 eq) and $TsNH_2$ (1.88 g; 11 mmol; 1.1 eq) in MeOH (40 mL) at 0 °C in absence of light. The solution was stirred for 2 h at 0-10 °C, 1 h at r.t. and poured into H_2O (230 mL). The solution was left to stand overnight, filtered and the precipitate was washed with ice-cold MeOH (12 mL), DCM (500 mL) and hexanes (200 mL). The product was obtained as a white solid in 1.17 g; 3.13 mmol; 31.3% isolated yield.

^{1}H NMR (400 MHz, DMSO-*d*$_6$) δ 7.69 (d, *J* = 7.8 Hz, 2H), 7.43 (d, *J* = 7.6 Hz, 3H), 7.29 (t, *J* = 7.7 Hz, 2H), 7.06 (d, *J* = 7.8 Hz, 2H), 2.27 (s, 3H).

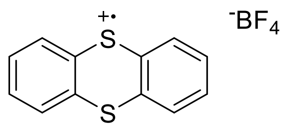

(Thi)BF$_4$

Thianthrenium tetrafluoroborate ((Thi)BF_4) was synthesized according to a literature procedure.[23] Under strict water-free conditions and under constant argon flow in a three neck round bottom, thianthrene (510 mg, 2.36 mmol, 1.0 eq.) and $(NO)BF_4$ (290 mg, 2.48 mmol, 1.05 eq.) were dissolved in MeCN (40 mL) and stirred for 1 h. to afford a blue solution. The reaction mixture was closed and stirred under argon for 1h., after which under argon flow Et_2O (6 × 20 mL portions) was added to yield a purple suspension, which was filtered under aerobic conditions. The purple solid was dried *in vacuo* and stored under nitrogen. Isolated yield: 555 mg, 1.83 mmol, 77.5%.

X-band EPR: g_{iso} = 2.009 (MeCN, microwave freq. 9.394585 GHz, mod. amp. 0.100 G, power 0.6325 mW).

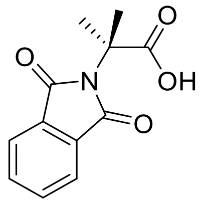

C1

Compound **C1** was synthesized according to a literature procedure.[24] Phthalic anhydride (40.0 g, 0.27 mol, 1.4 eq.) and 2-amino-*iso*-butyric acid (20.0 g, 0.19 mol, 1.0 eq.) were placed in a flame-dried round-bottom flask and heated to 190 °C under aerobic conditions. The colourless liquid was kept at 190 °C for 2 h., after which water vapour formation ceased. After stirring at 180 °C for 30 min., the reaction mixture was cooled to r.t., suspended in DCM (400 mL), stirred and filtered. The filtrate was concentrated under reduced pressure and the resulting white powder was suspended in an aqueous $NaHCO_3$ solution (10%, 200 mL), stirred vigorously and filtered. The filtrate was acidified with conc. HCl until precipitation had stopped. The white solid was collected by filtration, washed with pentane and dried overnight in a vacuum oven at 60 °C. **C1** was obtained as a white powder in 23.4 g; 0.10 mol; 53.1% isolated yield.

^{1}H NMR (500 MHz, DMSO-*d*$_6$) δ 12.90 (s, 1H, O*H*), 7.85 (s, 4H, Ar*H*), 1.72 (s, 6H, C*H*$_3$).

^{13}C NMR (126 MHz, DMSO-*d*$_6$) δ 174.36, 168.46, 135.15, 131.62, 123.42, 60.24, 24.74.

HRMS-FD$^+$ (*m/z*) calcd for $C_{12}H_{12}N_1O_4$: 234.0766, found 234.0775 [M$^+$].

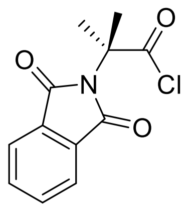
C2

Compound **C2** was synthesized according to a literature procedure.[24] **C1** (40.0 g, 0.171 mol, 1.0 eq.) and $SOCl_2$ (115 mL, 1.65 mol, 9.72 eq.) were refluxed at 85 °C for 2 h in a flame-dried round-bottom. The resulting yellow suspension was concentrated under reduced pressure after which Et_2O (3 × 50 mL) was added, followed by concentration. The obtained white solid was then suspended in petroleum ether (60-80, 250 mL), stirred at 85 °C for 15 min. and filtered while still hot. The filtrate was heated again to 85 °C until a clear solution was obtained, which was slowly cooled to r.t. to afford white crystals, which were obtained by filtration and washed with cold petroleum ether. The product was dried overnight in a vacuum oven at 60 °C and obtained as a white crystalline solid in 30.2 g; 0.12 mol; 70.6% isolated.

^{1}H NMR (500 MHz, DMSO-*d*$_6$) δ 7.85 (s, 4H, Ar*H*), 1.73 (s, 6H, C*H*$_3$).

^{13}C NMR (126 MHz, DMSO-*d*$_6$) δ 174.29, 168.45, 135.15, 131.62, 123.42, 60.21, 24.72.

HRMS-FD$^+$ (*m/z*) calcd for $C_{12}H_{11}Cl_1N_1O_3$: 251.0349, found 252.0432 $[M+H]^+$, 188.0719 $[M-COCl]^+$, 189.0781 $[M-COCl+H]^+$.

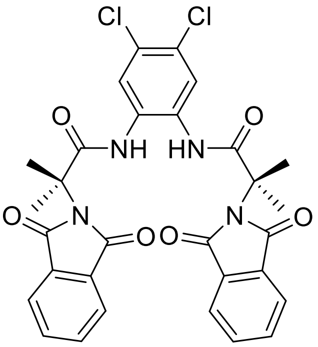
C3

Compound **C3** was synthesized according to a literature procedure.[24] Under argon, a solution of 4,5-dichloro-1,2-phenylenediamine (1.56 g, 8.81 mmol, 1.0 eq.) and NEt_3 (2.70 mL, 19.733 mmol, 2.2 eq.) in THF (55 mL) was added dropwise to a solution of **C2** (4.43 g, 17.62 mmol, 2.0 eq.) in THF (55 mL) at 0 °C. The red solution was stirred for 23 h. at 27 °C and then heated to 50 °C for 1 h and to 60 °C for 1.5 h, after which the red suspension was cooled to r.t., filtered, the filtrate concentrated under reduced pressure and residual THF was removed by co-evaporation with DCM. The solid was dissolved in DCM (150 mL), washed with aqueous HCl (0.1M, 3 × 50 mL) and aqueous $NaHCO_3$ (5%, 3 × 60 mL). Concentration under reduced pressure of the DCM fraction afforded a rose coloured solid as the product. **C3** was obtained in 4.66 g; 7.67 mmol; 87.1% isolated yield.

^{1}H NMR (500 MHz, DMSO-*d*$_6$) δ 9.45 (s, 2H), 7.91 – 7.81 (m, 4H), 7.82 (s, 2H), 7.74 (dd, *J* = 5.5, 3.0 Hz, 4H), 1.70 (s, 12H).

^{13}C NMR (126 MHz, DMSO-*d*$_6$) δ 172.30, 168.76, 135.00, 132.04, 131.13, 127.13, 125.68, 123.40, 61.39, 24.60.

HRMS-FD$^+$ (*m/z*) calcd for $C_{30}H_{24}Cl_2N_4O_6$: 606.1073, found 606.1046 $[M^+]$.

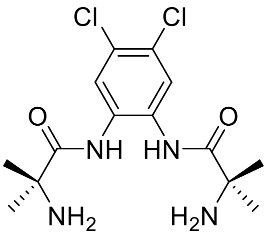
C4

Compound **C4** was synthesized according to a literature procedure.[24] Under argon, **C3** (2.69 g, 4.43 mmol, 1.0 eq) was suspended in EtOH (65 mL) and refluxed at 95 °C, upon which hydrazine (65% in H_2O, 0.81 mL, 17.10 mmol, 3.86 eq.) was added. The brown suspension was refluxed for 18 h. and then cooled to r.t. and concentrated under reduced pressure. To the white-red solid, aqueous HCl (2M, 250 mL) was added and the suspension was heated to 80 °C for 10 min and filtered. The red filtrate was brought to pH 13 with concentrated $NaOH_{aq}$ to afford a yellow solution. The product was extracted in DCM (4 × 100 mL) and the combined organic layers were concentrated under reduced pressure, followed by washing of the obtained oil with Et_2O to afford the product as a white-brown solid. Isolated yield: 1.20 g, 3.46 mmol, 78.1%.

^{1}H NMR (300 MHz, DMSO-*d*$_6$) δ 7.94 (s, 2H), 4.87 (s, 4H), 3.36 (s, 2H), 1.30 (s, 12H).

^{13}C NMR (75 MHz, DMSO-*d*$_6$) δ 177.52, 131.74, 126.45, 125.15, 55.50, 28.95.

HRMS-FD$^+$ (*m/z*) calcd for $C_{14}H_{20}Cl_2N_4O_2$: 346.0963, found 346.0978 $[M^+]$.

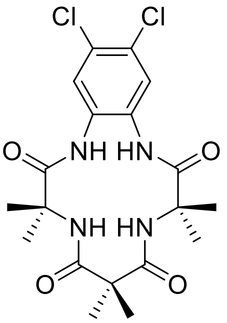

TAMLH4

TAMLH4 was synthesized according to a literature procedure.[24] Under argon, a solution of **C4** (1.00 g, 2.88 mmol, 1.0 eq) and Et_3N (0.82 mL, 5.88 mmol, 2.04 eq) in THF (30 mL) and a solution of dimethylmalonyl chloride (0.42 mL, 3.17 mmol, 1.1 eq) in THF (30 mL) were added to THF (10 mL) at 0 °C over the course of 2h. using a syringe pump. The yellow-white suspension was stirred at r.t. for 24 h. and H_2O (100 mL) was added. The THF was removed under reduced pressure to afford a brown suspension, which was filtered and the residue was washed with H_2O and Et_2O and dried in a vacuum oven at 60 °C to afford the product as an off-white powder. Isolated yield: 1.27 g, 2.86 mmol, 84.3%.

^1H NMR (300 MHz, DMSO-*d*$_6$) δ 8.48 (s, 2H), 7.80 (s, 2H), 7.70 (s, 2H), 1.46 (s, 12H, CH_3), 1.44 (s, 6H, CH_3).

^{13}C NMR (75 MHz, DMSO-*d*$_6$) δ 173.22, 172.48, 130.63, 127.04, 126.83, 57.56, 50.27, 24.81, 21.98.

IR-ATR (cm^{-1}); 3344 (w, br, NH), 2970 (w, sh, aliphatic), 1689 (m, sh, CO), 1646 (m, sh, CO).

HRMS-FD$^+$ (*m/z*) calcd for $C_{19}H_{24}Cl_2N_4O_4$: 442.1175, found 442.1190 [M^+].

XRD quality single crystals were grown by vapour diffusion of pentane into a concentrated THF solution of **TAMLH4** at r.t and the 50% thermal ellipsoid probability plot with relevant bond lengths is depicted in Figure S1. **TAML4**, $C_{19}H_{24}Cl_2N_4O_4$, fw = 443.32, 0.517 mm x 0.231 mm x 0.170 mm, orthorhombic, a = 21.4066(19) Å, b = 43.288(3) Å, c = 10.1268(7) Å, α = 90°, β = 90°, γ = 90°, V = 9384.1(13) Å^3, Z = 16, D_x = 1.408 g/cm^3, μ = 0.307 mm^{-1}; 66404 reflections were measured up to a resolution of 0.84 Å at a θ_{max} of 24.987°.; 4107 reflections were unique of which 4006 were observed [$I > 2\sigma(I)$]. Residual electron density between -0.406 and 1.480 e$^-$/Å^3. CCDC 1961659 contains the supplementary crystallographic data for this paper. This data can be obtained free of charge from The Cambridge Crystallographic Data Centre via www.ccdc.cam.ac.uk/data_request/cif.

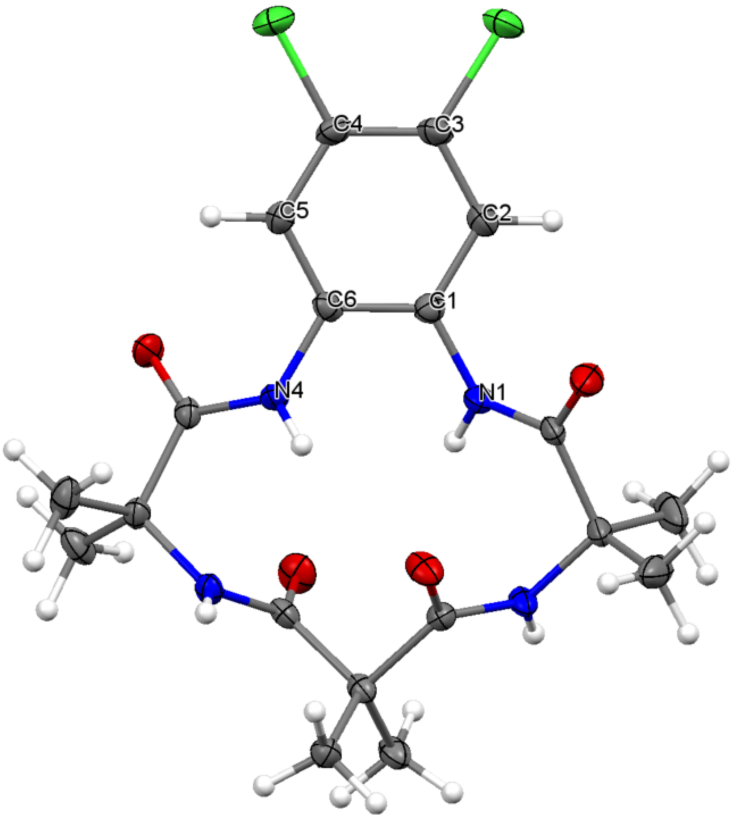

N1-C1 = 1.423(3) Å
N4-C6 = 1.420(3) Å
C1-C2 = 1.389(3) Å
C2-C3 = 1.379(3) Å
C3-C4 = 1.381(3) Å
C4-C5 = 1.380(3) Å
C5-C6 = 1.384(3) Å
C6-C1 = 1.394(3) Å

Figure S1. 50% thermal ellipsoid probability plot of the crystal structure of **TAMLH$_4$** and relevant bond lengths.

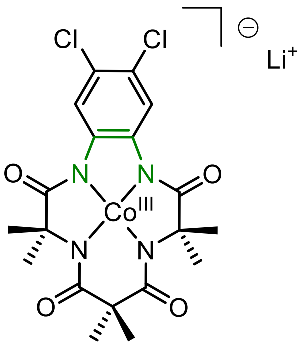

Li[Co^{III}(TAML^{red})]

Li[Co^{III}(TAML^{red})] was synthesized according to a literature procedure.[25] **TAMLH$_4$** (554.2 mg, 1.25 mmol, 1.0 eq.) was dissolved in dry THF (70 mL) under argon. The solution was frozen at –198 °C and *n*BuLi (2.5M in hexanes, 2.00 mL, 5.00 mmol, 4.0 eq.) was added slowly, upon which the solid started to melt. Just before the solid finished thawing, $CoCl_2$ (anhydrous, 211.6 mg, 1.63 mmol, 1.3 eq) was added in one portion under argon flow. The solution was stirred at r.t. for 30 min. and became brown-green, after which the solution was bubbled with air for 90 min. to form a purple suspension. The suspension was transferred onto a silica column with THF and the purple band eluted with acetone. Concentration of the purple solution, washing with DCM (500 mL), filtration, stirring of the residue in Et_2O (200 mL) and filtration afforded the desired product as a purple crystalline powder, which was dried in a vacuum oven at 50 °C. Isolated yield: 528 mg, 1.04 mmol, 83.6%.

^{1}H-NMR (CD_3CN) 4.99 (s (br), 12 H, CH_3), 3.61 (s (br), 6H, CH_3), -6.21 (s (br), 2H, ArH).

^{13}C-NMR (CD_3CN) 388.20 (s), 347.07 (s), 188.61 (s), 149.69 (s), 126.27 (s), 107.95 (s), 90.56 (s), 73.33 (s), 49.56 (s).

IR (IR-ATR, cm^{-1}) 2962 (w, br, aliphatic), 1633 (m, sh, CO),1600 (s, sh, CO).

UV-Vis (MeCN) λ_{max} [nm] (ε) = 240 (29747), 269 (18510), 510 (7664).

HRMS-CSI$^-$ (*m/z*) calcd for $C_{19}H_{20}Cl_2CoN_4O_4^-$: 497.0194, found 497.0205 [M$^-$].

X-band EPR silent (20K in EtOH).

Evans' method: CD_3CN with toluene as internal standard, c = 0.02178 M, δ = 125.44 Hz, μ_{eff} = 2.941 μ_B (S = 1), χ_d = –201.59 emu mol^{-1}.

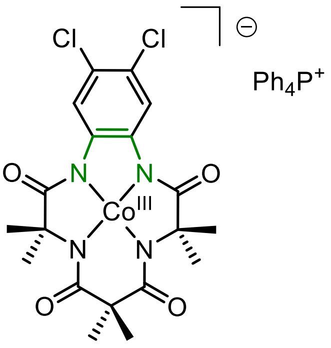

PPh_4[Co^{III}(TAML^{red})]

PPh_4[Co^{III}(TAML^{red})] was synthesized according to a literature procedure.[26] Under aerobic conditions, **Li[Co^{III}(TAML^{red})]** (84 mg, 0.166 mmol, 1.0 eq.) was dissolved in H_2O (50 mL) and PPh_4Cl (187 mg, 0.50 mmol, 3.0 eq.) was added while stirring. After 30 min. the purple suspension was filtered and the residue washed with H_2O. The residue was dissolved in DCM and dried over Naq_2SO_4, filtered and the filtrate was concentrated under reduced pressure to afford the product as a fine purple powder, which was dried *in vacuo* overnight. Isolated yield: 128 mg, 0.153 mmol, 92.3%.

^{1}H-NMR (d_3-CD_3CN) 7.78 (t, 4H, phenyl), 7.64 (m, 16H, phenyl), 5.09 (s (br), 12H, CH_3), 3.58 (s (br), 6H, CH_3), -6.11 (s (br), 2H, ArH).

^{31}P-NMR (d_3-CD_3CN) 22.84 (s, P).

IR (IR-ATR, cm^{-1}) 2929 (w, sh, aliphatic), 1647 (m, sh, CO), 1615 (s, sh, CO).

HRMS-ESI$^-$ *(m/z)* calcd for $C_{19}H_{20}Cl_2CoN_4O_4^-$: 497.0194, found 497.0217 [M$^-$].

HRMS-ESI$^+$ *(m/z)* calcd for $C_{24}H_{20}P^+$: 339.1301, found 339.1322.

UV-Vis (DCM) λ_{max} [nm] (ε) = 234 (69614), 269 (30103), 510 (9113).

X-band EPR silent (r.t. or 20K in toluene and 20K in MeCN).

Evans' method: CD_2Cl_2 with toluene as internal standard, c = 0.01357 M, δ = 70.82 Hz, μ_{eff} = 2.901 μ_B (S = 1), χ_d = –426.2 emu mol^{-1}.

Redox potentials: $E°_{½}$ = -1.18 V, +0.53 V and +1.13 V vs Fc$^{+/0}$ in DCM (see electrochemistry section).

Co-K edge XANES: **PPh_4[Co^{III}(TAML^{red})]** (33.5 mg; 0.040 mmol) was dissolved in toluene (4.0 mL) in an argon filled glovebox. A shoulder was determined to be at approximately 7715 eV and the edge position was found at 7721 eV (Figure S2).

XRD quality single crystals were grown by vapour diffusion of pentane into a concentrated THF solution of **PPh_4[Co^{III}(TAML^{red})]** at 4 °C and the 50% thermal ellipsoid probability plot with relevant bond lengths is depicted in Figure S3. 50% thermal ellipsoid probability plot of the crystal structure of **PPh_4[CoTAML-Cl_2] · THF** with relevant bond lengths.. **PPh_4[CoTAML-Cl_2]·THF**, $C_{47}H_{48}Cl_2CoN_4O_5P$, fw = 905.66, metallic dark brown-red block-like, 0.136 mm x 0.289 mm x 0.317 mm, monoclinic, P1 (21/c 1), a = 14.6681(9) Å, b = 15.5580(10) Å, c = 19.0036(12) Å, α = 90°, β = 99.766(2)°, γ = 90°, V = 4273.9(5) Å^3, Z = 4, D_x = 1.408 g/cm^3, μ = 0.616 mm^{-1}; 138208 reflections were measured up to a resolution of 0.71 Å at a θ_{max} of 30.1412575 reflections were unique (R_{int} = 0.0643) of which 9036 were observed [I > 2σ(I)]. Residual electron density between –0.528 and 0.515 e$^-$/Å^3. S = 0.965. 1959461. CCDC 1959461 contains the supplementary crystallographic data for this paper. This data can be obtained free of charge from The Cambridge Crystallographic Data Centre via www.ccdc.cam.ac.uk/data_request/cif.

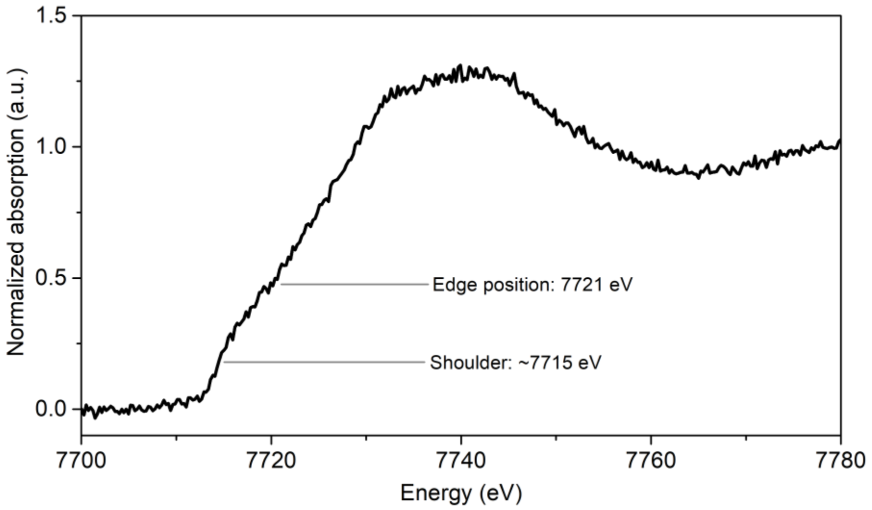

Figure S2. Co-K edge XANES analysis of **PPh$_4$[Co^{III}(TAML^{red})]** in toluene.

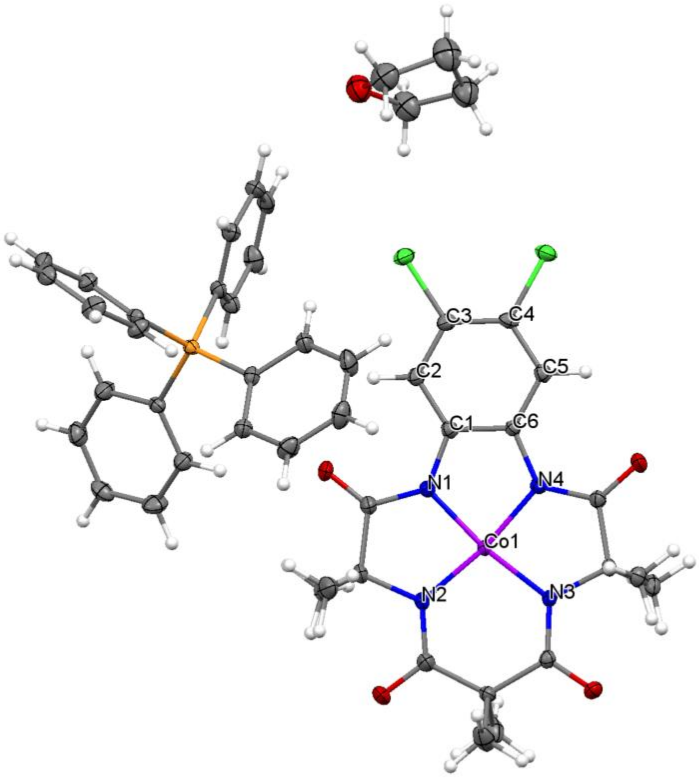

Co1-N1 = 1.8244(15)
Co1-N2 = 1.8273(15)
Co1-N3 = 1.8337(15)
Co1-N4 = 1.8267(15)
N1-C1 = 1.410(2)
N4-C6 = 1.407(2)
C1-C2 = 1.386(3)
C2-C3 = 1.391(3)
C3-C4 = 1.390(3)
C4-C5 = 1.397(3)
C5-C6 = 1.390(2)
C6-C1 = 1.410(2)

Figure S3. 50% thermal ellipsoid probability plot of the crystal structure of **PPh$_4$[CoTAML-Cl$_2$] ·THF** with relevant bond lengths.

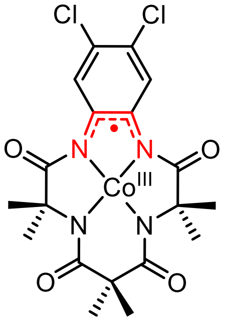

[Co^{III}(TAML^{sq})]

[Co^{III}(TAML^{sq})] can be synthesized according to a literature procedure with cerium ammonium nitrate (CAN) (*method 1*[25]), an (*in situ*) procedure with (Thi)BF$_4$ (*method 2),* of which the spectral data (UV-Vis and EPR) were in accordance with literature,[25] or via spectro-electrochemical (UV-Vis) one-electron oxidation of **PPh$_4$[Co^{III}(TAML^{red})]**.

Method 1:

CAN and **Li[Co^{III}(TAML^{red})]** were ground separately with a mortar to obtain two fine powders. Under argon, **Li[Co^{III}(TAML^{red})]** (111.7 mg; 0.221 mmol; 1 eq.) and CAN (1.632 g; 2.98 mmol; 13.5 eq.) were placed in a Schlenk flask. To this, dry toluene (40 mL) was added and the suspension was stirred for 1 h. Under argon, the blue-yellow suspension was filtered with a cannula filter to obtain a blue solution. The toluene was removed *in vacuo* to yield a dark coloured solid. To increase the yield, this procedure was repeated five times. Isolated yield: 38.8 mg; 0.078 mmol; 37.1%.

Method 2:

Under argon, **PPh$_4$[Co^{III}(TAML^{red})]** (1.0 eq) and Thi)BF$_4$ (1.05 eq) were stirred under argon at room temperature in either benzene, toluene or MeCN for 5 minutes, upon which the colour of the solution changed from purple to blue. In a similar fashion, **Li[Co^{III}(TAML^{red})]** (1.0 eq) and (Thi)BF$_4$ (1.05 eq) were stirred under argon at room temperature in MeCN for 5 minutes To remove unreacted (Thi)BF$_4$, the solution was concentrated *in vacuo* and **[Co^{III}(TAML^{sq})]** was extracted in DCM and filtered. It should be noted that **Li[Co^{III}(TAML^{red})]** is insoluble in DCM, and therefore unreacted **Li[Co^{III}(TAML^{red})]** is also removed during this work-up.

According to a UV-Vis titration study (see UV-Vis studies section), the oxidation of **PPh$_4$[Co^{III}(TAML^{red})]** to **[Co^{III}(TAML^{sq})]** occurs in a stoichiometric manner.

^{1}H NMR: silent.

HRMS-FD$^+$ (*m/z*) calcd for $C_{19}H_{20}Cl_2CoN_4O_4$+H: 498.0272, found 497.9892 [M$^+$+H].

UV-Vis (DCM) λ_{max} [nm] (ε) = 623 ($10.8 \cdot 10^3$). Characteristic for the TAML^{sq} oxidation state (see CASSCF section).

Evans' method: CD_2Cl_2 with toluene as internal standard, c = 0.01495 M, δ = 23.23 Hz, μ_{eff} = 1.882 μ_B (S = 0.5), χ_d = –249.113 emu mol^{-1}.

Co-K edge XANES: sample preparation was performed as described in *method 2* in an argon filled glovebox to afford a 10 mM solution of **[Co^{III}(TAML^{sq})]** in toluene. A shoulder was observed at approximately 7715 eV and the edge position was determined to be at 7721 eV (Figure S4).

EPR spectra and parameters are depicted in Figure S5, Figure S6 and Figure S7.

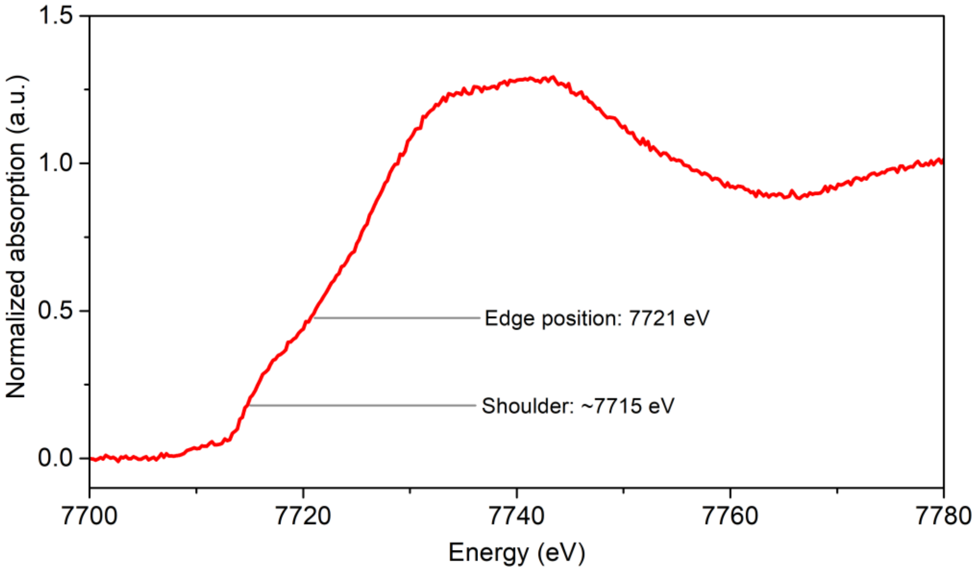

Figure S4. Co-K edge XANES analysis of **[Co^{III}(TAML^{sq})]** in toluene.

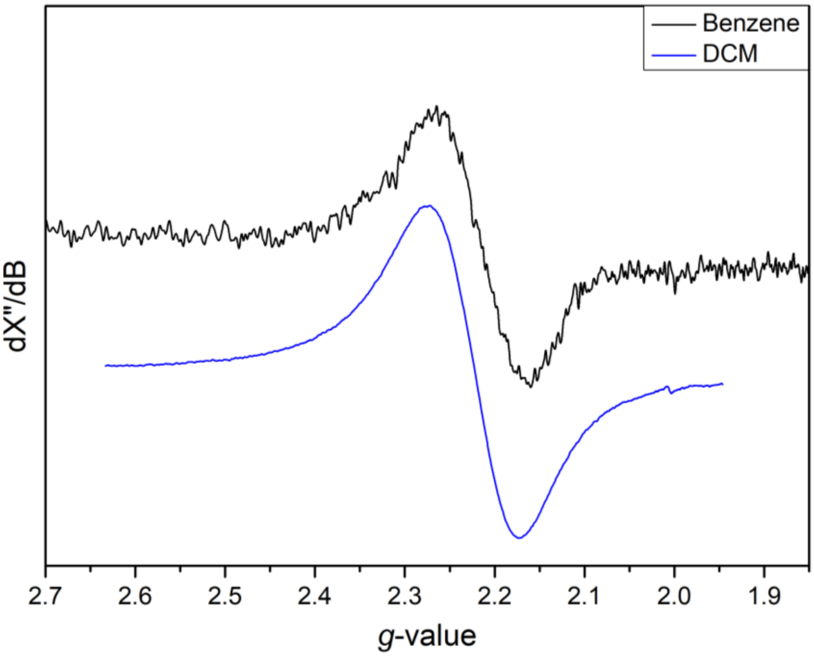

Figure S5. X-Band EPR spectrum of **[Co^{III}(TAML^{sq})]** at r.t. in benzene (black, Microwave freq. 9.390167 GHz, Mod. Amp. 4.000 G, Power 2.518 mW) and CH_2Cl_2 (blue, Microwave freq. 9.396621 GHz, Mod. Amp. 5.000 G, Power 2.000 mW) with g_{iso} = 2.22.

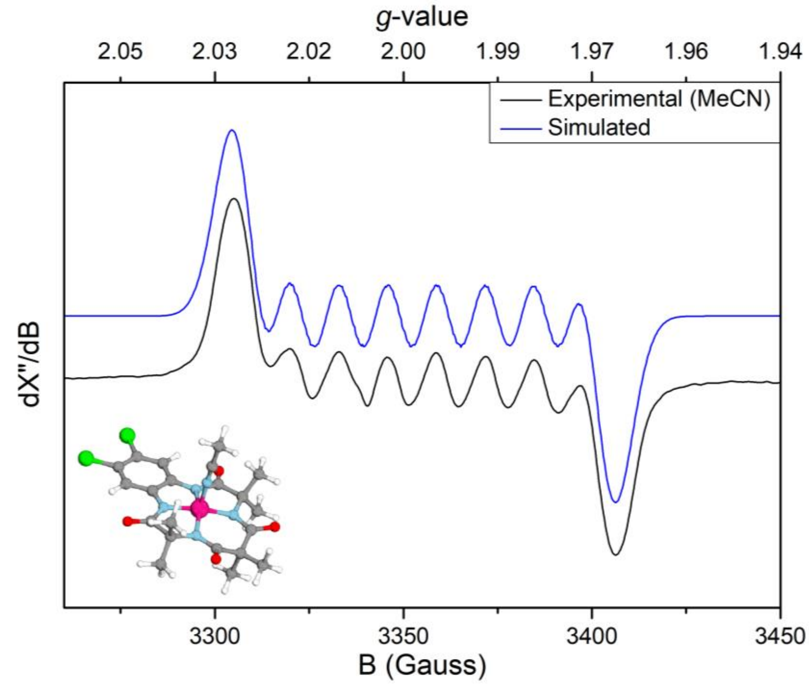

Figure S6. Experimental (black) and simulated (blue) X-Band EPR spectrum of **[Co^{III}(TAML^{sq})(MeCN)]** at r.t. in MeCN and DFT (BP86/def2-TZVP/disp3) optimized structure. Microwave freq. 9.388626 GHz, mod. amp. 2.999 G, power 0.7962 mW. Simulated and calculated (in parenthesis, B3LYP/def2-TZVP) parameters: g_{iso} = 2.00 (2.00) and A^{Co}_{iso} = 36.0 (34.2) MHz.

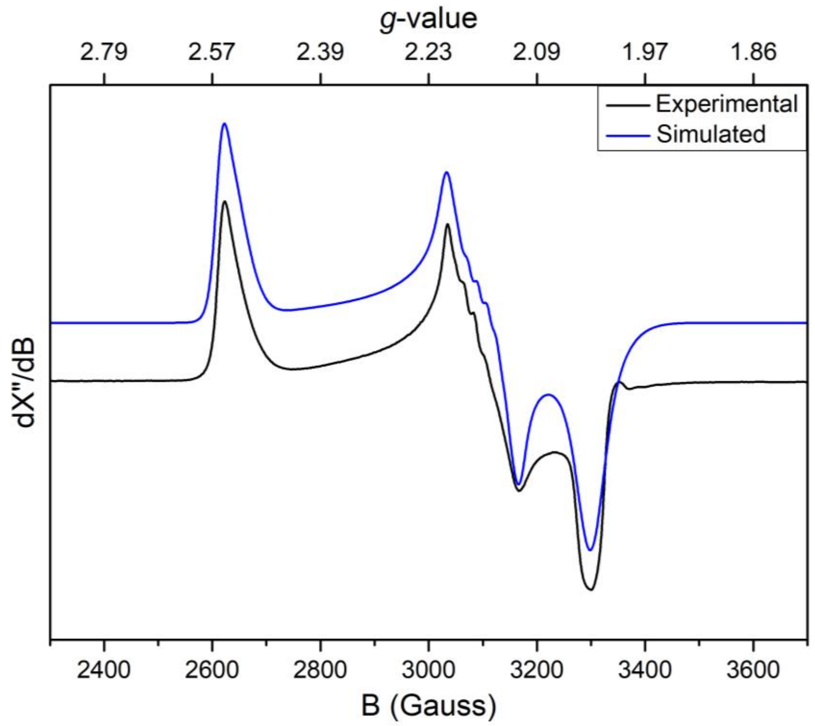

Figure S7. Experimental (black) and simulated (blue) X-Band EPR spectrum of **[Co^{III}(TAML^{sq})]** at 10 K in toluene. Microwave freq. 9.365984 GHz, mod. amp. 4.000 G, power 2.000 mW. Simulation parameters: g_x = 2.03, g_y = 2.16, g_z = 2.54, A^{Co}_x = 5.0 MHz, A^{Co}_y = 50.0 MHz, A^{Co}_z = 20.0 MHz, Linear A-strain in z direction: –0.018, Quadratic A strain in x direction: –18 and y direction: –2.

Synthesis and characterization of nitrene-complexes

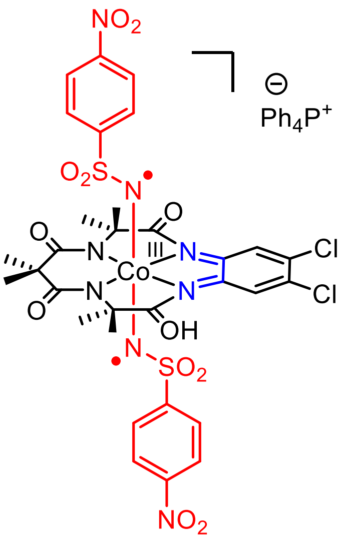

PPh$_4$[Co^{III}(TAML^{q})(NNs)$_2$]

PPh$_4$[Co^{III}(TAML^{red})] (6.6 mg; 8.0 µmol; 1.0 eq) was dissolved in toluene or DCM (2.0 mL) under argon and added to PhINNs (32.3 mg; 80 µmol; 10.0 eq) at r.t. and stirred for 15 minutes. The suspension was filtered over a syringe filter (PTFE 0.45 µm) to afford an olive-green solution of **PPh$_4$[Co^{III}(TAML^{q})(NNs)$_2$]**.

HRMS-ESI$^-$ (*m/z*) calcd for $C_{31}H_{28}Cl_2Co_1N_8O_{12}S_2$: 896.9977, found 896.9965 [M$^-$] (see Figure S8). No mono-nitrene adduct was detected.

Evans's method: CD_2Cl_2 with toluene as internal standard, c = 0.01537 M, δ = 71.28 Hz, μ_{eff} = 2.746 μ_B (S = 1), χ_d = –449.281 emu mol^{-1}.

X-band EPR: silent at r.t. and 20 K in toluene.

^{1}H NMR: silent.

UV-Vis: no characteristic absorption bands in the 400-880 nm region. Very intense absorption in the 300-400 nm region. See also the UV-Vis studies section.

Co-K edge XANES: Sample preparation was performed as described above in an argon filled glovebox to afford 4.0 mL of a toluene solution of **PPh$_4$[Co^{III}(TAML^{q})(NNs)$_2$]** (initial concentration of **PPh$_4$[Co^{III}(TAML^{red})]** was 5.0 mM). The solubility of **PPh$_4$[Co^{III}(TAML^{q})(NNs)$_2$]** in toluene was too low to achieve a concentration of 5.0 mM, which led to reduced data quality. The edge position was determined to be at 7721 eV (Figure S9).

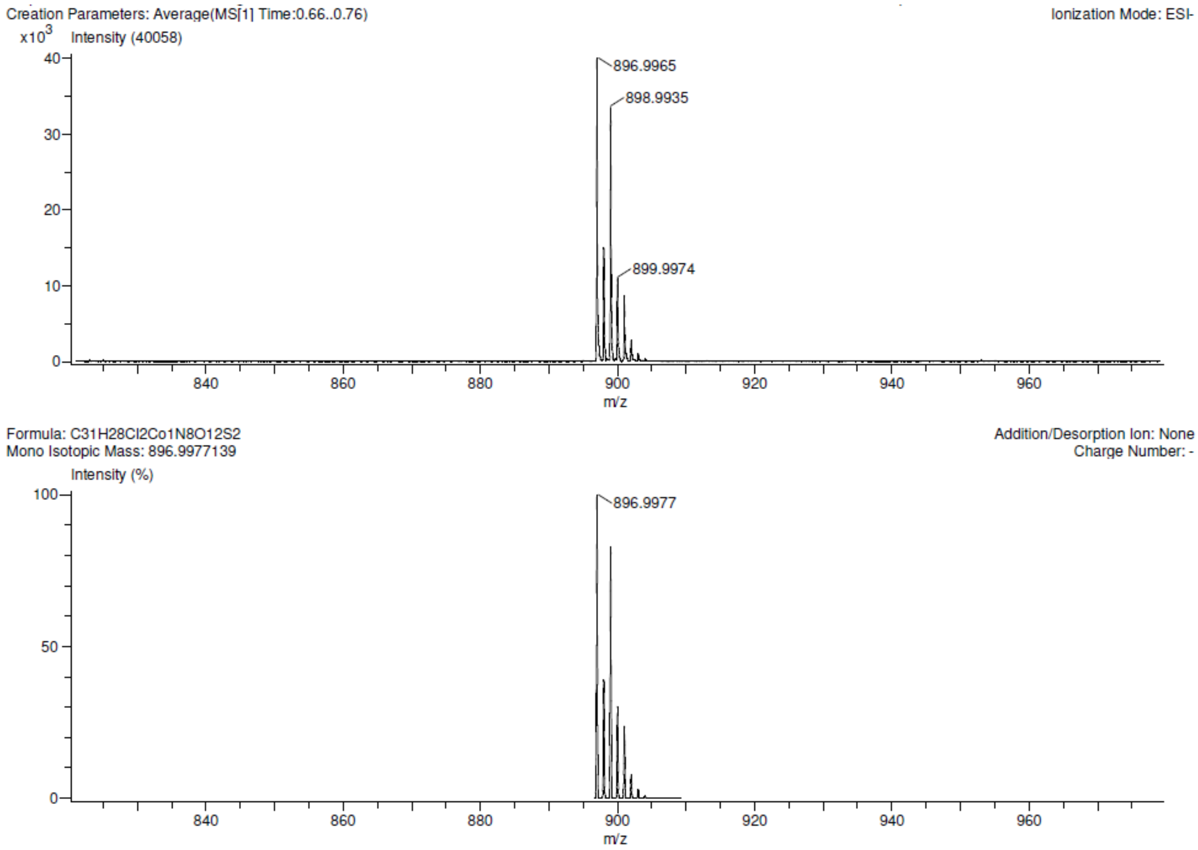

Figure S8. HRMS-ESI$^-$ experimental (top) and simulated (bottom) spectrum of **[Co^{III}(TAML^{q})(NNs)$_2$]$^-$**.

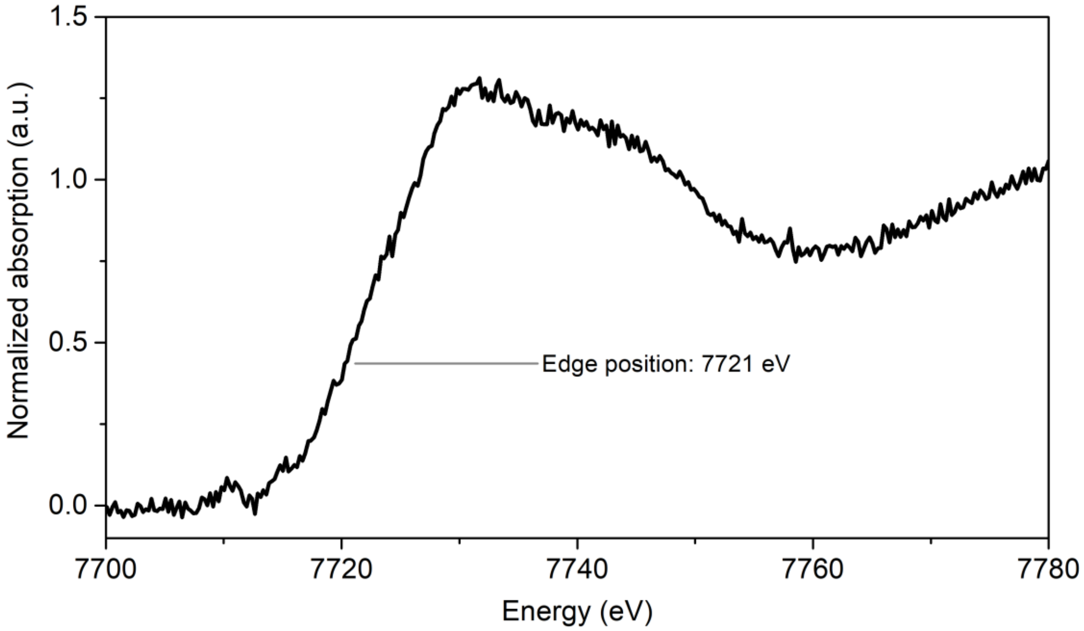

Figure S9. Co-K edge XANES analysis of **PPh$_4$[Co^{III}(TAML^q)(NNs$_2$)]** in toluene.

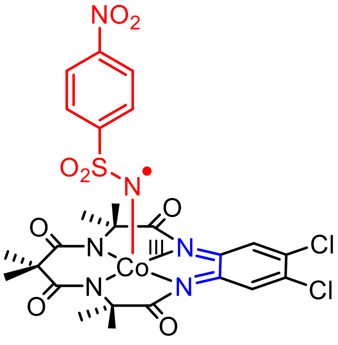

Co^{III}(TAML^q)(NNs)

[Co^{III}(TAML^{sq})] was first generated under argon by reaction of **Li[Co^{III}(TAML^{red})]** (5.23 mg; 10.4 µmol; 1.0 eq) and (Thi)BF$_4$ (3.45 mg; 11.4 µmol; 1.1 eq) in acetonitrile (1.0 mL). The blue solution was stirred for 10 minutes, concentrated *in vacuo* and **[Co^{III}(TAML^{sq})]** was then extracted in toluene or DCM (1.0 mL) to remove unreacted **Li[Co^{III}(TAML^{red})]**, filtered over a syringe filter (PTFE 0.45 µm) and added to PhINNs (40.0 mg; 100.0 µmol; 10 .0 eq) in a nitrogen filled glovebox. The suspension was stirred for 15 min. and filtered over a syringe filter (PTFE 0.45 µm) to afford a turquoise-green solution of **[Co^{III}(TAML^q)(NNs)]**.

HRMS-ESI$^-$ (*m/z*) calcd for $C_{25}H_{24}Cl_2Co_1N_6O_8S_1$: 697.0085, found 697.0045 [M$^-$] (see Figure S10). No bis-nitrene adduct was detected.

Evans's method: toluene-*d*$_8$ with 1,3,5-tris-*tert*-butylbenzene as internal standard, c = 0.01294 M, δ = 10.29 Hz, μ_{eff} = 1.530 μ_B (S = 0.5), χ_d = –349.197 emu mol^{-1}.

^{1}H NMR: silent.

UV-Vis: λ_{max} = 752 nm. See also the UV-Vis studies section.

Co-K edge XANES: Sample preparation was performed as described above in an argon filled glovebox to afford 4.0 mL of a toluene solution of **[Co^{III}(TAML^q)(NNs)]** (5.0 mM). The edge position was determined to be at 7721 eV and a pre-edge feature was observed at 7711 eV (Figure S11).

X-Band EPR: r.t. in toluene: g_{iso} = 2.091, A^{Co}_{iso} = 89.5 MHz and A^{N}_{iso} = 18.9 MHz (Figure S12). 20K in toluene glass slightly rhombic spectrum with multiple hyperfine coupling interactions, of which simulation was not successful (Figure S13).

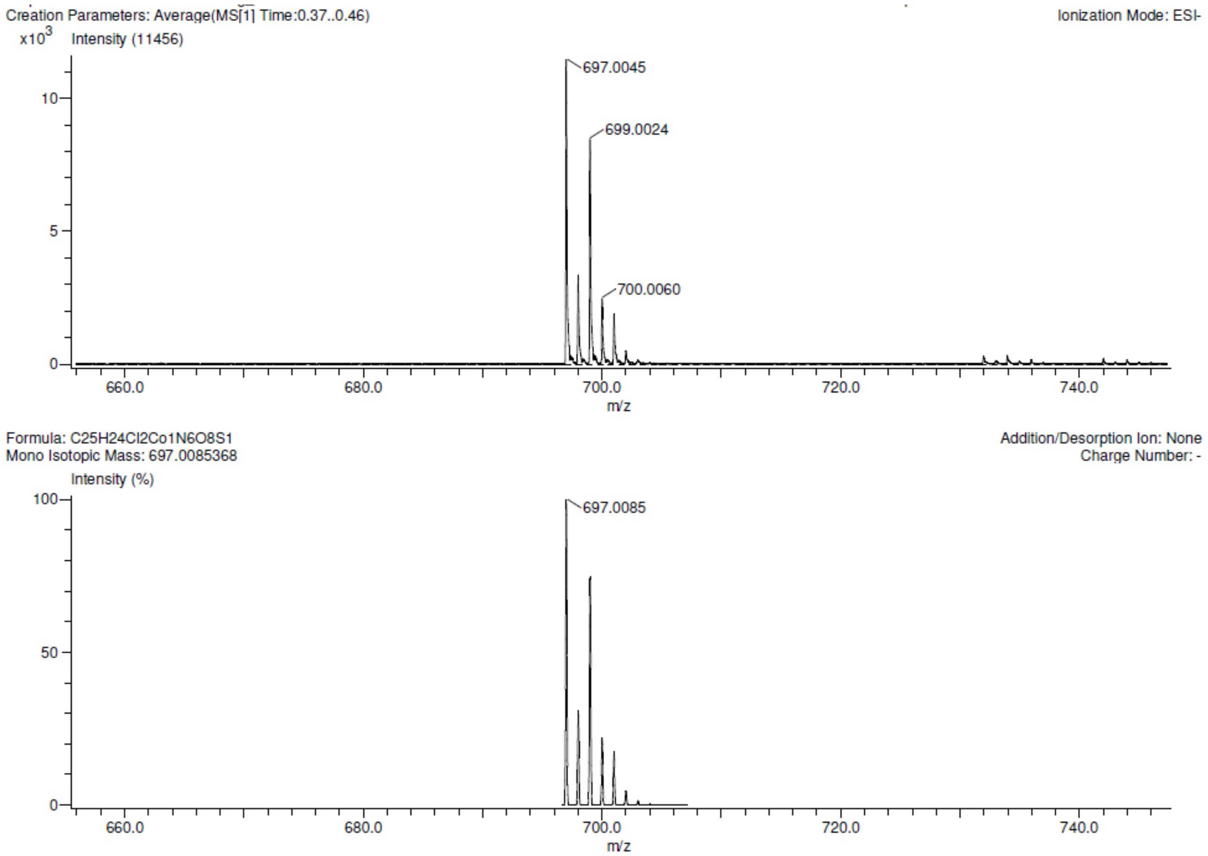

Figure S10. HRMS-ESI^{-} experimental (top) and simulated (bottom) spectrum of **[Co^{III}(TAML^{q})(NNs)]**.

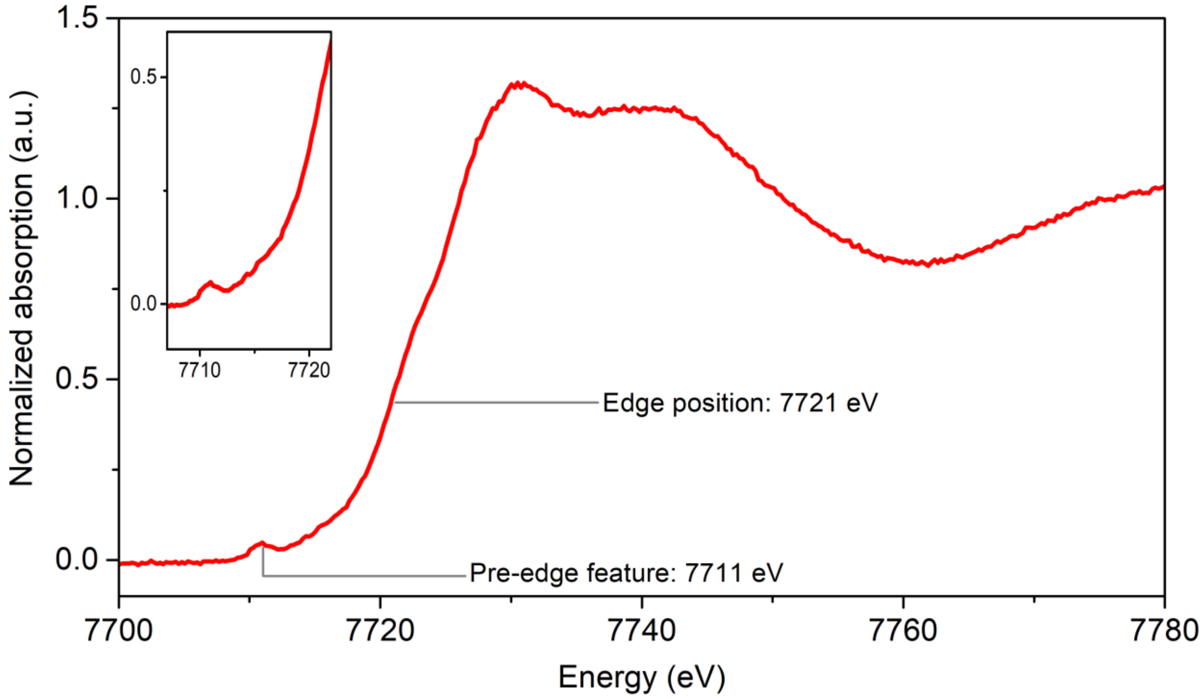

Figure S11. Co-K edge XANES analysis of **[Co^{III}(TAML^{q})(NNs)]** in toluene with an insert showing the pre-edge feature.

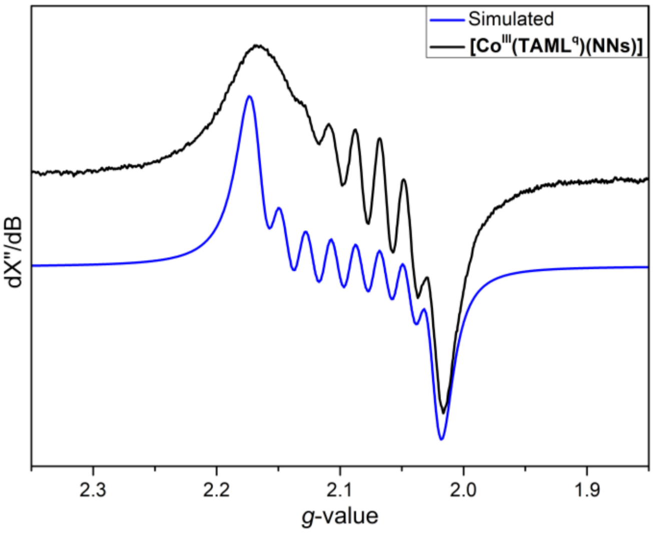

Figure S12. Experimental (black) and simulated (blue) X-Band EPR spectrum of **[Co^{III}(TAML^{q})(NNs)]** at r.t. in toluene. Microwave freq. 9.371643 GHz, mod. amp. 2.000 G, power 6.325 mW. Simulated parameters: g_{iso} = 2.091, A^{Co}_{iso} = 89.5 MHz and A^{N}_{iso} = 18.9 MHz.

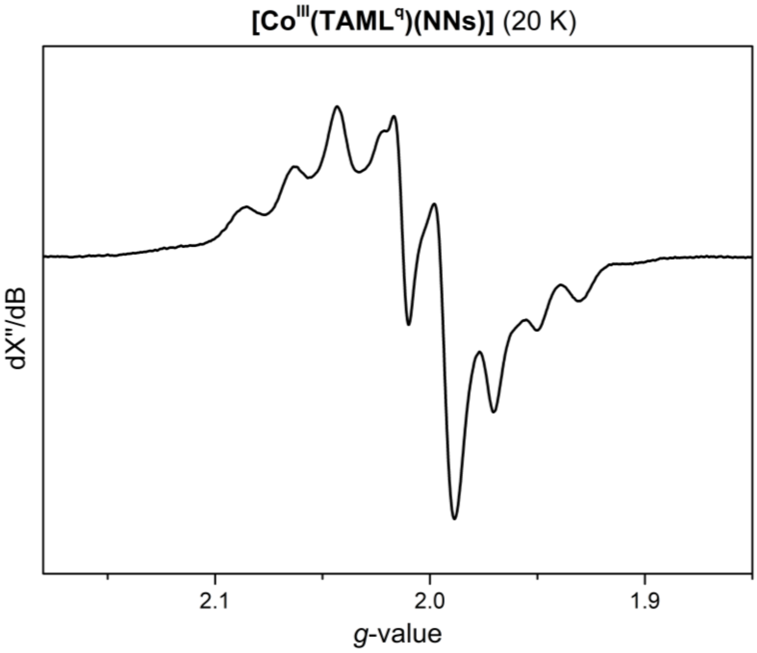

Figure S13. X-Band EPR spectrum of **[Co^{III}(TAML^{q})(NNs)]** in toluene-glass at 20 K. Microwave freq. 9.37624 GHz, mod. amp. 2.000 G, power 6.325 mW.

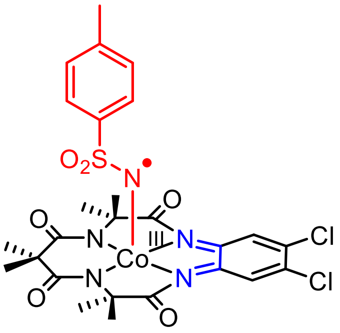

Co^{III}(TAML^{q})(NTs)

[Co^{III}(TAML^{q})(NTs)] was prepared in a similar manner as **[Co^{III}(TAML^{q})(NNs)]**, but PhINTs was used as the nitrene precursor and benzene was used as the solvent to afford a green solution of **[Co^{III}(TAML^{q})(NTs)]**.

HRMS-CSI$^-$ (*m/z*) calcd for $C_{26}H_{27}Cl_2Co_1N_5O_6S_1$: 666.03911, found 666.03952 [M$^-$], 511.01921 [M-$SO_2C_6H_4CH_3$$^-$].

X-band EPR: r.t. in benzene shows an identical eight-line pattern around g_{iso} = 2.091 as was observed for **[Co^{III}(TAML^{q})(NNs)]** (Figure S12). See Figure S15.

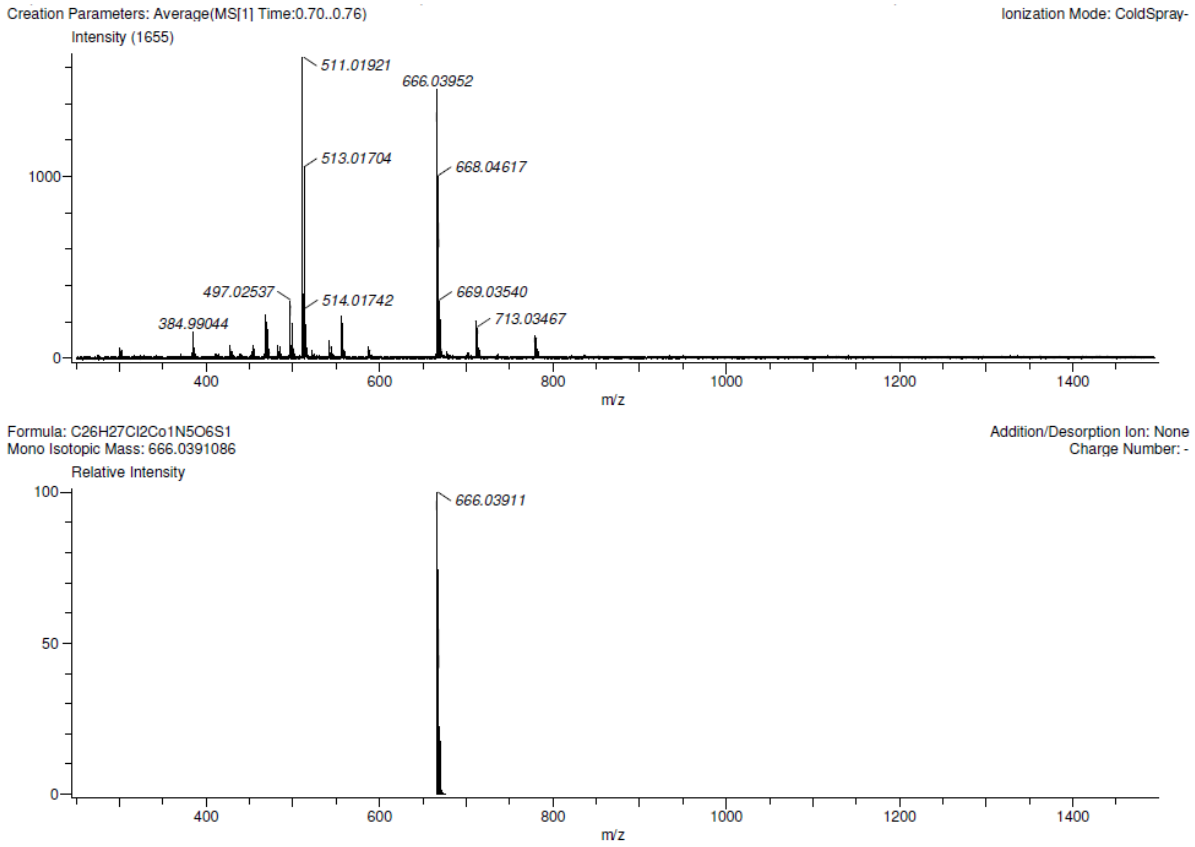

Figure S14. HRMS-CSI⁻ experimental (top) and simulated (bottom) spectrum of **[Co^{III}(TAML^q)(NTs)]**.

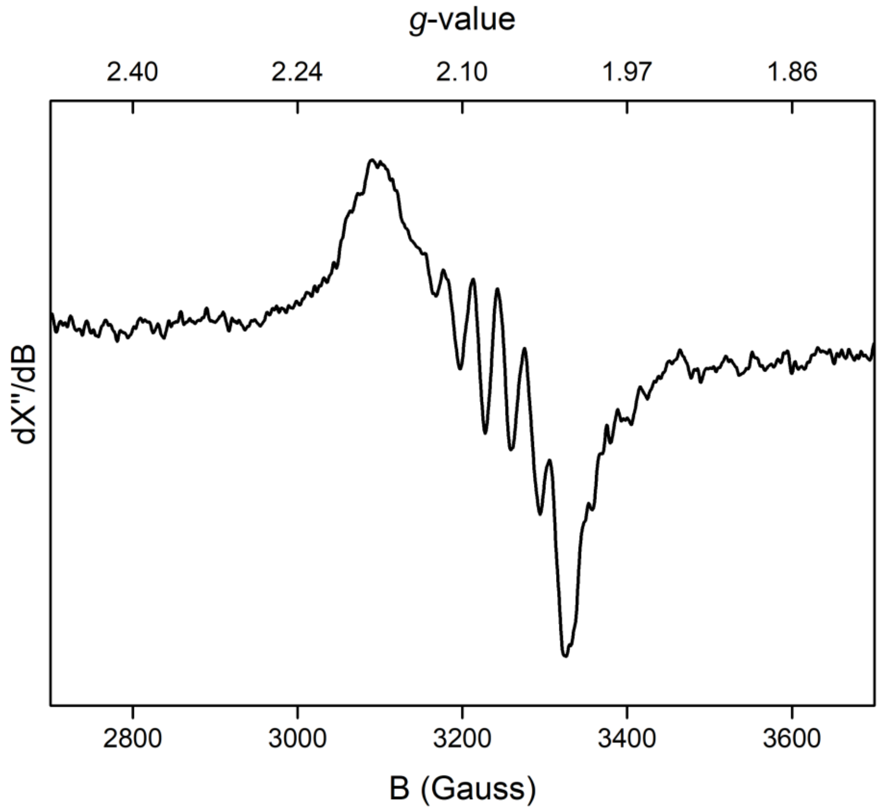

Figure S15. X-Band EPR spectrum of **[Co^{III}(TAML^q)(NTs)]** at r.t. in benzene. Microwave freq. 9.392329 GHz, mod. amp. 6.001 G, power 0.6325 mW.

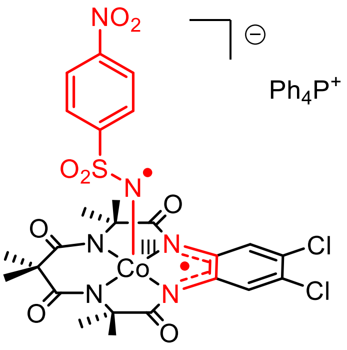

PPh$_4$[Co^{III}(TAML^{sq})(NNs)]

PPh$_4$[Co^{III}(TAML^{red})] (1.34 mg; 1.6 µmol; 1.0 eq) was dissolved in DCM (2.0 mL) under argon and added to PhINNs (0.65 mg; 1.6 µmol; 1.0 eq) at r.t. and stirred for 15 minutes. The suspension was filtered over a syringe filter (PTFE 0.45 µm) to afford a purple solution which contained mainly starting material and **PPh$_4$[Co^{III}(TAML^{q})(NNs)]** according to HRMS-ESI$^-$. HRMS-ESI$^-$ (*m/z*) calcd for $C_{25}H_{24}Cl_2Co_1N_6O_8S_1$: 697.0085, found 697.0075 [M$^-$], 497.1094 [Starting material$^-$] (see Figure S16).

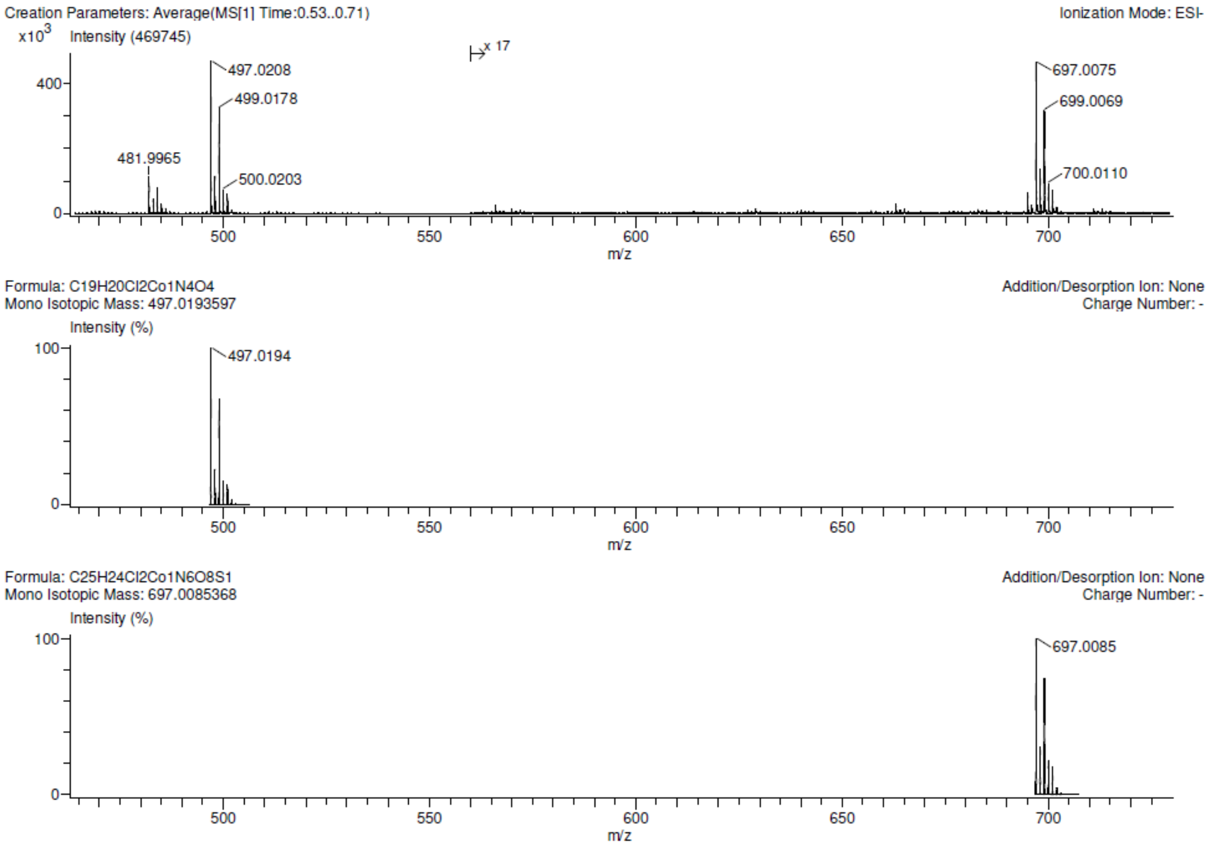

Figure S16. HRMS-CSI$^-$ experimental (top) and simulated spectrum of **[Co^{III}(TAML^{sq})(NNs)]**$^-$ (bottom) and starting material (middle).

(Spectro)electrochemistry

Cyclic voltammetry on **PPh$_4$[Co^{III}(TAML^{red})]** (1.0 mM in DCM) with [NBu$_4$]PF$_6$ (100 Mm) as supporting electrolyte and a glassy carbon working electrode, Pt auxiliary electrode and leak-free Ag/AgCl (3.5 M KCl) afforded three fully reversible redox couples at multiple scan rates (10-200 mV s^{1}) (see Figure S17). The redox potentials were found at –1.18 V, +0.53 V and +1.13 V versus Fc$^{+/0}$, which are assigned to **[Co$^{III/II}$(TAML^{red})]$^{2–/1–}$**, **[Co^{III}(TAML$^{sq/red}$)]$^{–/0}$** and **[Co^{III}(TAML$^{q/sq}$)]$^{+/0}$** couples, respectively, based on the combined experimental (magnetic moment, XANES, EPR) and theoretical (CASSCF) data.

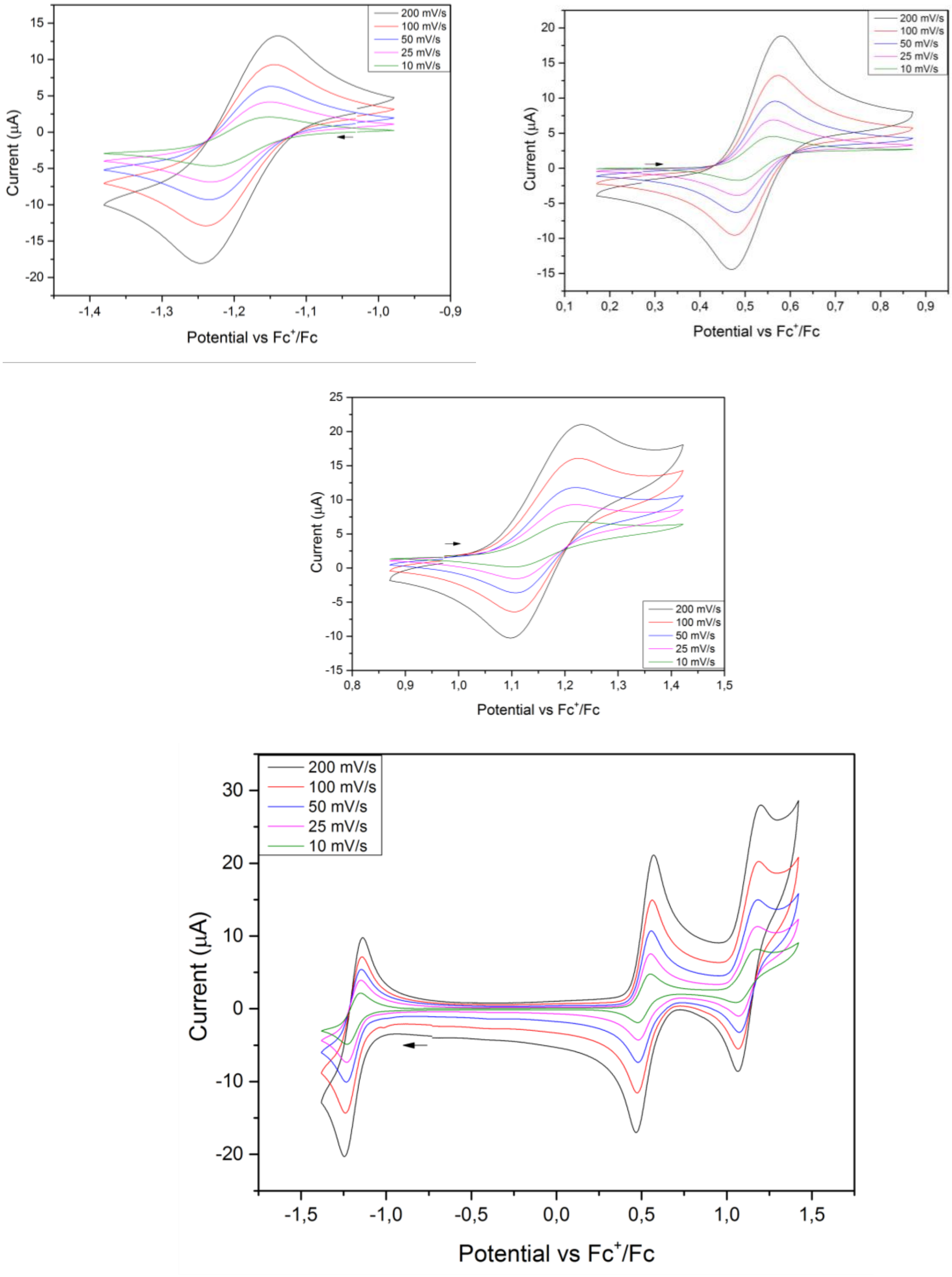

Figure S17. Reversible reduction (top left, –1.18 V vs Fc$^{+/0}$), first oxidation (top right, +0.53 V vs Fc$^{+/0}$) and second oxidation (+1.13 V vs Fc$^{+/0}$) of **PPh$_4$[Co^{III}(TAML^{red})]** at multiple scan rates. Bottom: all three redox events combined at multiple scan rates.

Spectroelectrochemical monitoring in the UV-Vis region of the first oxidation event (+0.53 V vs $Fc^{+/0}$) in a standard OTTLE cell with a Pt working and auxiliary electrode and Ag reference electrode was performed on a 1.0 mM solution of **PPh_4[Co^{III}(TAML^{red})]** in CH_2Cl_2 with $[NBu_4]PF_6$ (100 Mm) as supporting electrolyte (Figure S18). Disappearance of the absorption band at 510 nm (**PPh_4[Co^{III}(TAML^{red})]**) is concomitant with appearance of a band at 623 nm (which is characteristic for **[Co^{III}(TAML^{sq}]**, see CASSCF section for more details)[25]). An isosbestic point is observed at 545 nm, thus indicating clean stoichiometric conversion of **PPh_4[Co^{III}(TAML^{red})]** to **[Co^{III}(TAML^{sq})]**.

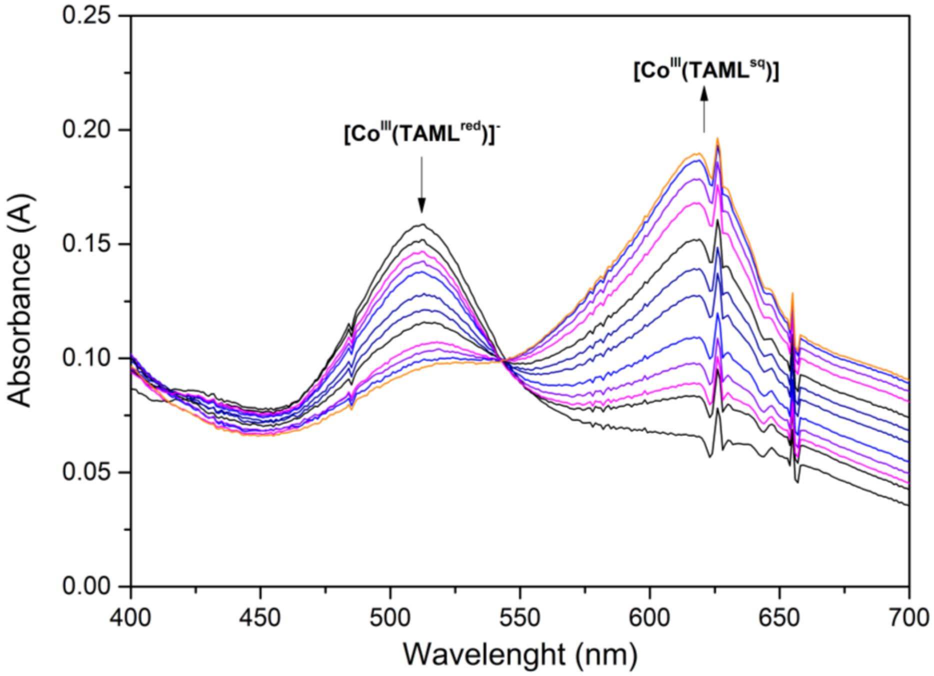

Figure S18. Spectro-electrochemical monitoring of the first oxidation event for **PPh_4[Co^{III}(TAML^{red})]**.

UV-Vis studies

Stepwise oxidation of **PPh$_4$[Co^{III}(TAML^{red})]** with (Thi)BF$_4$ was performed in CH$_2$Cl$_2$ (0.15 mM) by stepwise addition of increasing amounts (Thi)BF$_4$ in CH$_2$Cl$_2$ and followed by UV-Vis spectroscopy (Figure S19). The total concentration of cobalt complex was kept at 0.15 mM. The disappearance of **PPh$_4$[Co^{III}(TAML^{red})]** (λ_{max} = 510 nm) goes concomitant with formation of **[Co^{III}(TAML^{sq})]** (λ_{max} = 623 nm). After 1.0 eq (Thi)BF$_4$ the absorption of **PPh$_4$[Co^{III}(TAML^{red})]** has almost completely vanished, and is not present anymore after 1.25 eq (Thi)BF$_4$. The isosbestic points at 338 and 545 nm indicate clean stoichiometric conversion of **PPh$_4$[Co^{III}(TAML^{red})]** to **[Co^{III}(TAML^{sq})]**.

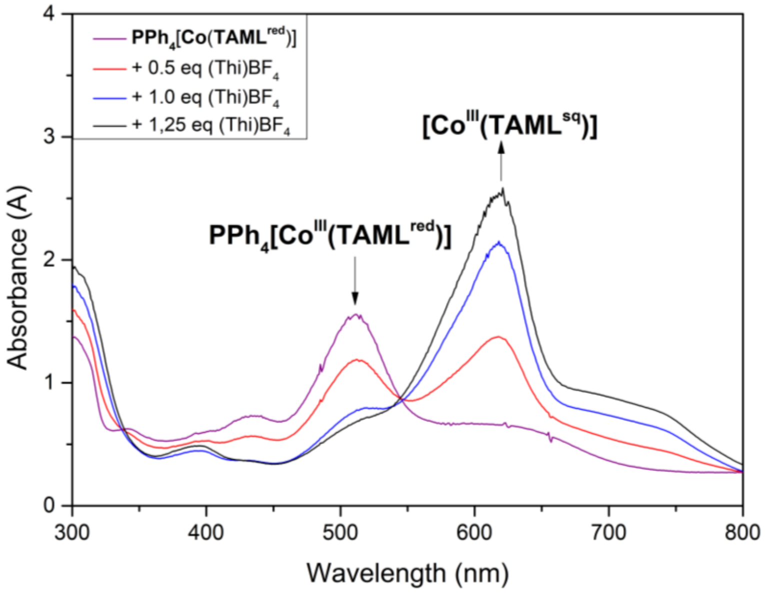

Figure S19. UV-Vis titration of **PPh$_4$[Co(TAML^{red})]** in DCM (0.15 mM) with increasing amounts [Thi]BF$_4$, measured in a 1.0 cm quartz cuvette.

Addition of 10 equivalents PhINNs to a 150 µM solution of **PPh$_4$[Co^{III}(TAML^{red})]** in DCM afforded an olive-green solution of **PPh$_4$[Co^{III}(TAML^{q})(NNs)$_2$]**, which was transferred to a 1.0 cm quartz cuvette under nitrogen and the UV-Vis spectrum was measured (Figure S20). No characteristic bands were observed between 400 and 880 nm, but a very intense absorption was observed in the 300-400 nm region. No absorption band of **PPh$_4$[Co^{III}(TAML^{red})]** was observed anymore, thus indicating complete conversion of the starting material.

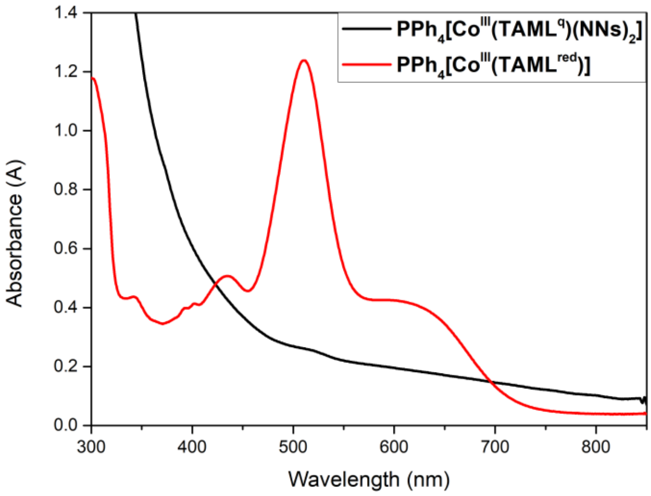

Figure S20. UV-Vis spectrum of the formation of **PPh$_4$[Co^{III}(TAML^{q})(NNs)$_2$]** (black) from **PPh$_4$[Co^{III}(TAML^{red})]** (150 µM in DCM, red) by addition of 10 equivalents PhINNs.

Addition of 10 equivalents PhINNs to a 78 µM solution of **[Co^{III}(TAML^{sq})]** in CH_2Cl_2 afforded a turquoise-green solution of **[Co^{III}(TAML^{q})(NNs)]**, which was transferred to a 1.0 cm quartz cuvette under nitrogen and the UV-Vis spectrum was measured (Figure S21). A band at λ_{max} = 752 nm was observed, in combination with an intense absorption 300-400 nm region. No absorption band of **Co^{III}(TAML^{sq})** was observed anymore, thus indicating complete conversion of the starting material.

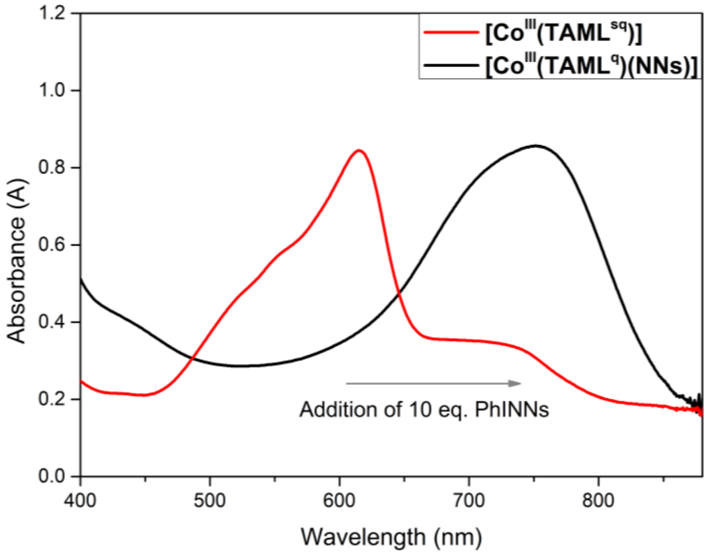

Figure S21. UV-Vis spectrum of the formation of **[Co^{III}(TAML^{q})(NNs)]** (black) from **PPh$_4$[Co^{III}(TAML^{red})]** (78 µM in DCM, red) by addition of 10 equivalents PhINNs.

Catalytic aziridination

*Procedure for the aziridination with **$PPh_4[Co^{III}(TAML^{red})]$***

An oven-dried reaction tube was charged with PhINNs (96.0 µmol, 1.0 eq.) and brought under argon, followed by addition of DCM (1.0 mL). Styrene was filtered over basic alumina prior to use and sparged with argon in a vial and then added (480 µmol, 5.0 eq) in the tube under argon flow. A solution of **$PPh_4[Co^{III}(TAML^{red})]$** (2.4 µmol, 2.5 mol%) in CH_2Cl_2 (2.0 mL) and 1.0 mL extra CH_2Cl_2 were then added. The reaction mixture was stirred at 35 °C for 2 hours and cooled to r.t. 1,3,5-trimethoxybenzene was added as an internal standard, the mixture was concentrated under reduced pressure and analyzed by ^1H NMR. Yield: 64%.

*Standard procedure for the aziridination with **$[Co^{III}(TAML^{sq})]$***

An oven-dried reaction tube was charged with PhINNs (96.0 µmol, 1.0 eq.) and brought under argon, followed by addition of CH_2Cl_2 (1.0 mL). Styrene was filtered over basic alumina prior to use and sparged with argon in a vial and then added (480 µmol, 5.0 eq) in the tube under argon flow. A solution of **$[Co^{III}(TAML^{sq})]$** (2.4 µmol, 2.5 mol%) (prepared according to *method 2*) in CH_2Cl_2 (2.0 mL) and 1.0 mL extra CH_2Cl_2 were then added. The reaction mixture was stirred at 35 °C for 2 hours and cooled to r.t. 1,3,5-trimethoxybenzene was added as an internal standard, the mixture was concentrated under reduced pressure and analyzed by ^1H NMR. Yield: 35%.

Characterization of **1** from the aziridination reaction was performed by ^1H NMR, and is reported in Figure S22.

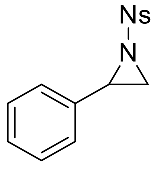

1

1 was prepared from styrene and PhINNs according to the aziridination method described for **$PPh_4[Co^{III}(TAML^{red})]$** or **$Co^{III}(TAML^{sq})$** as the catalyst, and its spectral data are in accordance with literature.[27] A crude ^1H NMR spectrum for the formation of **1** is depicted in Figure S22. The resonance for trimethoxybenzene at δ = 6.08 and the characteristic signal for the aziridine between δ = 2.5 and 4.0 ppm were used to calculate the yield

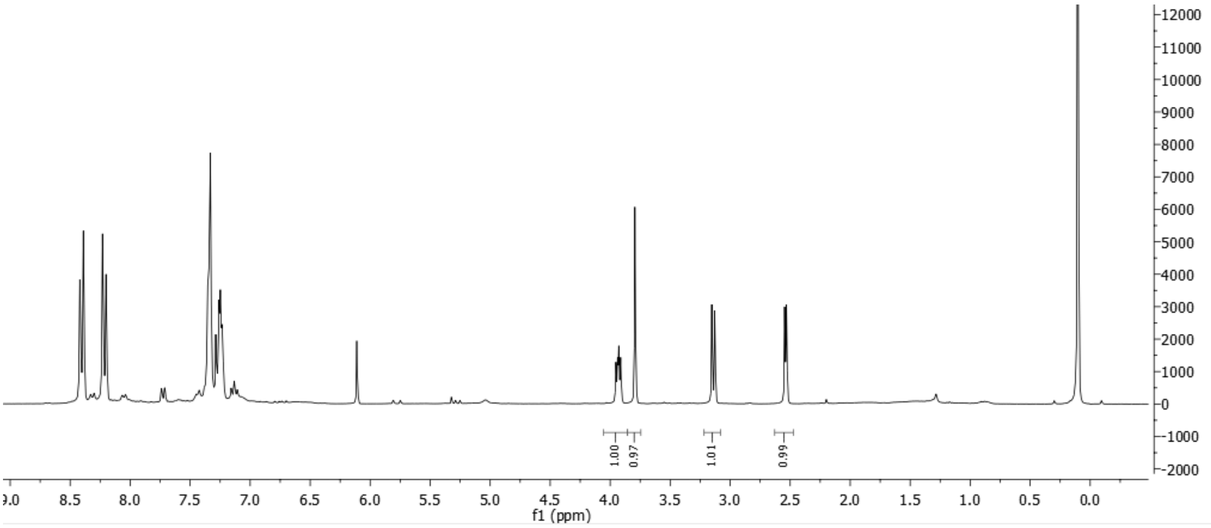

Figure S22. Crude ^1H NMR spectrum of **1** in $CDCl_3$ wherein **$PPh_4[Co^{III}(TAML^{red})]$** was used as the catalyst. 6.6 µmol 1,3,5-trimethoxybenzene was added as internal standard.

Density Functional Theory Calculations

All calculations were performed according to the methods described in the general considerations.

Influence of the functional

The influence of the functional to correctly describe the spin-state of the complexes was investigated first by comparison to the experimentally determined spin-state. We used the BP86, B3LYP, PBE, OPBE or BP86 geometry optimization followed by a B3LYP SCF (BP86//B3LYP) functionals. As evident from Table S1, the overall performance of the BP86 functional is best for predicting the (net) spin state of Co(TAML)-type complexes and was therefore used for all further DFT calculations.

Table S1. Comparison between the calculated most stable spin state and the experimental spin-state for different functionals.

Entry	Functional	Compound	Relative energies of spin states (kcal mol^{-1}) and ($\langle s^2 \rangle$)	Experimental spin state	Accordance DFT and experiment
1	BP86	**[Co^{III}(TAML^{sq})]**	Doublet = 0 (0.9656) Quartet = +6.9 (3.7641)	Doublet	Yes
2		**[Co^{III}(TAML^{q})(NNs$_2$)]$^-$**	CSS = no convergence OSS = +0.3 (1.5491) Triplet = +0.8 (2.501) Quintet = 0 (6.0161) Septet = +21.6 (12.0326)	Triplet	Yes[a]
3		**[Co^{III}(TAML^{q})(NNs)]**	Doublet = 0 (0.8274) Quartet = +6.0 (3.7641)	Doublet	Yes
4	B3LYP	**[Co^{III}(TAML^{sq})]**	Doublet = 0 (1.5347) Quartet = +5.1 (3.7782)	Doublet	Yes
5		**[Co^{III}(TAML^{q})(NNs)]**	Doublet = 0 (1.3327) Quartet = +0.6 (3.8695)	Doublet	
6	BP86//B3LYP	**[Co^{III}(TAML^{q})(NNs$_2$)]$^-$**	CSS = no convergence OSS = - (1.707) Triplet = no convergence Quintet = 0 (6.0286) Septet = +14.1 (12.0565)	Triplet	No
7	PBE	**[Co^{III}(TAML^{sq})]**	Doublet = 0 (0.9511) Quartet = +6.8 (3.7637)	Doublet	Yes
8		**[Co^{III}(TAML^{q})(NNs$_2$)]$^-$**	CSS = no convergence OSS = no convergence Triplet = +0.4 (2.4915) Quintet = 0 (6.0157)	Triplet	No
9		**[Co^{III}(TAML^{q})(NNs)]**	Doublet = 0 (0.8201) Quartet = +6.2 (3.7643)	Doublet	Yes
10	OPBE	**[Co^{III}(TAML^{sq})]**	Doublet = +0.7 (1.0239) Quartet = 0 (3.7692)	Doublet	No

All calculations were performed with TURBOMOLE at the functional/def2-TZVP/disp3/m4 level of theory. [a] A 1 : 1 : 1 mixture of the OSS, triplet and quintet is undistinguishable from a 100% triplet ground state by Evans' method.

*Bond metrics and spin densities for **[Co^{III}(TAML^{red})]$^-$**, **[Co^{III}(TAML^{sq})]** and **[Co^{III}(TAML^{sq})(MeCN)]***

As can be seen in Table S2, the bond metrics for the DFT (BP86/def2-TZVP/disp3) optimized geometry are in close agreement with the experimentally (XRD) observed bond lengths for **[Co^{III}(TAML^{red})]$^-$**, and the calculated spin density is solely localized on cobalt. Moreover, one-electron oxidation to afford **[Co^{III}(TAML^{sq})]** results in alternating bond (C1 until C6) elongation or shortening compared to **[Co^{III}(TAML^{red})]$^-$**, according to DFT calculations (Table S3). Moreover, the calculated α spin density is mostly localized on cobalt, whereas β spin density is observed on the ligand. This indicated loss of aromaticity and therefore ligand-centered oxidation. Moreover, all Co–N and C–N bonds are shortened, which also indicates stronger C–N bonds and therefore ligand-centered oxidation. Similar ligand bond metrics are observed for **[Co^{III}(TAML^{sq})(MeCN)]** (Table S4), thus indicating that the TAML scaffold is also one-electron oxidized. The calculated spin density displays only α spin density (contrary to **[Co^{III}(TAML^{sq})]**), which we attribute to the formation of a formally low spin cobalt(III) center and one ligand-centered unpaired electron, which is partially delocalized on cobalt.

Table S2. Bond metrics for the XRD and DFT (BP86/def2-TZVP/disp3) optimized structure of **[Co^{III}(TAML^{red})]$^{-}$** and spin density plot (isosurface 0.005, yellow: spin up, purple: spin down).

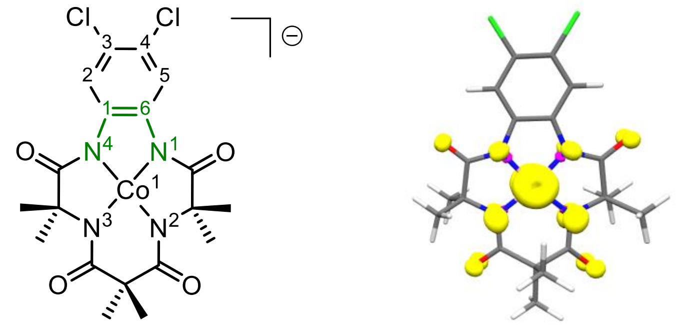

Bond	DFT (Å)	XRD (Å)
Co1-N1	1.841	1.8244(15)
Co1-N2	1.839	1.8273(15)
Co1-N3	1.839	1.8337(15)
Co1-N4	1.841	1.8267(15)
N1-C6	1.398	1.410(2)
N4-C1	1.399	1.407(2)
C1-C2	1.399	1.390(2)
C2-C3	1.399	1.397(3)
C3-C4	1.403	1.390(3)
C4-C5	1.399	1.391(3)
C5-C6	1.398	1.386(3)
C6-C1	1.427	1.410(2)

Table S3. Bond metrics for the DFT (BP86/def2-TZVP/disp3) optimized structure of **[Co^{III}(TAML^{sq})]** and spin density plot (isosurface 0.005, yellow: spin up, purple: spin down).

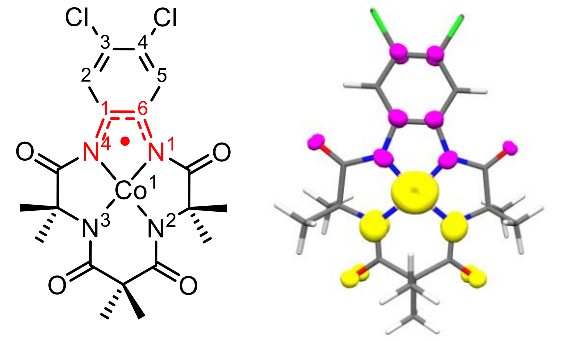

Bond	DFT
Co1-N1	1.832
Co1-N2	1.817
Co1-N3	1.820
Co1-N4	1.832
N1-C6	1.373
N4-C1	1.373
C1-C2	1.405
C2-C3	1.388
C3-C4	1.430

C4-C5	1.388
C5-C6	1.406
C6-C1	1.444

Table S4. Bond metrics for the DFT (BP86/def2-TZVP/disp3) optimized structure of **[Co^{III}(TAML^{sq})(MeCN)]** and spin density plot (isosurface 0.002, yellow: spin up).

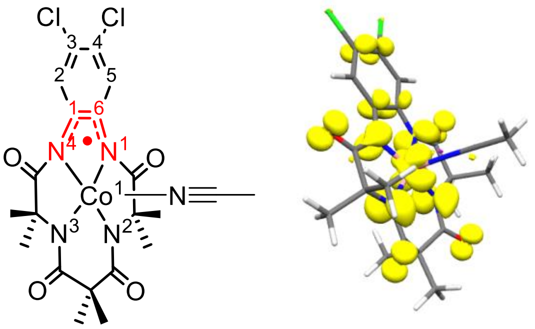

Bond	DFT
Co1-N1	1.860
Co1-N2	1.872
Co1-N3	1.872
Co1-N4	1.861
N1-C6	1.374
N4-C1	1.375
C1-C2	1.407
C2-C3	1.389
C3-C4	1.424
C4-C5	1.388
C5-C6	1.407
C6-C1	1.441

Calculated EPR parameters

The EPR parameters (Table S5) were calculated using ORCA (B3LYP/def2-TZVP) with geometries optimized in TURBOMOLE (BP86/def2-TZVP). The correlation between experiment and DFT is good in the case of **[Co^{III}(TAML^{sq})(MeCN)]**, but poor for **[Co^{III}(TAML^{sq})]**. We attribute the large difference in calculated and experimental hyperfine coupling constants (*A*) of **[Co^{III}(TAML^{sq})]** to the erroneous description of multireference systems with DFT. As can be seen in the spin density plot for **[Co^{III}(TAML^{sq})(MeCN)]** (Table S4), the electronic structure does not have multireference character and is therefore accurately described by DFT.

Table S5. Calculated (ORCA, B3LYP/def2-TZVP) and simulated EPR parameters for **[Co^{III}(TAML^{sq})]** and **[Co^{III}(TAML^{red})(MeCN)]**.

Compound	*g*-values (DFT)	*A* values (DFT)	*g*-values (simulated)	*A* values (simulated)
[Co^{III}(TAML^{sq})]	$g_x = 2.04$	$A^{Co}{}_x = 166.3$	$g_x = 2.03$	$A^{Co}{}_x = 5.0$ MHz
	$g_y = 2.25$	$A^{Co}{}_z = 199.8$	$g_y = 2.16$	$A^{Co}{}_y = 50.0$ MHz
	$g_z = 2.26$	$A^{Co}{}_z = 641.3$	$g_z = 2.54$	$A^{Co}{}_z = 20.0$ MHz
[Co^{III}(TAML^{sq})(MeCN)]	$g_{iso} = 2.00$	$A^{Co}{}_{iso} = 34.2$ MHz	$g_{iso} = 2.00$	$A^{Co}{}_{iso} = 36.0$ MHz

Energies of formation for nitrene adducts

As can be seen in

Table S6, formation of a mono- (**[Co^{III}(TAML^{sq})(NNs)]$^{-}$**) or bis-nitrene (**[Co^{III}(TAML^{q})(NNs)$_2$]$^{-}$**) adduct of **[Co^{III}(TAML^{red})]$^{-}$** is almost equally exergonic, whereas formation of the mono-nitrene species (**[Co^{III}(TAML^{q})(NNs)]**) from **[Co^{III}(TAML^{sq})]** is favored by 5.8 kcal mol^{-1} compared to formation of the bis-nitrene (**[Co(TAML^{q})(NNs)$_2$]**).

Table S6. ΔG^{o}_{298K} for the formation of neutral and anionic mono- and bis-nitrene adducts.

Compound	**ΔG^{o}_{298K} (kcal mol^{-1})**
$[Co^{III}(TAML^{red})]^{-}$	= 0
$[Co^{III}(TAML^{sq})(NNs)]^{-}$	–27.9
$[Co^{III}(TAML^{q})(NNs)_{2}]^{-}$	–29.9
$[Co^{III}(TAML^{sq})]$	= 0
$[Co^{III}(TAML^{q})(NNs)]$	–20.3
$[Co(TAML^{q})(NNs)_{2}]$	–14.5

Absolute energies for all DFT optimized structures with the BP86 functional

The relevant $<s^2>$, ΔH^{o}_{298K}, ΔS^{o}_{298K} and ΔG^{o}_{298K} (in Hartree) for all relevant compounds is depicted in Table S7.

Table S7. Calculated $<s^2>$ and energies for all relevant compounds.

Compound + spin state	**Spin state**	**$<s^2>$**	**SCF** (Hartree)	**ZPE correction** (Hartree)	**Enthaply correction** (Hartree)	**Entropy correction** (Hartree)	**ΔG^{o}_{298K}** (Hartree)
$[Co^{III}(TAML^{red})]^{-}$	Triplet	2.0112	-3560.45169	0.36334	0.39355	0.30505	-3560.14664
$[Co^{III}(TAML^{sq})]$	Doublet	0.9656	-3560.30626	0.36357	0.39390	0.30453	-3560.00172
	Quartet	3.7641	-3560.29462	0.36274	0.39320	0.30388	-3559.99074
$[Co^{III}(TAML^{sq})(MeCN)]$	Doublet	0.7568	-3693.12693	0.40858	0.44386	0.34262	-3692.78430
$[Co^{III}(TAML^{q})(NNs)]$	Doublet	0.8274	-4600.19427	0.46717	0.50998	0.39150	-4599.80276
	Quartet	3.7641	-4600.18309	0.46647	0.50953	0.38987	-4599.79322
$[Co^{III}(TAML^{q})(NNs)]$ nitrene on other side	Doublet	0.7762	-4600.19171	0.46700	0.50989	0.39017	-4599.80154
	Quartet	3.7630	-4600.18763	0.46686	0.50977	0.39053	-4599.79710
	Sextet	8.7768	-4600.15425	0.46441	0.50811	0.38584	-4599.76842
$[Co(TAML^{q})(NNs)_{2}]$	Doublet	1.8926	-5640.03801	0.56920	0.62496	0.47566	-5639.56234
	Quartet	3.9472	-5640.03947	0.56927	0.62502	0.47523	-5639.56424
$[Co^{III}(TAML^{sq})(NNs)]^{-}$	Triplet	2.0119	-4600.35180	0.46728	0.50993	0.39198	-4599.95981
$[Co^{III}(TAML^{q})(NNs_{2})]^{-}$	CSS			No convergence			
	OSS	1.5491	-5640.20781	0.56904	0.62483	0.47424	-5639.73357
	Corrected OSS [a]	-	-	-	-	-	-5639.73660
	Triplet	2.5010	-5640.20623	0.56876	0.62456	0.47452	-5639.73171
	Quintet	6.0161	-5640.20834	0.56915	0.62484	0.47528	-5639.73306
	Septet	12.0326	-5640.17032	0.56775	0.62422	0.47163	-5639.69869

Calculations were performed at the BP86/def2-TZVP/disp3/m4-grid level of theory. Conversion from Hartree to kcal mol^{-1} can be achieved by multiplication with 627.503. [a] Although the energy for this OSS species is slightly (0.6 kcal mol^{-1}) lower in energy than the triplet at the BP86 level DFT, CASSCF calculations demonstrated that the triplet spin-state is the most stable.

Graphical representations of complexes

All relevant converged geometries (BP86/def2-TZVP/disp3) are depicted below.

[Co^{III}(TAML^{red})]$^{–}$

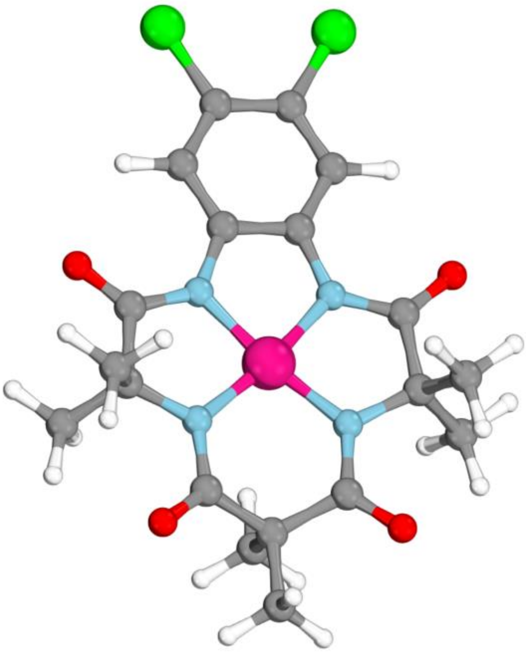

[Co^{III}(TAML^{sq})]

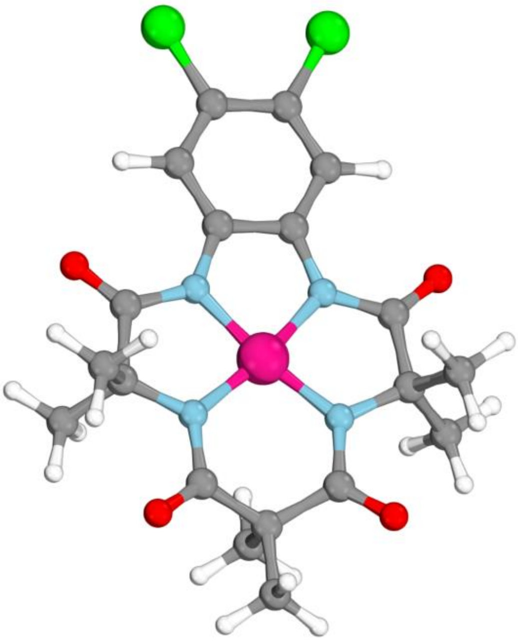

[Co^{III}(TAML^{sq})(MeCN)]

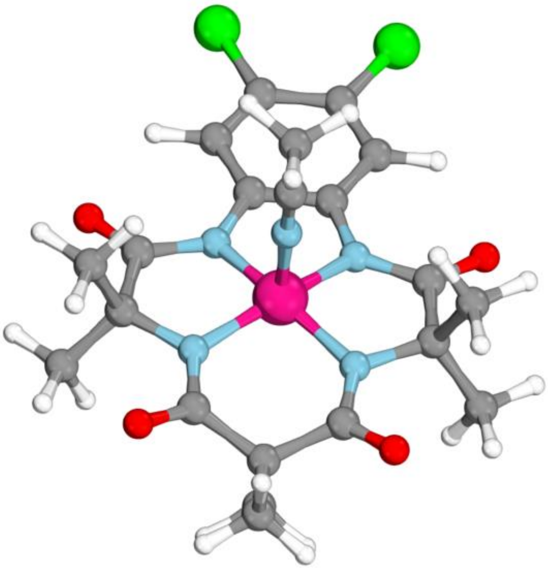

[Co^{III}(TAML^{q})(NNs)]

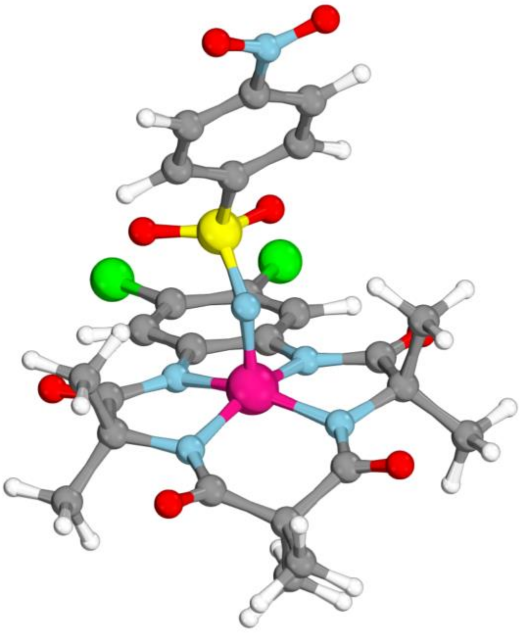

$[\mathrm{Co^{III}(TAML^{q})(NNs)}]$ nitrene on other side

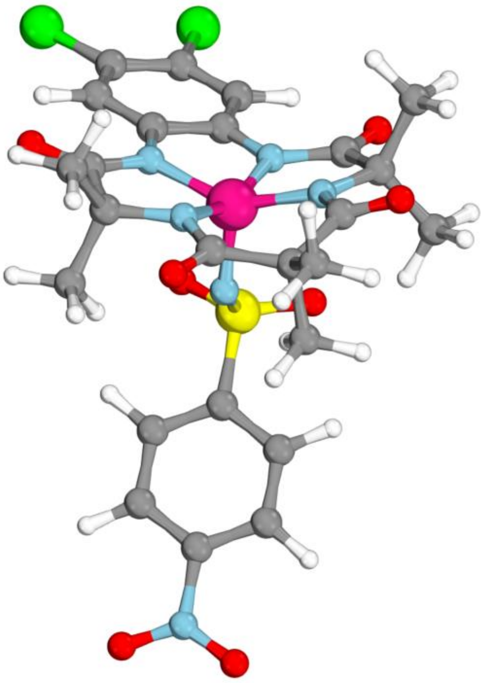

$[\mathrm{Co^{III}(TAML^{sq})(NNs)}]^{-}$

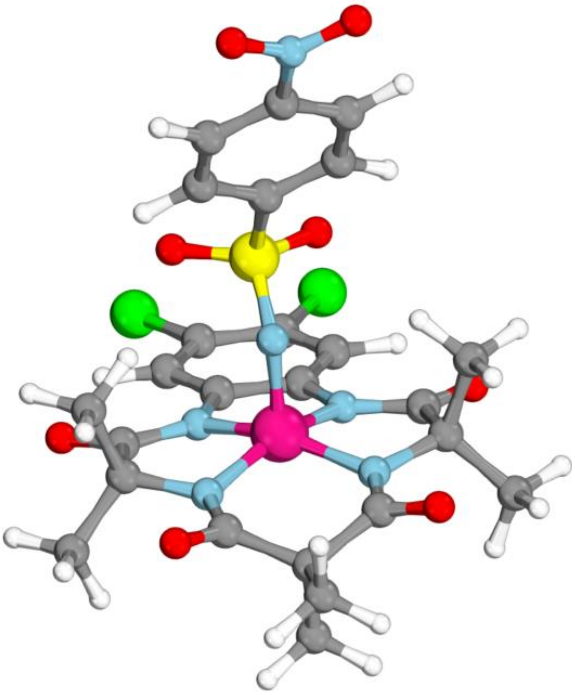

[Co^{III}(TAML^{q})(NNs)$_2$]$^{-}$

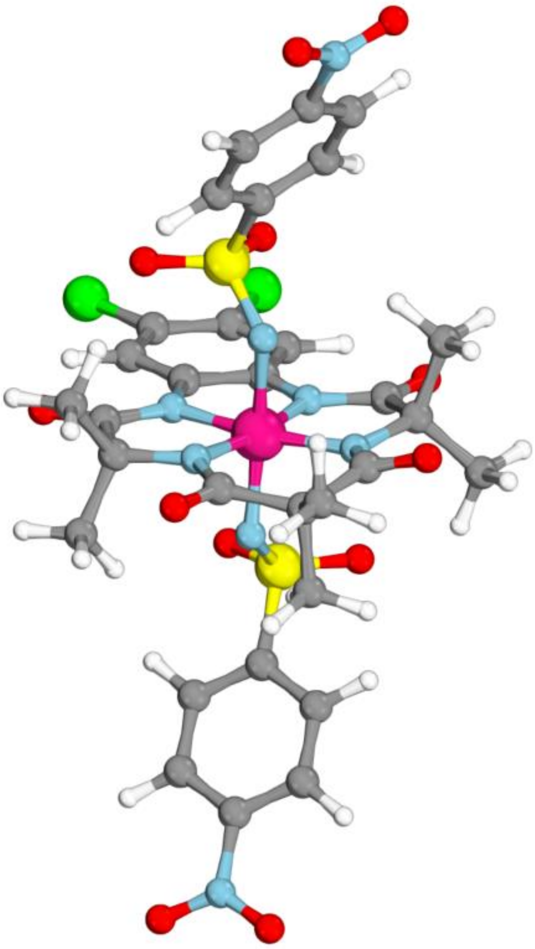

Complete Active Space Self Consistent Field Calculations

All NEVPT2 corrected CASSCF calculations were performed according to the methods described in the general considerations.

$[\mathrm{Co^{III}(TAML^{red})}]^{-}$ NEVPT2-CASSCF(14,13)

The total and relative energies for the singlet, triplet and quintet spin state and their states and contributions for **$[\mathrm{Co^{III}(TAML^{red})}]^{-}$** were obtained from NEVPT2 corrected CASSCF(14,13) calculations and are reported in Table S8. The d_{xy} orbital was not preserved in the active space as this orbital was found to be non-correlated. The triplet spin state is the most stable and has diminishable multi-reference character. A quantitative orbital analysis is shown in Scheme S1. The most relevant active orbitals and an assignment of the electronic structure (from Löwdin population analysis) are shown in Scheme S2.

Table S8. Total and relative energies (NEVPT2 corrected) for multiple spin states and their contributions for the single-root NEVPT2-CASSCF(14,13) calculation on **$[\mathrm{Co^{III}(TAML^{red})}]^{-}$**.

Multiplicity	**Total energy (kcal $\mathrm{mol^{-1}}$)**	**Relative energy (kcal $\mathrm{mol^{-1}}$)**	**Contribution : state**
1 (singlet)	–2230783,076	+29.4	0.33606 : 2222222000000
			0.33220 : 2222220200000
			0.13762 : 2222221100000
			0.01703 : 2122220200100
			0.01699 : 2122222000100
			0.01577 : 2222121200000
			0.01275 : 2222212100000
			0.00688 : 2222022002000
			0.00683 : 2222020202000
			0.00679 : 2211222000011
			0.00672 : 2211220200011
			0.00639 : 2222112011000
			0.00635 : 2222110211000
			0.00609 : 2222122100000
			0.00558 : 2222211200000
			0.00545 : 2222202020000
			0.00540 : 2222200220000
			0.00283 : 2222021102000
			0.00278 : 2211221100011
			0.00265 : 2222111111000
3 (triplet)	–2230812,509	= 0.0	0.88588 : 2222221100000
			0.01742 : 2222201120000
			0.01364 : 2222111111000
			0.01243 : 2211221100110
			0.00963 : 2222021102000
			0.00655 : 2022221100002
			0.00609 : 2211221101100
			0.00457 : 2222021101010
			0.00435 : 2220221100200
			0.00409 : 2202221100200
			0.00316 :2222111110010
5 (quintet)	–2230771,475	+41.0	0.89548 : 2222211110000
			0.01218 : 2221111111100
			0.00996 : 2222011112000
			0.00935 : 2220211110200
			0.00646 : 2112211110011
			0.00397 : 2202211110020
			0.00358 : 2112211111010
			0.00345 : 2022211110002
			0.00339 : 2220211110110
			0.00330 : 2112211110101

0.00327 : 2222011111001

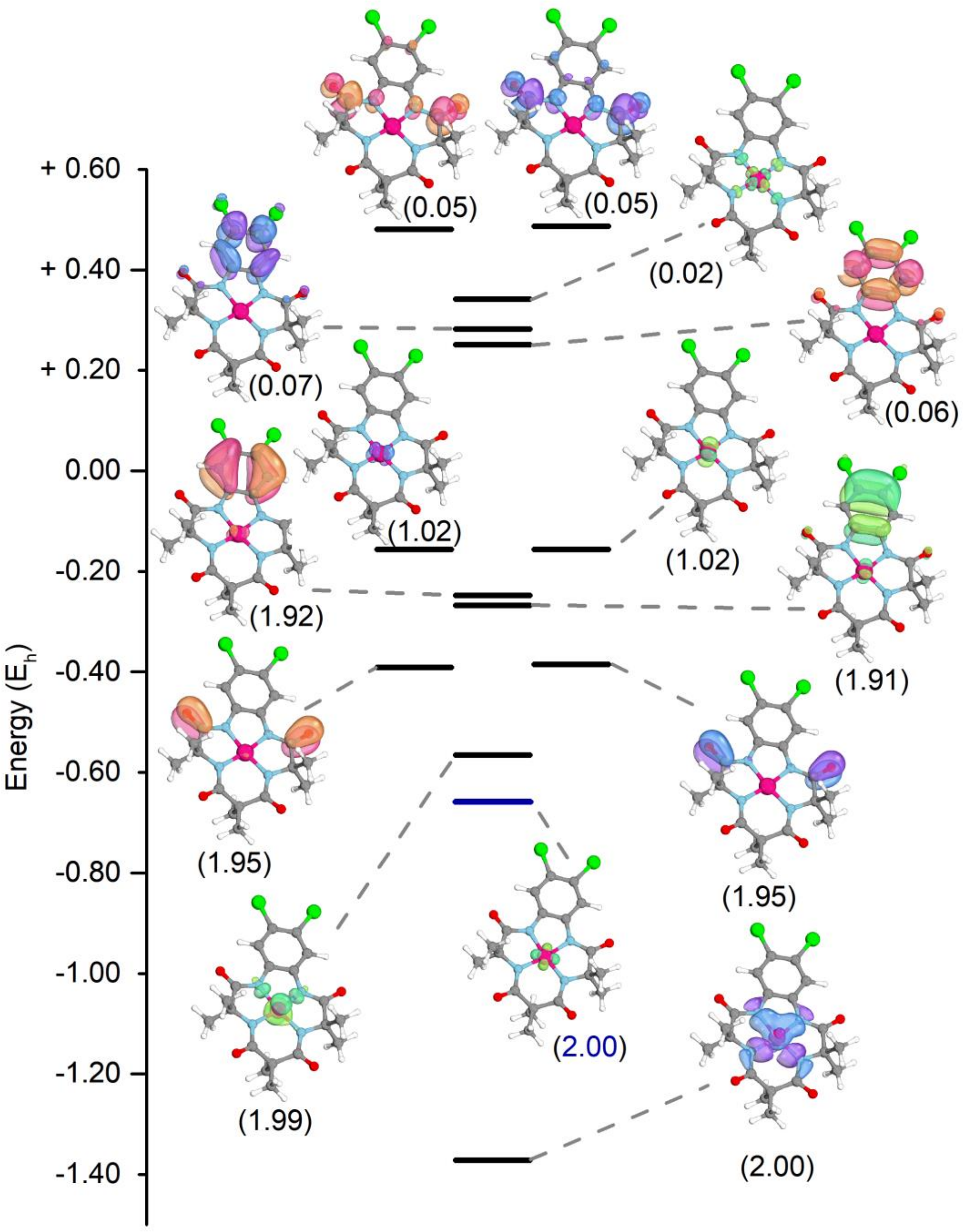

Energy (E_h)
+ 0.60
+ 0.40
+ 0.20
0.00
-0.20
-0.40
-0.60
-0.80
-1.00
-1.20
-1.40
(0.05)
(0.05)
(0.02)
(0.07)
(0.06)
(1.02)
(1.02)
(1.92)
(1.91)
(1.95)
(1.95)
(2.00)
(1.99)
(2.00)

Scheme S1. Energies of active orbitals (black) and inactive orbitals (blue) with their occupancies in parenthesis obtained from NEVPT2-CASSCF(14,13) calculations on **[Co^{III}(TAML^{red})]$^{-}$**. Isosurface for canonical orbitals set at 80.0.

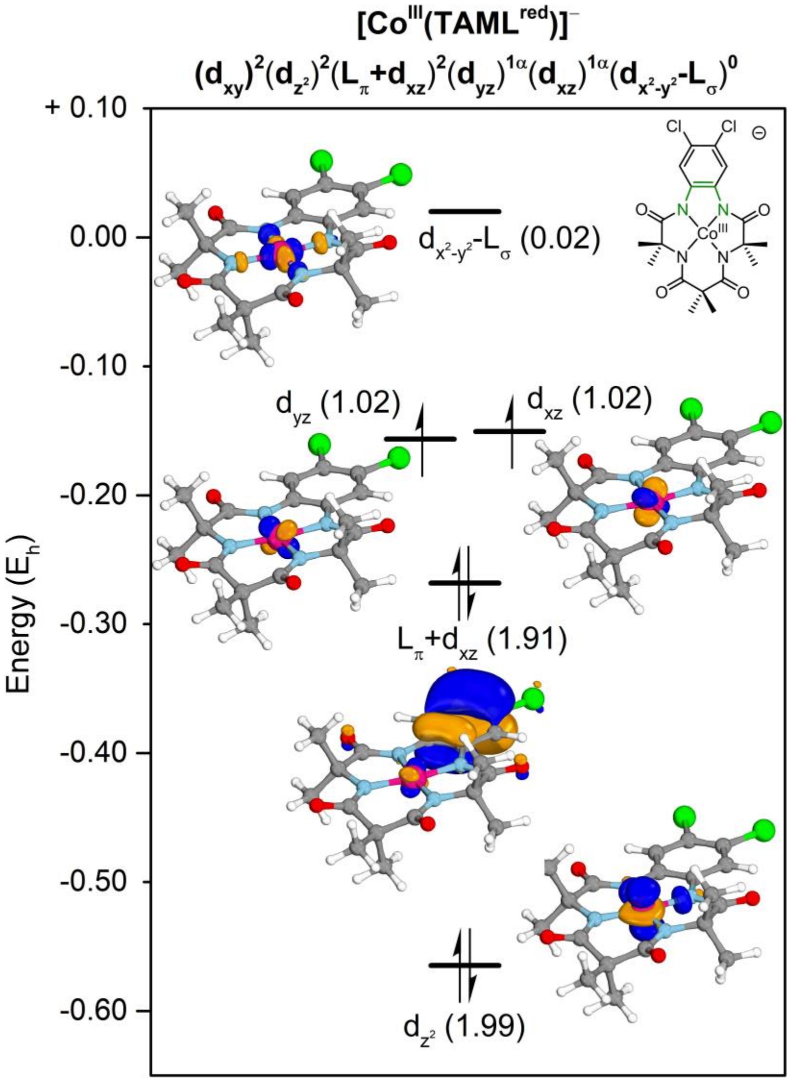

Scheme S2. Most relevant active orbitals, occupancies (in parenthesis) and assignment of the electronic structure of NEVPT2-corrected CASSCF(14,13) calculations on **[Co^{III}(TAML^{red})]$^{-}$**. Isosurface for canonical orbitals set at 80.0.

[Co^{III}(TAML^{sq})] NEVPT2-CASSCF(13,12)

The total and relative energies for the doublet and quartet spin state and their states and contributions for **[Co^{III}(TAML^{sq})]** were obtained from NEVPT2 corrected CASSCF(13,12) calculations and are reported in Table S9. The d_{xy} and d_{z^2} orbitals were not preserved in the active space as these orbitals were found to be non-correlated. The doublet spin state is the most stable and has significant multi-reference character (total of 30.2%) due to single- and double-excitation from the bonding d_{xz}+L_π orbital into the antibonding L_π-d_{xz} orbital. The doublet state results from antiferromagnetic coupling of the triplet spin state of cobalt and an unpaired electron on the ligand backbone. A quantitative orbital analysis can be found in Scheme S3. The most relevant active orbitals and an assignment (from Löwdin population analysis) of the electronic structure are shown in Scheme S4.

Table S9. Total and relative energies (NEVPT2 corrected) for multiple spin states and their contributions for the single-root NEVPT2-CASSCF(13,12) calculation on **[Co^{III}(TAML^{sq})]**.

Multiplicity	Total energy (kcal mol^{-1})	Relative energy (kcal mol^{-1})	Contribution : state
2 (doublet)	–2230756.561	= 0.0	0.48501 : 222222100000
			0.16500 : 222220120000
			0.13677 : 222221110000
			0.02335 : 222122200000
			0.00956 : 122221110100
			0.00940 : 222120220000
			0.00765 : 222121210000

			0.00756 : 222202102000
			0.00611 :022222100200
			0.00592 : 221212101010
			0.00575 : 202222100002
			0.00487 :221221111000
			0.00430 : 222202111000
			0.00424 : 221212110010
			0.00380 : 222212200000
			0.00370 : 022220120200
			0.00361 : 211222100002
			0.00353 : 122122200100
			0.00346 : 122222100100
			0.00296 : 222211101010
			0.00296 : 022221110200
			0.00292: 222200122000
			0.00285 : 122121210100
4 (quartet)	–2230744.127	+12.4	0.85212 : 222221110000
			0.01462 : 220221110200
			0.01425 : 222201112000
			0.00945 : 221221110100
			0.00767 : 222111111010
			0.00578 : 121221210100
			0.00575 : 202221110002
			0.00529 : 222121111000
			0.00492 : 212121110011
			0.00489 : 222202111000
			0.00472 : 222112110010
			0.00469 : 212121110002
			0.00421 : 212211111010
			0.00297 : 222210111010
			0.00284 : 222201110020
			0.00274 : 212221111000

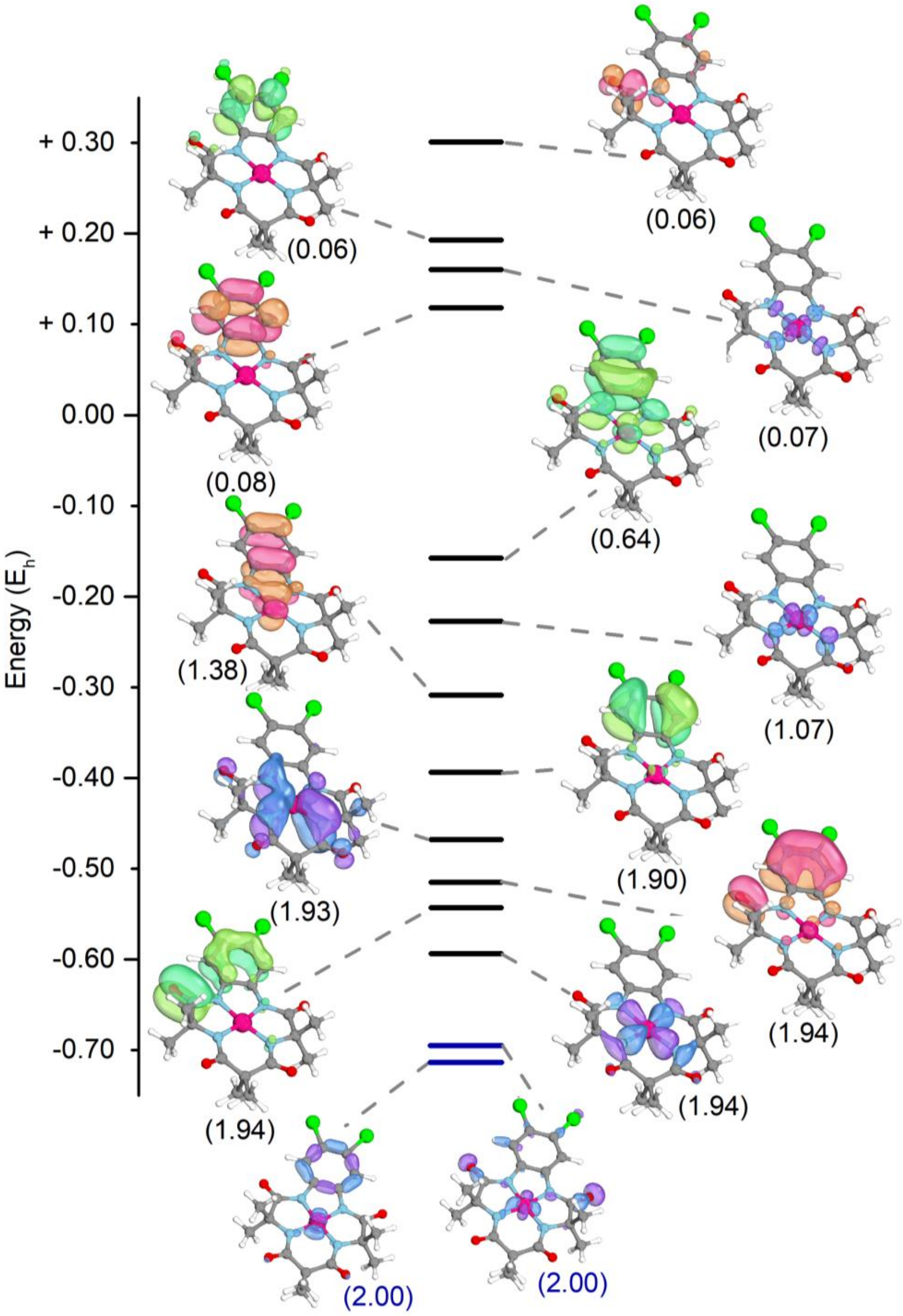
+ 0.30
+ 0.20
+ 0.10
0.00
-0.10
-0.20
-0.30
-0.40
-0.50
-0.60
-0.70
Energy (E$_h$)
(0.06)
(0.06)
(0.08)
(0.07)
(0.64)
(1.38)
(1.07)
(1.93)
(1.90)
(1.94)
(1.94)
(1.94)
(2.00)
(2.00)

Scheme S3. Energies of active orbitals (black) and inactive orbitals (blue) with their occupancies in parenthesis obtained from NEVPT2-CASSCF(13,12) calculations on **[Co^{III}(TAML^{sq})]**. Isosurface for canonical orbitals set at 80.0.

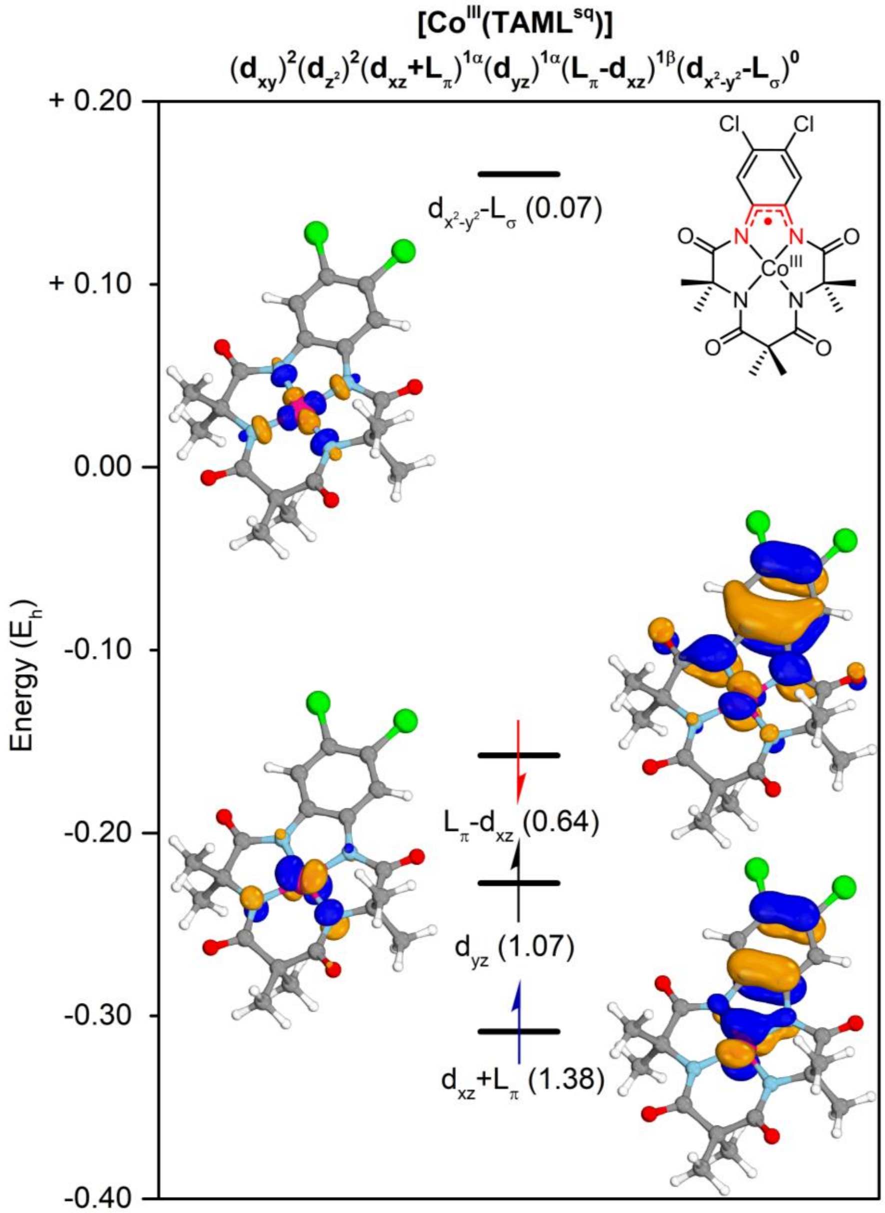
[Co^{III}(TAML^{sq})]
(d$_{xy}$)^2(d$_{z^2}$)^2(d$_{xz}$+L$_\pi$)$^{1\alpha}$(d$_{yz}$)$^{1\alpha}$(L$_\pi$-d$_{xz}$)$^{1\beta}$(d$_{x^2-y^2}$-L$_\sigma$)^0
+ 0.20
+ 0.10
0.00
-0.10
-0.20
-0.30
-0.40
Energy (E$_h$)
d$_{x^2-y^2}$-L$_\sigma$ (0.07)
L$_\pi$-d$_{xz}$ (0.64)
d$_{yz}$ (1.07)
d$_{xz}$+L$_\pi$ (1.38)
Cl
Cl
O
N
N
O
Co^{III}
N
N
O
O

Scheme S4. Most relevant active orbitals, occupancies (in parenthesis) and assignment of the electronic structure of NEVPT2-corrected CASSCF(13,12) calculations on **[Co^{III}(TAML^{sq})]**. The red and blue arrows indicate the multireference character. Isosurface for canonical orbitals set at 80.0.

The UV-Vis absorption of **[Co^{III}(TAML^{sq})]** at 623 nm was reproduced (624.9 nm) very well by calculation of the first 10 roots in the CASSCF(13,12) calculation (Table S10 and Table S11). The first ten roots were chosen because we were mainly interested in the low-energy UV-Vis transitions and to reduce computational costs. The various states for the excitation at 624.9 nm are reported in Table S12, and the three most important contributors are shown in Table S13. The excitations are comprised of ligand-centered $L_{\pi}\rightarrow L_{\pi}\text{-}d_{xz}$ and metal-to-ligand ($d_{xz}+L_{\pi}\rightarrow L_{\pi}\text{-}d_{xz}$ and $d_{yz}\rightarrow L_{\pi}\text{-}d_{xz}$) charge-transfer processes, with the ligand-centered radical being the acceptor orbital in all cases.

Table S10. CASSCF(13,12) (nroots = 10) calculation on **[Co^{III}(TAML^{sq})]** and the relevant absorptions in the UV-Vis region.

States	Energy (cm^{-1})	Wavelength (nm)	fosc	T2 (D**2)	TX (D)	TY (D)	TZ (D)
0(0)-> 1(0) 2	16003.8	624.9	0.010304195	136.724	0.86201	-0.78970	0.02379
0(0)-> 2(0) 2	17947.3	557.2	0.003570785	0.42249	-0.39821	0.51356	-0.01334
0(0)-> 3(0) 2	18523.8	539.8	0.000209118	0.02397	0.15391	0.01512	0.00738
0(0)-> 4(0) 2	29988.2	333.5	0.000746538	0.05286	-0.06595	-0.21758	-0.03427
0(0)-> 5(0) 2	30043.8	332.8	0.000646016	0.04566	0.08757	0.16638	-0.10153
0(0)-> 6(0) 2	32696.3	305.8	0.001507122	0.09788	0.25364	0.18315	0.00166
0(0)-> 7(0) 2	33154.6	301.6	0.000972966	0.06232	-0.21462	0.12743	-0.00423
0(0)-> 8(0) 2	34754.9	287.7	0.049464335	302.224	141.481	100.980	0.02929
0(0)-> 9(0) 2	38858.1	257.3	0.000171988	0.00940	-0.09687	-0.00383	0.00025

Table S11. CASSCF(13,12) (nroots = 10) derived absorptions and intensities of **[Co^{III}(TAML^{sq})]** in the UV-Vis region.

Energy (cm^{-1})	Wavelength (nm)	Intensity
16003.80	624.9	1490.399524247968
17947.30	557.2	516.478605576834
18523.80	539.8	30.246842932581
29988.20	333.5	107.979311341937
30043.80	332.8	93.439801853185
32696.30	305.8	217.990237159103
33154.60	301.6	140.729873950313
34754.90	287.7	7154.525060059725
38858.10	257.3	24.876356995996

Table S12. All contributing states to the excitation at 624.9 nm from a CASSCF(13,12) calculation on **[Co^{III}(TAML^{sq})]**.

Contribution	State
0.28728	222212110000
0.20163	222211120000
0.18101	222222010000
0.05422	222211111000
0.03233	222221200000
0.02470	222221020000
0.01903	122222110000
0.01861	222220210000
0.00797	212221110010
0.00762	222212101000
0.00491	222121110010
0.00459	220211120200
0.00365	220212110200
0.00362	121222110100
0.00341	221212110100
0.00329	212212111000
0.00326	221211120100
0.00317	222210121000
0.00302	212221110001
0.00297	222201111010
0.00257	222202012000

Table S13. Most important donating and accepting orbitals to the excitation at 624.9 nm from a CASSCF(13,12) calculation on **[Co^{III}(TAML^{sq})]**.

State and contribution	**Donating orbital(s)**	**Accepting orbital**
222212110000 (0.28728)	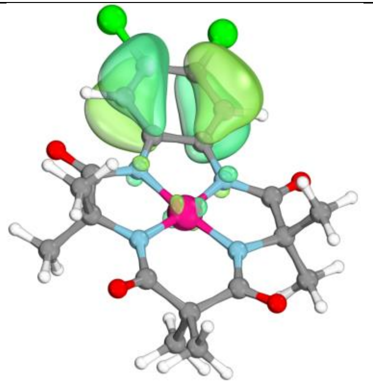 L_π	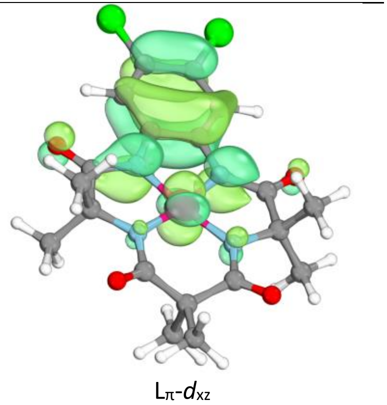 L_π-d_{xz}
222211120000 (0.20163)	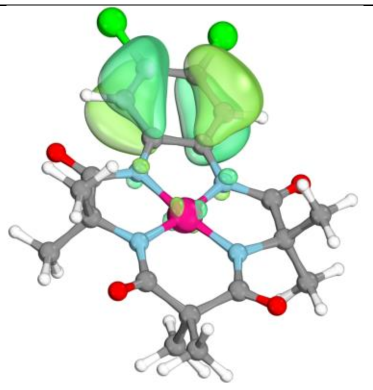 L_π 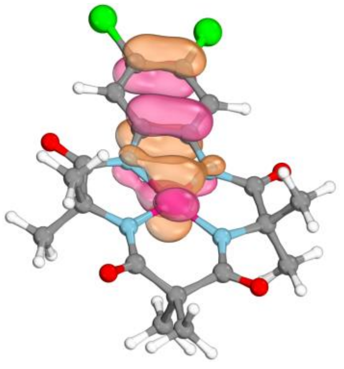 L_π+d_{xz}	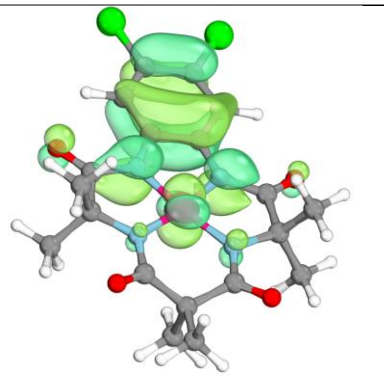 L_π-d_{xz}
222222010000 (0.18101)	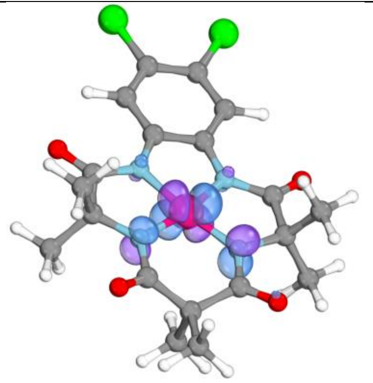 d_{yz}	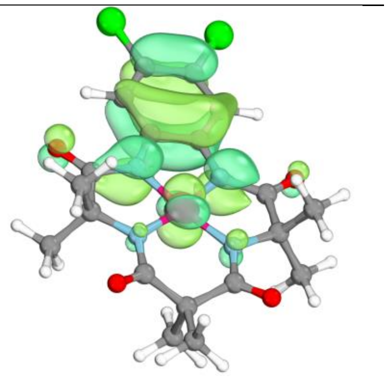 L_π-d_{xz}

[Co^{III}(TAML^{q})(NNs)$_2$]$^{–}$ *NEVPT2-CASSCF(14,13)*

The total and relative energies for the singlet, triplet and quintet spin state and their states and contributions for **[Co^{III}(TAML^{q})(NNs)$_2$]$^{–}$** were obtained from NEVPT2 corrected CASSCF(14,13) calculations and are reported in Table S14. The d_{xy} orbital was not preserved in the active space as this orbital was found to be non-correlated. The triplet spin state is the most stable and has diminishable multi-reference character. A quantitative orbital analysis is shown in Scheme S5. The most relevant active orbitals and an assignment (from Löwdin population analysis) of the electronic structure are shown in Scheme S6.

Table S14. Total and relative energies (NEVPT2 corrected) for multiple spin states and their contributions for the single-root NEVPT2-CASSCF(14,13) calculation on [**Co^{III}(TAML^{q})(NNs)$_2$**]$^{-}$.

Multiplicity	**Total energy (kcal mol^{-1})**	**Relative energy (kcal mol^{-1})**	**Contribution : state**
1 (singlet)	-3533366.778	+6.8	0.45886 : 2222222000000
			0.43046 : 2222220200000
			0.01173 : 2222202020000
			0.01100 : 2222200220000
			0.00460 : 2212122001100
			0.00435 : 2212120201100
			0.00324 : 2222022002000
			0.00301 : 2222020202000
			0.00298 : 0222222020000
			0.00296 : 2202222000200
			0.00279 : 0222220220000
			0.00275 : 2202220200200
3 (triplet)	-3533373.53	= 0.0	0.86886 : 2222221100000
			0.02501 : 2222201120000
			0.00905 : 2212121101100
			0.00878 : 1222211110010
			0.00644 : 2222021102000
			0.00574 : 2202221100200
			0.00556 : 0222221120000
			0.00545 : 2221121101001
			0.00470 : 2221121111000
			0.00443 : 2211221100101
			0.00400 : 2122121101010
			0.00375 : 2211221110100
			0.00331 : 2112221100110
			0.00287 : 2022221100200
5 (quintet)	-3533328.706	+44.8	0.83004 : 2222211110000
			0.03336 : 2221111111010
			0.03301 : 2222011112000
			0.00883 : 2022211110200
			0.00722 : 2212221100100
			0.00673 : 2122211110100
			0.00664 : 2220211112000
			0.00597 : 2112211110101
			0.00536 : 2220211110020
			0.00427 : 2222011110020
			0.00387 : 2212221010100
			0.00344 : 1122211120100
			0.00324 : 2202211110200
			0.00314 : 2212111111010
			0.00286 : 2112211111100

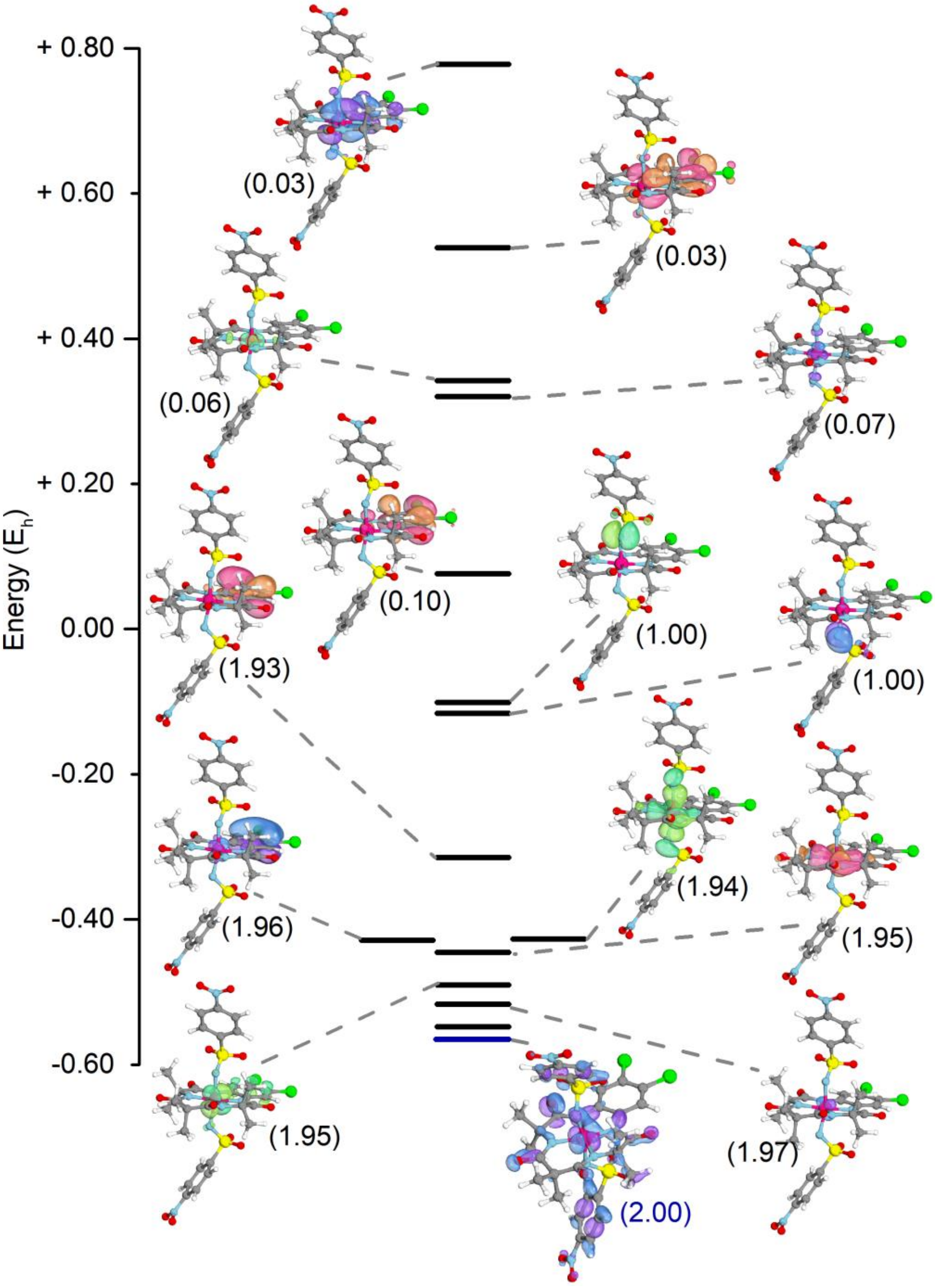
+ 0.80
+ 0.60
+ 0.40
+ 0.20
0.00
-0.20
-0.40
-0.60
Energy (E_h)
(0.03)
(0.03)
(0.06)
(0.07)
(0.10)
(1.93)
(1.00)
(1.00)
(1.96)
(1.94)
(1.95)
(1.95)
(1.97)
(2.00)

Scheme S5. Energies of active orbitals (black) and inactive orbitals (blue) with their occupancies in parenthesis obtained from NEVPT2-CASSCF(14,13) calculations on **[Co^{III}(TAML^{q})(NNs)$_2$]$^{-}$**. Isosurface for canonical orbitals set at 80.0.

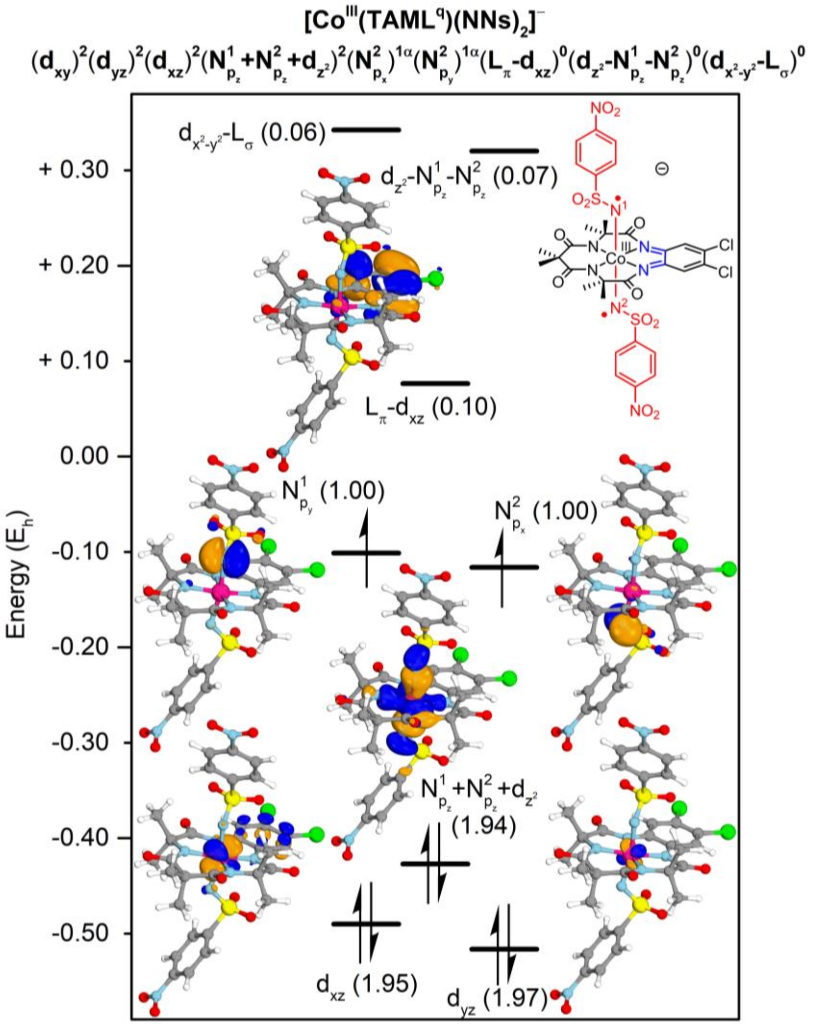
[Co^III(TAML^q)(NNs)2]^-
(dxy)^2(dyz)^2(dxz)^2(N1pz+N2pz+dz2)^2(N2px)^1α(N2py)^1α(Lπ-dxz)^0(dz2-N1pz-N2pz)^0(dx2-y2-Lσ)^0
dx2-y2-Lσ (0.06)
dz2-N1pz-N2pz (0.07)
Lπ-dxz (0.10)
N1py (1.00)
N2px (1.00)
N1pz+N2pz+dz2 (1.94)
dxz (1.95)
dyz (1.97)
+ 0.30
+ 0.20
+ 0.10
0.00
-0.10
-0.20
-0.30
-0.40
-0.50
Energy (Eh)
NO2
O2S
N1
N2
SO2
Co
III
Cl
Cl
O
N
⊖

Scheme S6. Most relevant active orbitals, occupancies (in parenthesis) and assignment of the electronic structure of NEVPT2-corrected CASSCF(14,13) calculations on **[Co^{III}(TAML^{q})(NNs)$_2$]$^-$**. Isosurface for canonical orbitals set at 80.0.

The UV-Vis absorption of **[Co^{III}(TAML^{q})(NNs)$_2$]$^-$** was calculated by the first 10 roots in the CASSCF(14,13) calculation (Table S15). The first ten roots were chosen because we were mainly interested in the low-energy UV-Vis transitions and to reduce computational costs. In accordance with the experimental section, no intense absorptions were observed in the 400-850 nm region.

Table S15. CASSCF(14,13) (nroots = 10) derived absorptions and intensities of **[Co^{III}(TAML^{q})(NNs)$_2$]$^-$** in the UV-Vis region.

Energy (cm^{-1})	**Wavelength (nm)**	**Intensity**
12128.10	824.5	8.140054067846
12612.40	792.9	2.380197052853
15894.60	629.1	5.388565945798
16060.90	622.6	2.802835348213
17657.90	566.3	0.098644530265
17692.50	565.2	0.961422569902
19150.80	522.2	0.076659239062
20969.70	476.9	1.907947212214
21191.70	471.9	0.860463798458

[Co^{III}(TAML^{q})(NNs)] *NEVPT2-CASSCF(13,12)*

The total and relative energies for the doublet and quartet spin state and their states and contributions for **[Co^{III}(TAML^{sq})]** were obtained from NEVPT2 corrected CASSCF(13,12) calculations and are reported in Table S16. The d_{xy} orbital was not preserved in the active space as this orbital was found to be non-correlated. The doublet spin state is the most stable and has diminishable multi-reference character. A quantitative orbital analysis is shown in Scheme S7. The most relevant active orbitals and an assignment (from Löwdin population analysis) of the electronic structure are shown in Scheme S8.

Table S16. Total and relative energies (NEVPT2 corrected) for multiple spin states and their contributions for the single-root NEVPT2-CASSCF(13,12) calculation on **[Co^{III}(TAML^{q})(NNs)]**.

Multiplicity	**Total energy (kcal mol^{-1})**	**Relative energy (kcal mol^{-1})**	**Contribution : state**
2 (doublet)	–2882015.513	= 0.0	0.77915 : 222222100000
			0.02706 : 122212201000
			0.01859 : 222202102000
			0.01776 : 222220120000
			0.01173 : 211222110100
			0.00894 : 221212111000
			0.00802 :221222110000
			0.00743 : 222212101000
			0.00603 : 211222100110
			0.00537 : 221212101010
			0.00535 : 202222100200
			0.00489 : 122222200000
			0.00431 : 222112201000
			0.00424 : 212212101100
			0.00391 : 212222100100
			0.00346 : 222220110010
			0.00339 : 222121110010
			0.00317 : 220222110010
			0.00294 : 112222200100
			0.00278 : 220222120000
4 (quartet)	–2882010.361	+5.2	0.80812 : 222221110000
			0.03561 : 222201112000
			0.02738 : 221212111000
			0.01553 : 222021110200
			0.01485 : 202221110020
			0.00977 : 222111111100
			0.00870 : 222211111000
			0.00619 : 122211211000
			0.00518 : 222121110100
			0.00458 : 221122110100
			0.00382 : 122121210100
			0.00323 : 121222210000
			0.00306 : 222201211000
			0.00280 : 202221120010
			0.00280 : 221121110101

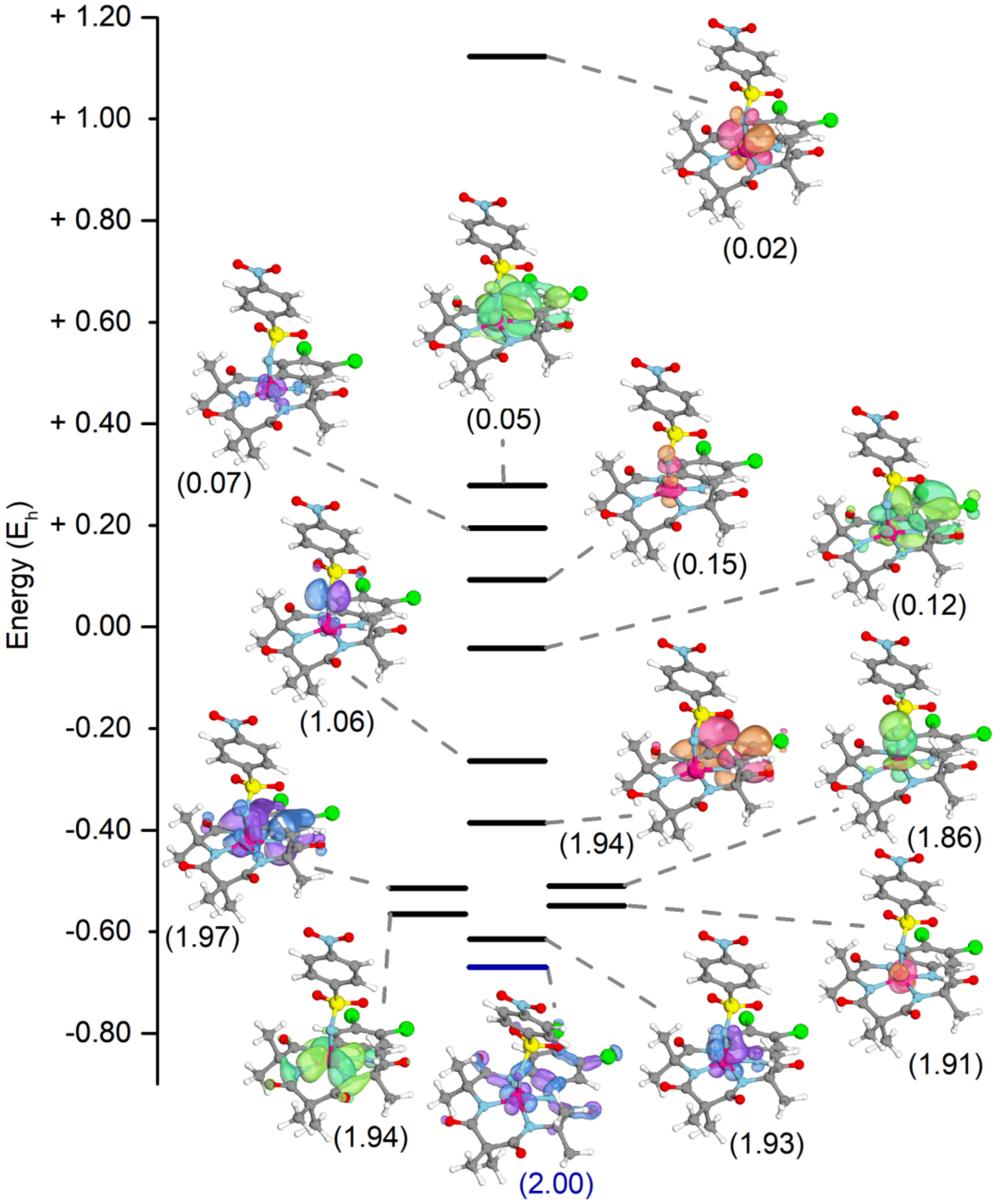

Scheme S7. Energies of active orbitals (black) and inactive orbitals (blue) with their occupancies in parenthesis obtained from NEVPT2-CASSCF(13,12) calculations on **[Co^{III}(TAML^{q})(NNs)]**. Isosurface for canonical orbitals set at 80.0.

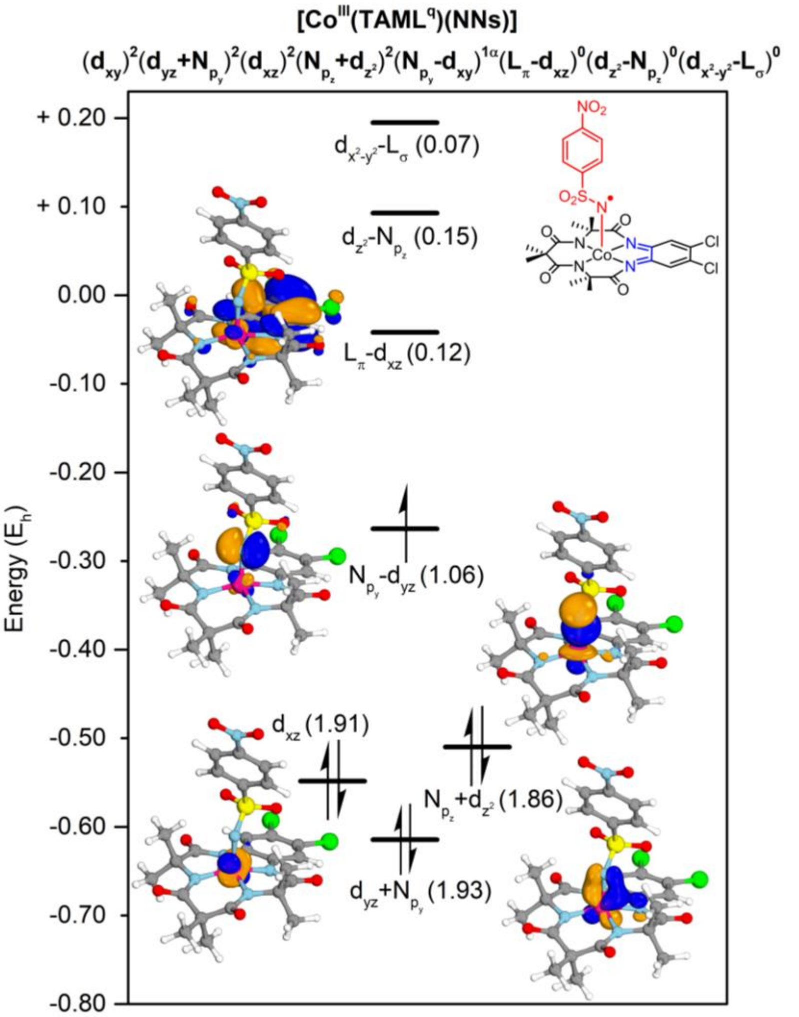
[Co^III(TAML^q)(NNs)]
(d_xy)^2(d_yz+N_py)^2(d_xz)^2(N_pz+d_z²)^2(N_py-d_xy)^1α(L_π-d_xz)^0(d_z²-N_pz)^0(d_x²-y²-L_σ)^0
+ 0.20
+ 0.10
0.00
-0.10
-0.20
-0.30
-0.40
-0.50
-0.60
-0.70
-0.80
Energy (E_h)
d_x²-y²-L_σ (0.07)
d_z²-N_pz (0.15)
L_π-d_xz (0.12)
N_py-d_yz (1.06)
d_xz (1.91)
N_pz+d_z² (1.86)
d_yz+N_py (1.93)
NO2
O2S
N•
N
Co
N
N
N
N
O
O
O
O
Cl
Cl

Scheme S8. Most relevant active orbitals, occupancies (in parenthesis) and assignment of the electronic structure of NEVPT2-corrected CASSCF(13,12) calculations on **[Co^{III}(TAML^{q})(NNs)]**. Isosurface for canonical orbitals set at 80.0.

The UV-Vis absorption spectrum and EPR *g*-values of **[Co^{III}(TAML^{q})(NNs)]** were calculated by inclusion of the first 10 roots in the CASSCF(13,12) calculation. The first ten roots were chosen because we were mainly interested in the low-energy UV-Vis transitions and to reduce computational costs. However, as was evident form XANES analysis (Figure 8 in the main text), an unidentified sixth axial ligand is possibly coordinating to **[Co^{III}(TAML^{q})(NNs)]**. It is, however, computationally not feasible to calculate all possible coordinating axial ligands that might be present in the solution (e.g. solvent, NsNH$_2$, NsNH^{-}, PhI, H_2O, OH^{-}) with the computationally very expensive CASSCF calculations. We therefore evaluated the calculated EPR *g*-values and UV-Vis absorptions of the **[Co^{III}(TAML^{q})(NNs)]** complex and found that these are close to the experimentally found values, but not exactly the same, perhaps indeed pointing to coordination of a sixth axial ligand.

The *g* values were calculated to be $g_1 = 1.983$, $g_2 = 1.986$ and $g_3 = 2.025$ ($g_{iso} = 1.998$). These values are close the experimental *g* values ($g_{iso} = 2.091$ and small *g*-anisotropy, Figure 7 in the main text). The absorption energies in the 400-850 nm region were found at 666.3, 450.1 and 414.5 nm with intensities of 2.15, 298.36 and 105.27, respectively. These absorptions do not reflect the absorption observed in the 700-800 nm region characteristic for MLCT bands (Figure 6 in the main text), which we attribute to the possible presence of an unidentified sixth axial ligand.

List of xyz coordinates for all DFT calculated structures (BP86/def2-TZVP/disp3/m4)

[Co^{III}(TAML^{red})]$^{-}$ (Triplet)

Co	0.00000000	0.00000000	0.00000000
Cl	5.91572996	3.24889119	-0.21671688
O	3.69837564	-1.39281770	0.11496289
O	-0.89721875	-3.87637713	0.46127304
N	1.84121319	-0.00000000	-0.00000000
N	0.10130006	-1.83417955	0.08321454
C	2.47853102	-1.21061592	0.11031340
C	1.47162427	-2.37726475	0.28717294
C	-0.96842886	-2.68823629	0.11341613
C	-2.31088775	-2.13796554	-0.44631171
C	2.43165107	1.26628321	-0.06912997
C	3.79618126	1.56898599	-0.10565882
C	4.20081718	2.90689750	-0.16912990
C	1.66885021	-2.90061310	1.72518073
C	1.81421360	-3.45653377	-0.75261499
C	-3.42318480	-3.15381400	-0.16064899
H	4.52811552	0.76675420	-0.08245526
H	1.03627490	-3.77830844	1.89077779
H	1.39164114	-2.11751184	2.44578363
H	2.72666091	-3.15955525	1.87306752
H	1.61359804	-3.07885362	-1.76524381
H	1.21237618	-4.35546211	-0.58188554
H	2.88282206	-3.69848085	-0.67507433
H	-3.14700549	-4.13294344	-0.57079594
H	-4.36413559	-2.80975429	-0.60541919
N	0.15367748	1.83436104	-0.04534075
N	-1.82096675	0.25541064	0.03113656
C	-2.76270289	-0.73900409	0.06202965
C	-2.12426189	-2.00658277	-1.98376687
C	1.46544029	2.31545307	-0.09459288
C	3.25089839	3.93938912	-0.19340626
C	-1.00108668	2.57227350	0.01742018
C	-2.25246269	1.67077675	0.18345543
O	-3.94968385	-0.56022656	0.37129456
H	-3.06415631	-1.67006085	-2.44617413
H	-1.85353767	-2.98307262	-2.41169792
C	1.88255658	3.64900517	-0.15556673
Cl	3.73645542	5.61867917	-0.27438339
O	-1.08119365	3.80346649	-0.01019720
C	-3.26937155	2.07328798	-0.89729574
C	-2.79876282	1.94944388	1.60015257
H	1.14438948	4.44460727	-0.17120729
H	-4.21992415	1.55230050	-0.73950543
H	-2.88025746	1.81540336	-1.89219360
H	-3.42390770	3.15983842	-0.85309505
H	-2.06245752	1.62655504	2.35099631
H	-3.73213816	1.39782631	1.75397558
H	-2.97077331	3.02837493	1.71397790
H	-1.33328776	-1.28365266	-2.22086596
H	-3.57969736	-3.27018745	0.91894493

[Co^{III}(TAML^{sq})] (Doublet)

Co	0.00000000	0.00000000	0.00000000
Cl	5.91183043	3.19855482	0.07626219
O	3.67184872	-1.41981401	-0.09650990
O	-0.91283757	-3.82499388	0.52360897
N	1.83189220	-0.00000000	0.00000000
N	0.09300983	-1.81369079	0.05020869
C	2.46727401	-1.25030618	0.00429124
C	1.45808198	-2.40069155	0.19522297

C	-1.00026247	-2.66762829	0.11522708
C	-2.33472146	-2.14165930	-0.45610981
C	2.43935753	1.23180122	-0.00810088
C	3.81493412	1.52281790	0.01767415
C	4.22020960	2.85010104	0.02690732
C	1.71814258	-2.95271728	1.61393826
C	1.72675882	-3.46079223	-0.88483736
C	-3.45133684	-3.13280369	-0.11071600
H	4.54351411	0.71806148	0.03435599
H	1.09739317	-3.83656640	1.79031828
H	1.47707491	-2.19046017	2.36891408
H	2.77931038	-3.21898196	1.70386617
H	1.49581073	-3.05870410	-1.88094033
H	1.11220354	-4.34882399	-0.70431753
H	2.78817717	-3.73852289	-0.85880365
H	-3.18881921	-4.13361287	-0.47210980
H	-4.39406754	-2.80892206	-0.56602856
N	0.18540939	1.82217037	-0.05240710
N	-1.79881655	0.27073652	-0.04383765
C	-2.76626978	-0.72330713	-0.02093609
C	-2.14770554	-2.07873357	-2.00067330
C	1.47155876	2.30253844	-0.03510712
C	3.26136278	3.91062895	0.00300469
C	-0.99324076	2.57933082	-0.10128335
C	-2.25054564	1.69380095	0.00525896
O	-3.94551384	-0.49496091	0.24610404
H	-3.08850708	-1.76003731	-2.47184116
H	-1.88735016	-3.07565974	-2.38075525
C	1.90030670	3.64075683	-0.03182913
Cl	3.77943039	5.55873304	0.02630385
O	-1.03416839	3.79627239	-0.19584093
C	-3.16085849	2.03034102	-1.18918204
C	-2.91750957	2.05869427	1.35012327
H	1.17424379	4.44814188	-0.04937975
H	-4.11744426	1.50696371	-1.09542783
H	-2.67796435	1.73329376	-2.13114656
H	-3.33572850	3.11346675	-1.21225004
H	-2.27291869	1.76070661	2.18830936
H	-3.87935656	1.54561716	1.44138240
H	-3.06955509	3.14545604	1.38692028
H	-1.35382312	-1.37241500	-2.27704766
H	-3.60121629	-3.19205380	0.97473164

[Co^{III}(TAML^{sq})(MeCN)] (Doublet)
56
CoTAML_MeCN_BP86_Doublet-163105

Cl	8.3421002	6.1476903	0.8007750
O	5.6410313	2.1508376	2.5437395
O	1.0816098	-0.3532190	2.1566062
N	4.2030973	3.0258840	0.9468808
N	2.4146458	1.2562480	1.2128845
C	4.5663252	2.1381760	1.9576154
C	3.4354243	1.1361102	2.2802286
C	1.3271359	0.4150164	1.2190259
C	0.4900277	0.3341686	-0.0805096
C	4.9317808	4.0862476	0.4643100
C	6.1965699	4.5291040	0.8923746
C	6.7858722	5.6135211	0.2567783
C	2.9007990	1.5172971	3.6794436
C	4.0571927	-0.2738210	2.2950384
C	-0.7720404	-0.4937586	0.1851355
H	6.7023044	4.0197534	1.7073898
H	2.1368796	0.7960965	3.9872875

H	2.4591142	2.5226589	3.6594819
H	3.7322212	1.5136115	4.3969128
H	4.3842918	-0.5533030	1.2841599
H	3.3235253	-1.0044983	2.6490499
H	4.9317705	-0.2693732	2.9579389
H	-0.4985612	-1.4696060	0.6013197
H	-1.3335877	-0.6292921	-0.7457774
N	3.0512380	4.1839050	-0.9201811
N	1.0804317	2.5983602	-0.9472699
C	0.0914363	1.6582167	-0.7753933
C	1.3969875	-0.4103002	-1.1059362
C	4.2628337	4.7586910	-0.6204828
C	6.1246695	6.2781541	-0.8159482
C	2.1677695	4.5489253	-1.9338894
C	0.8625369	3.7231848	-1.8868358
O	-1.0393539	1.7824219	-1.2603582
H	0.8464987	-0.5589367	-2.0455476
H	1.6776492	-1.3938459	-0.7035981
C	4.8752274	5.8572888	-1.2506556
Cl	6.8615603	7.6355787	-1.6013370
O	2.3770987	5.4298863	-2.7577421
C	0.5879642	3.2069971	-3.3124411
C	-0.2502441	4.6933482	-1.4283675
H	4.3725977	6.3614113	-2.0707752
H	-0.3954953	2.7290314	-3.3563168
H	1.3557724	2.4777141	-3.6047488
H	0.6246072	4.0533775	-4.0098188
H	-0.0463885	5.0573014	-0.4122056
H	-1.2137972	4.1737177	-1.4367465
H	-0.2812872	5.5544231	-2.1093231
H	2.3087775	0.1635967	-1.3134709
H	-1.4277769	0.0105091	0.9063128
Co	2.4779124	2.8714584	0.2676405
N	1.5949789	3.9116000	1.4597979
C	1.0039103	4.5526582	2.2233785
C	0.2487839	5.3367661	3.1770019
H	-0.0042396	6.3160611	2.7469988
H	0.8367122	5.4885384	4.0931557
H	-0.6809012	4.8094102	3.4340133

[Co^{III}(TAML^{q})(NNs)] (Doublet)

Cl	5.86235270	3.09074634	-1.15900557
O	3.64699355	-1.43658346	-0.38560091
O	-0.98127249	-3.82943762	-0.17457615
N	1.81196334	-0.02275419	-0.36133240
N	0.10042343	-1.82766342	-0.37241448
C	2.44288814	-1.28246774	-0.30921040
C	1.42860410	-2.42048212	-0.10741805
C	-1.00107420	-2.64461653	-0.50638313
C	-2.23328091	-2.03168825	-1.20046999
C	2.41393107	1.18936588	-0.53138177
C	3.77652104	1.45552209	-0.75894815
C	4.18501526	2.76776117	-0.91745698
C	1.56738101	-2.90322184	1.35387360
C	1.78666626	-3.53548843	-1.10564972
C	-3.38182339	-3.04412363	-1.18898945
H	4.49637829	0.64260426	-0.77568559
H	0.90937053	-3.76676580	1.50417671
H	1.27396996	-2.10475550	2.04665528
H	2.61014948	-3.18744196	1.54631806
H	1.60528482	-3.20012718	-2.13632503
H	1.18584405	-4.42769839	-0.90973122
H	2.85110584	-3.77491462	-0.99820448

H	-3.06178426	-3.97479767	-1.67144028
H	-4.24743059	-2.63336475	-1.72257293
N	0.18874673	1.82017290	-0.32497888
N	-1.77890128	0.30669823	-0.45081087
C	-2.71052787	-0.70912677	-0.58093192
C	-1.81012403	-1.71724630	-2.66383204
C	1.46245324	2.27373385	-0.48802243
C	3.24135766	3.84673446	-0.85701721
C	-0.99019637	2.58483256	-0.31650714
C	-2.23864424	1.69132066	-0.19286103
O	-3.89181597	-0.53463306	-0.28320658
H	-2.66849014	-1.31014438	-3.21699085
H	-1.48298172	-2.64173845	-3.15829656
C	1.89524326	3.60321056	-0.64577057
Cl	3.77152811	5.47943830	-1.02639983
O	-1.01729784	3.79677183	-0.40918798
C	-3.24350734	2.17295851	-1.25550684
C	-2.79613871	1.86405549	1.23641034
H	1.18052892	4.41861860	-0.58417391
H	-4.19916570	1.65550280	-1.13431825
H	-2.85493705	1.98254641	-2.26560503
H	-3.38965027	3.25334559	-1.13541514
H	-2.10003236	1.43931807	1.96864943
H	-3.75910980	1.34786626	1.31006032
H	-2.92102221	2.93414225	1.44725964
H	-0.99058668	-0.98876572	-2.69615233
H	-3.69089693	-3.27839525	-0.16429664
Co	0.00000000	0.00000000	0.00000000
N	0.00000000	0.00000000	1.76681635
S	0.88037563	1.05034012	2.66758455
O	2.31206854	0.83646762	2.43954954
O	0.36176248	2.41623726	2.60881897
H	-1.27866839	1.63110085	4.48535016
C	-0.68470749	0.83385328	4.92955367
C	0.92014519	-1.19589074	6.04011392
C	0.45098187	0.35817074	4.26326484
C	-1.02446910	0.28610094	6.16360043
C	-0.21686009	-0.72050708	6.69473317
C	1.25677848	-0.64877492	4.80472235
H	-1.89602545	0.62552806	6.71867228
H	2.14131896	-0.98208063	4.26413987
H	1.51973199	-1.97726781	6.50238607
N	-0.58094848	-1.30771581	8.01445607
O	0.15492615	-2.18827965	8.46689926
O	-1.59455340	-0.87732213	8.56839141

[Co^{III}(TAML^{q})(NNs)] nitrene on other side (Doublet)
67
CoTAML_NNs_BP86_Doublet-177089

Co	2.3228155	3.2069426	-0.2052319
Cl	6.7221491	7.8894063	1.8558106
O	4.8659030	3.2321893	2.8401195
O	0.6586421	0.3438485	2.0461139
N	3.6258029	3.8395979	0.9809166
N	1.9430378	1.9870030	1.1283947
C	3.9423890	3.0265095	2.0727997
C	2.9123290	1.9054034	2.2550967
C	0.9249490	1.0478626	1.0708764
C	0.2515442	0.7470295	-0.2732029
C	4.0832080	5.1062083	0.7613916
C	5.1386455	5.7683300	1.4121744
C	5.4035077	7.0877407	1.0818965
C	2.2513482	2.1873975	3.6245231

C	3.6636966	0.5618926	2.2382551
C	-1.0453082	-0.0411859	-0.0216800
H	5.7440669	5.2405419	2.1421764
H	1.5901244	1.3621894	3.9001688
H	1.6659644	3.1164472	3.5821131
H	3.0447646	2.3033793	4.3742342
H	4.1092827	0.3945777	1.2494387
H	2.9804539	-0.2566329	2.4878926
H	4.4720675	0.6059127	2.9794157
H	-0.8259454	-0.9489706	0.5508460
H	-1.5013291	-0.3096719	-0.9804158
N	2.2972871	4.9835812	-0.7265402
N	0.6751640	3.0801479	-1.0974807
C	-0.0668642	1.9345956	-1.1966963
C	1.2646929	-0.1499515	-1.0458528
C	3.2916296	5.7872532	-0.2260077
C	4.6118132	7.7690150	0.1054531
C	1.3321092	5.3453917	-1.6719988
C	0.4213632	4.1770379	-2.0619566
O	-0.9447880	1.7922883	-2.0564468
H	0.8096067	-0.4625935	-1.9950471
H	1.4921237	-1.0420049	-0.4463422
C	3.5599890	7.1294118	-0.5372955
Cl	4.9572933	9.4072569	-0.3132443
O	1.2571653	6.4609113	-2.1621379
C	0.8561418	3.7594672	-3.4874420
C	-1.0284816	4.6928096	-2.0263335
H	2.9660047	7.6502295	-1.2811321
H	0.1849677	2.9744909	-3.8525739
H	1.8850064	3.3727479	-3.4708985
H	0.8061206	4.6320451	-4.1516065
H	-1.3378827	4.8904877	-0.9908045
H	-1.7060215	3.9571279	-2.4669172
H	-1.0773132	5.6323757	-2.5916804
H	2.1977268	0.3890287	-1.2614041
H	-1.7655549	0.5580986	0.5506193
N	3.3393824	2.4428930	-1.3981242
S	4.9801949	2.5631920	-1.4167664
O	5.3678583	3.9324624	-1.7527701
O	5.6015536	1.9077150	-0.2684108
C	5.2422929	1.5208777	-2.8514895
C	5.6044755	-0.0764660	-5.0519991
C	5.4173251	0.1446690	-2.6714486
C	5.2487370	2.1055149	-4.1223762
C	5.4356837	1.2960414	-5.2398363
C	5.6016274	-0.6671022	-3.7876916
H	5.4220573	-0.2744801	-1.6660552
H	5.1216143	3.1827007	-4.2236461
H	5.4533612	1.7069934	-6.2473950
H	5.7454951	-1.7418925	-3.6959960
N	5.7987256	-0.9442902	-6.2471960
O	5.9427195	-2.1532558	-6.0534157
O	5.8014878	-0.3967712	-7.3517395

[Co(TAML^q)(NNs)$_2$] (Doublet)
84
CoTAML_2xNNs_BP86_Doublet-177087

Cl	7.9757177	7.2981418	0.8435411
O	5.4903246	3.1511935	2.5288478
O	0.8502319	0.8082797	2.3463373
N	4.0523677	3.9703518	0.8933343
N	2.3014471	2.1416510	1.2099884
C	4.4324439	3.0882835	1.9405114

C	3.2871807	2.1280329	2.3132574
C	1.1440111	1.3854640	1.2966190
C	0.2763789	1.2077722	0.0390973
C	4.7115627	5.0499172	0.4481715
C	5.9594317	5.5439925	0.8889944
C	6.4572719	6.6900776	0.3136247
C	2.7019615	2.7341388	3.6219016
C	3.8554368	0.7212782	2.5552264
C	-1.0358973	0.5234575	0.4539448
H	6.5072349	5.0191468	1.6652259
H	1.9241287	2.0712427	4.0105617
H	2.2663679	3.7213910	3.4239552
H	3.5174959	2.8347729	4.3498369
H	4.2258697	0.3002251	1.6137433
H	3.0816169	0.0755382	2.9809310
H	4.6953625	0.8004503	3.2568117
H	-0.8190509	-0.4190576	0.9693018
H	-1.6444243	0.3260572	-0.4343467
N	2.8250495	5.1376930	-0.9173789
N	0.8227851	3.4872894	-0.9116945
C	-0.0739179	2.4614287	-0.8162578
C	1.0723882	0.2648888	-0.9085087
C	3.9796812	5.7460774	-0.6142316
C	5.7231737	7.3899992	-0.7249490
C	1.8685591	5.4946094	-1.9006162
C	0.6674445	4.5244392	-1.9630843
O	-1.1102846	2.4358547	-1.4914580
H	0.4597638	0.0393923	-1.7916901
H	1.3050655	-0.6739942	-0.3870306
C	4.5080701	6.9278371	-1.1786133
Cl	6.3715401	8.8285566	-1.4055593
O	2.0049876	6.4406387	-2.6487938
C	0.7282346	3.8798128	-3.3712405
C	-0.6159145	5.3591990	-1.7827342
H	3.9554476	7.4551238	-1.9498858
H	-0.1563068	3.2519180	-3.5188752
H	1.6321768	3.2637451	-3.4636599
H	0.7464103	4.6760885	-4.1257895
H	-0.6594910	5.7628097	-0.7653287
H	-1.4910813	4.7321519	-1.9737123
H	-0.5931113	6.1971902	-2.4912820
H	2.0073595	0.7363550	-1.2433504
H	-1.6116945	1.1588978	1.1385934
N	3.1834288	2.5585732	-1.4147337
S	4.7587207	2.1928765	-1.4827300
O	5.4939342	3.3979658	-1.8892960
O	5.2317015	1.4512767	-0.3110246
C	4.7541958	1.0508280	-2.8632087
C	4.6705053	-0.6915284	-4.9840467
C	4.6194021	-0.3190931	-2.6152444
C	4.8513038	1.5555643	-4.1642699
C	4.8121806	0.6730658	-5.2404142
C	4.5755350	-1.2038916	-3.6898505
H	4.5615367	-0.6812608	-1.5895817
H	4.9682976	2.6270059	-4.3224473
H	4.8899871	1.0213359	-6.2684913
H	4.4742479	-2.2773594	-3.5427874
Co	2.4393656	3.5993003	0.0644050
N	1.2791223	4.5513100	1.3063241
S	1.4837793	6.1258550	1.6509424
O	2.8068322	6.3756618	2.2378298
O	1.0547752	6.9773747	0.5371186
H	-1.3534040	6.6395167	1.5854685

C	-1.0636543	6.5355374	2.6302475
C	-0.2538034	6.2950567	5.3131998
C	0.2745339	6.2998933	2.9634386
C	-2.0080053	6.6500754	3.6462315
C	-1.5864878	6.5242654	4.9710928
C	0.6885464	6.1809348	4.2936534
H	-3.0584843	6.8363775	3.4319989
H	1.7412168	6.0163734	4.5202324
H	0.0255788	6.2128708	6.3617210
N	4.6241486	-1.6358149	-6.1339400
O	4.4890697	-2.8349304	-5.8796391
O	4.7230166	-1.1575541	-7.2662802
N	-2.5949586	6.6445027	6.0587398
O	-2.1967937	6.5227207	7.2197225
O	-3.7641786	6.8575128	5.7293325

[Co^{III}(TAML^{sq})(NNs)]$^{-}$ (Triplet)

Cl	3.60628844	-5.64316688	-0.85985110
O	-1.14498320	-3.75579178	-0.49227461
O	-3.92792988	0.63374977	-0.04972282
N	0.12256161	-1.82170578	-0.35978693
N	-1.82719846	-0.23412533	-0.35274259
C	-1.06003207	-2.53949323	-0.35164734
C	-2.28481224	-1.62444890	-0.13466058
C	-2.73906015	0.78619401	-0.36215640
C	-2.26093518	2.14121159	-0.93571800
C	1.40346604	-2.32164697	-0.48206538
C	1.79279447	-3.66363352	-0.60069800
C	3.14495504	-3.96809824	-0.71362359
C	-2.76298316	-1.85570549	1.31548326
C	-3.35917588	-2.04138196	-1.15399507
C	-3.36084045	3.18911910	-0.73563537
H	1.04222994	-4.44755225	-0.59000230
H	-3.68535868	-1.28888703	1.48470175
H	-1.99352221	-1.51015109	2.01766162
H	-2.94024485	-2.92871760	1.47342298
H	-3.02793569	-1.79736649	-2.17355801
H	-4.29892363	-1.51950575	-0.94927873
H	-3.50579430	-3.12718243	-1.08530877
H	-4.29880465	2.83464847	-1.17957057
H	-3.06131648	4.13715667	-1.19825155
N	1.82595807	-0.03294702	-0.34580013
N	0.13962572	1.83518502	-0.36827292
C	-0.92337885	2.69584883	-0.38760966
C	-2.03502678	1.90692005	-2.45633775
C	2.38897565	-1.28764460	-0.47086431
C	4.12099716	-2.94466066	-0.69982025
C	2.48290678	1.18585250	-0.35641038
C	1.50645198	2.36593878	-0.16444086
O	-0.82712259	3.89884972	-0.10796297
H	-1.73633631	2.84992720	-2.93758401
H	-2.96775420	1.55518578	-2.92145194
C	3.75017855	-1.61030974	-0.57437264
Cl	5.81811151	-3.32362695	-0.82810959
O	3.69292992	1.32842396	-0.50004423
C	1.86616754	3.43406127	-1.21257367
C	1.71800373	2.89090354	1.27200901
H	4.49652629	-0.82276830	-0.54547257
H	1.29871237	4.35145617	-1.02871971
H	1.63508652	3.06559743	-2.22233681
H	2.94353786	3.63590056	-1.15271576
H	1.43223986	2.11608544	1.99412602
H	1.09720065	3.78080596	1.42489554

H	2.77927594	3.13625401	1.41556444
H	-1.25059157	1.15827931	-2.62187967
H	-3.53766284	3.37200804	0.33150601
Co	0.00000000	0.00000000	0.00000000
N	0.00000000	0.00000000	1.77996626
S	1.00864913	-0.87697696	2.68761829
O	0.82872314	-2.32571214	2.55058439
O	2.38209492	-0.36271614	2.68792043
H	1.45612955	1.38611860	4.42864753
C	0.68625852	0.77312668	4.89633790
C	-1.27159856	-0.87469260	6.06004421
C	0.26840072	-0.40387538	4.26521408
C	0.12365879	1.13413811	6.11662811
C	-0.84865332	0.30327400	6.68155403
C	-0.70514514	-1.22868879	4.83877374
H	0.42254832	2.04113215	6.63820013
H	-0.99727206	-2.14416657	4.32524321
H	-2.03014676	-1.49110211	6.53840400
N	-1.44280350	0.67878729	7.98211990
O	-2.29645438	-0.07395822	8.46779788
O	-1.05331911	1.72475223	8.51624500

[Co^{III}(TAML^{q})(NNs$_2$)]$^{-}$ (Triplet)

Cl	5.87098453	3.17790786	-0.76188406
O	3.68927528	-1.40630862	-0.18691703
O	-0.76840380	-3.81349011	1.01313317
N	1.84467067	-0.00145765	-0.17055782
N	0.13226769	-1.88746148	0.19681052
C	2.48733926	-1.24477193	-0.05522920
C	1.52093776	-2.37766657	0.35062658
C	-0.91483672	-2.66359629	0.55258173
C	-2.36041824	-2.18628798	0.23891337
C	2.41637611	1.21861458	-0.30755660
C	3.78728894	1.51152707	-0.45794697
C	4.18291292	2.82883914	-0.56720158
C	1.87483133	-2.68947532	1.82676873
C	1.79059511	-3.59214219	-0.55366921
C	-3.33547357	-3.03239139	1.07731729
H	4.50887701	0.70244443	-0.49271694
H	1.27218147	-3.53550330	2.17070307
H	1.65369472	-1.81685795	2.45546938
H	2.94418925	-2.92995833	1.89934670
H	1.52369785	-3.34861680	-1.58970794
H	1.19835507	-4.44386331	-0.20301001
H	2.86016375	-3.83778437	-0.51418715
H	-3.16428781	-4.09686775	0.88798553
H	-4.36704390	-2.76584336	0.82243541
N	0.17944717	1.85597866	-0.10552697
N	-1.84783905	0.28962220	0.27101258
C	-2.77556801	-0.69493995	0.39045447
C	-2.57017760	-2.50324007	-1.27024612
C	1.44579373	2.29951667	-0.27033417
C	3.22523877	3.89589485	-0.52272279
C	-1.00403985	2.59232112	-0.04262824
C	-2.26504073	1.70688021	0.12538124
O	-3.98980994	-0.44358933	0.49960299
H	-3.61362698	-2.29424839	-1.54505674
H	-2.35470451	-3.56595828	-1.45452402
C	1.87718753	3.63790869	-0.37488179
Cl	3.74725200	5.54508027	-0.65254068
O	-1.06344129	3.80741423	-0.15295606
C	-3.08169708	1.88963408	-1.17773942
C	-3.03444733	2.22971672	1.35231460

H	1.14914691	4.44231514	-0.33259531
H	-4.03521876	1.35806925	-1.08305976
H	-2.52097403	1.47623154	-2.02721100
H	-3.26347861	2.95944273	-1.34222016
H	-2.44546605	2.05382482	2.25990651
H	-3.99784815	1.71878126	1.42606982
H	-3.18388232	3.31171343	1.23968122
H	-1.90784820	-1.88391188	-1.88970826
H	-3.18193081	-2.85151525	2.14996329
N	-0.40187660	-0.13474964	-1.84117944
S	0.69663461	-0.15960152	-3.00235967
O	1.28048435	1.17540205	-3.19632599
O	1.61773892	-1.30011537	-2.93687687
C	-0.39049112	-0.47216790	-4.40278992
C	-2.11312310	-0.95678955	-6.49944702
C	-0.74909982	-1.79053217	-4.70756764
C	-0.88959502	0.60362283	-5.14567257
C	-1.75867308	0.36291312	-6.20538910
C	-1.62000193	-2.03845686	-5.76402579
H	-0.33865497	-2.60789191	-4.11603226
H	-0.58336429	1.61740317	-4.88696205
H	-2.16488800	1.17314803	-6.80757083
H	-1.92217392	-3.05003922	-6.02879401
Co	0.00000000	0.00000000	0.00000000
N	-0.00000000	-0.00000000	1.96048463
S	0.65730101	1.14363992	2.87329465
O	2.11451810	1.21280286	2.68732736
O	-0.09081141	2.40558933	2.85651715
H	-1.60810120	1.21332522	4.66086081
C	-0.84063114	0.60625440	5.14051873
C	1.18447506	-0.93210563	6.33487852
C	0.38837282	0.41490012	4.49944868
C	-1.06435220	0.02665047	6.38472538
C	-0.04631806	-0.73670763	6.96548687
C	1.40092803	-0.34754198	5.08991290
H	-2.00755087	0.15363551	6.91313248
H	2.35167713	-0.46802215	4.57123604
H	1.94877442	-1.53112085	6.82507467
N	-3.03163218	-1.21683633	-7.62719776
O	-3.33316640	-2.39194683	-7.86915936
O	-3.44704062	-0.24522027	-8.27124362
N	-0.27762154	-1.34770169	8.29062045
O	0.63817296	-2.01508376	8.78851061
O	-1.37384966	-1.15782309	8.83242118

References in the Supporting Information

1. Fulmer, G. R.; Miller, A. J. M.; Sherden, N. H.; Gottlieb, H. E.; Nudelman, A.; Stolz, B. M.; Bercaw, J. E.; Goldberg, K. I. NMR Chemical Shifts of Trace Impurities: Common Laboratory Solvents, Organics, and Gases in Deuterated Solvents Relevant to the Organometallic Chemist. *Organometallics* **2010**, *29*, 2176–2179.
2. (a) Evans, D. F. The determination of the paramagnetic susceptibility of substances in solution by nuclear magnetic resonance. *J. Chem. Soc.* **1959**, 2003–2005. (b) Deutsch, J. L.; Poling, S. M. The determination of paramagnetic susceptibility by NMR: A physical chemistry experiment. *J. Chem. Educ.* **1969**, *46*, 167–168. (c) Piguet, C. Paramagnetic Susceptibility by NMR: The "Solvent Correction" Removed for Large Paramagnetic Molecules. *J. Chem. Educ.* **1997**, *74*, 815–816. (d) Sur, S. K. Measurement of magnetic susceptibility and magnetic moment of paramagnetic molecules in solution by high-field fourier transform NMR spectroscopy. *J. Magn. Reson.* **1989**, *82*, 169–173. (e) Grant, D. H. Paramagnetic Susceptibility by NMR: The "Solvent Correction" Reexamined. *J. Chem. Educ.* **1995**, *72*, 39. (f) Hoppeé, J. I. Effective magnetic moment. *J. Chem. Educ.* **1972**, *49*, 505.
3. Bain, G. A.; Berry, J. F. Diamagnetic Corrections and Pascal's Constants. *J. Chem. Educ*. **2008**, *85*, 532–536.
4. Krejčik, M.; Daněl, M.; Hartl, F. Simple construction of an infrared optically transparent thin-layer electrochemical cell: Applications to the redox reactions of ferrocene, $Mn_2(CO)_{10}$ and $Mn(CO)_3$(3,5-di-t-butyl-catecholate)$^-$. *J. Electroanal. Chem.* **1991**, *317*, 179–187.
5. Bruker, *APEX2 software*, Madison WI, USA, **2014**.
6. G. M. Sheldrick, *SADABS*, University of Göttingen, Germany, **2008**.
7. Sheldrick, G. M. Crystal structure refinement with *SHELXL*. *Acta Cryst. C* **2015**, *71*, 3-8.
8. G. M. Sheldrick, *SHELXL2013*, University of Göttingen, Germany, **2013**.
9. Bartlett, S. A.; Wells, P. P.; Nachtegaal, M.; Dent, A. J.; Cibin, G.; Reid, G.; Evans, J.; Tromp, M. Insights in the mechanism of selective olefin oligomerisation catalysis using stopped-flow freeze-quench techniques: A Mo K-edge QEXAFS study. *J. Catal.* **2011**, *284*, 247–258.
10. TURBOMOLE *Version 7.3*; TURBOMOLE Gmbh, Karlsruhe, Germany, **2018**.
11. (a) *PQS Version 2.4*; Parallel Quantum Solutions, Fayetteville, AR, USA, **2001**. (b) Baker, J. An algorithm for the location of transition states. *J. Comput. Chem.* **1986**, *7*, 385−395.
12. Budzelaar, P. H. M. Geometry optimization using generalized, chemically meaningful constraints. *J. Comput. Chem.* **2007**, *28*, 2226−2236.
13. (a) Becke, A. D. Density-functional exchange-energy approximation with correct asymptotic behaviour. *Phys. Rev. A* **1988**, *38*, 3098–3110. (b) Perdew, J. P. Density-functional approximation for the correlation energy of the inhomogeneous electron gas. *Phys. Rev. B* **1986**, *33*, 8822–8824. (c) Perdew, J. P. Erratum: Density-functional approximation for the correlation energy of the inhomogeneous electron gas. *Phys. Rev. B* **1986**, *34*, 7406–7406.
14. (a) Weigend, F.; Ahlrichs, R. Balanced basis sets of split valence, triple zeta valence and quadruple zeta valence quality for H to Rn: Design and assessment of accuracy. *Phys. Chem. Chem. Phys*. **2005**, *7*, 3297−3305. (b) Weigend, F.; Haser, M.; Patzelt, H.; Ahlrichs, R. RI-MP2: optimized auxiliary basis sets and demonstration of efficiency. *Chem. Phys. Lett*. **1998**, *294*, 143−152.
15. Grimme, S.; Antony, J.; Ehrlich, S.; Krieg, H. A consistent and accurate ab initio parametrization of density functional dispersion correction (DFT-D) for the 94 elements H-Pu. *J. Chem. Phys.* **2010**, *132*, 154104−154119.
16. Neese, F. The ORCA program system, Wiley Interdiscip. Rev. *Comput. Mol. Sci.* **2012**, *2*, 73–78.
17. (a) Becke, A. D. Density-functional thermochemistry. III. The role of exact exchange. *J. Chem. Phys.* **1993**, *98*, 5648–5652. (b) Lee, C. Yang, W. Parr, R. G. Development of the Colle-Salvetti correlation-energy formula into a functional of the electron density. *Phys. Rev. B* **1988**, *37*, 785–789.
18. Available at www.iboview.org. (a) Knizia, G. Intrinsic Atomic Orbitals: An Unbiased Bridge between Quantum Theory and Chemical Concepts. *J. Chem. Theory Comput.* **2013**, *9*, 4834–4843. (b) Knizia, G.; Klein, J. E. M. N. Electron Flow in Reaction Mechanisms-Revealed from First Principles. *Angew. Chem. Int. Ed.* **2015**, *54*, 5118–5522.
19. Iszak, R.; Neese, F. An overlap fitted chain of spheres exchange method. *J. Chem. Phys.* **2011**, *135*, 144105–144111.
20. (a) Angeli, C.; Cimiraglia, R.; Evangelisti, S.; Leininger, T.; Malrieu, J.-P. Introduction of *n*-electron valence states for multireference perturbation theory. *J. Chem. Phys.* **2001**, *114*, 10252–10264. (b) Angeli, C.; Cimiraglia, R.; Malrieu, J.-P. *N*-electron valence state perturbation theory: a fast implementation of the strongly contracted variant. *Chem. Phys. Lett.* **2001**, *350*, 297–305. (c) Angeli, C.; Cimiraglia, R.; Malrieu, J.-P. *n*-electron valence state perturbation theory: A spinless formulation and an efficient implementation of the strongly contracted and of the partially contracted variants. *J. Chem. Phys.* **2002**, *117*, 9138–9153.
21. Wu, Q.; Hu, J.; Ren, X.; Zhou, J. S. An Efficient, Overall [4+1] Cycloadditon of 1,3-Dienes and Nitrene Precursors. *Chem. Eur. J.* **2011**, *17*, 11553–11558.
22. Yoshimura, A.; Luedtke, M. W.; Zhdankin, V. V. (Tosylimino)phenyl-λ^3-iodane as a Reagent for the Synthesis of Methyl Carbamates via Hofmann Rearrangement of Aromatic and Aliphatic Carboxamides. *J. Org. Chem.* **2012**, *77*, 2087–2091.
23. Boduszek, B.; Shine, H. J. Preparation of solid thianthrene cation radical tetrafluoroborate. *J. Org. Chem.* **1988**, *53*, 5142–4143.
24. Ramidi, P.; Sullivan, S. Z.; Gartia, Y.; Munshi, P.; Griffin, W. O.; Darsey, J. A.; Biswas, A.; Shaikh, A. U.; Ghosh, A. Catalytic Cyclic Carbonate Synthesis Using Epoxide and Carbon Dioxide: Combined Catalytic Effect of Both Cation and Anion of an Ionic CrV(O) Amido Macrocyclic Complex. *Ind. Eng. Chem. Res.* **2011**, *50*, 7800–7807.

---

25. Collins, T. J.; Powell, R. D.; Slebodnick, C.; Uffelman, E. S. Stable highly oxidizing cobalt complexes of macrocyclic ligands. *J. Am. Chem. Soc.* **1991**, *113*, 8419–8425.
26. Horwitz, C. P.; Ghosh, A. Improved synthesis TAML and TAML complexes. PCT/US2004/004985, 2004.
27. Ruppel, J. V.; Jones, J. E.; Huff, C. A.; Kamble, R. M.; Chen, Y.; Zhang, X. P. A Highly Effective Cobalt Catalyst for Olefin Aziridination with Azides: Hydrogen Bonding Guided Catalyst Design. *Org. Lett.*, **2008**, *10*, 1995–1998.